CD43 dependent mechanisms of Th17 cell recruitment to sites of inflammation and autoimmune reactions

A thesis submitted by:
Francisco Esteban Velázquez Planas

In partial fulfillment of the requirements for the degree of
Doctor of Philosophy
In
Immunology

Tufts University

May 20, 2017

Adviser: Pilar Alcaide

Abstract

Abstract:

IL17 producing T helper lymphocytes (Th17 cells) are often recruited at sites of tissue inflammation and participate in cell-mediated inflammatory reactions that involve interactions with the vascular endothelium. These interactions are quantitatively different from the Th1 T cell subset, and are highly dependent on E-selectin. T cell expressed E-selectin ligands were described before the existence of Th17 cells emerged, thus, their contribution to Th17 recruitment is unclear. One such ligand is syaloglycoprotein CD43, a protein with other pleiotropic functions but with unknown roles in Th17 cells. Chapter 3.1 of the present thesis dissertation tests the hypothesis that Th17 cells use specific E-selectin ligands that differ from other T cell subsets, and identifies CD43 as a major Th17 cell expressed E-selectin ligand in vitro and *in vivo*. We combine real time videomicroscopy and adhesion experiments under flow conditions in vitro, and the air pouch model of leukocyte recruitment as well as intravital microscopy of the inflamed cremaster muscle *in vivo*. In Chapter 3.2, we test the hypothesis that CD43 regulates antigen specific Th17 cell recruitment to sites of autoimmune reactions, using the mouse model of Experimental Autoimmune Encephalomyelitis (EAE). We find that CD43 regulates Th17 cell recruitment to the spinal cord in an E-selectin independent way, and hypothesize that CD43 regulates Th17 cell adhesion to ICAM-1. We present evidence that CD43 regulates Th17 cell adhesion and apical migration on ICAM-1, as well as ICAM-1 dependent transmigration in vitro. Lastly, in Chapter 3.3, we test the hypothesis that CD43 contributes to pathological cardiac remodeling and heart failure (HF), using the thoracic aortic constriction model (TAC) in which both E-selectin and ICAM-1 are upregulated in the heart. We demonstrate for the first time that CD43 contributes to T cell and monocyte recruitment to the heart, cardiac fibrosis and systolic dysfunction. In summary, we report several new roles for the sialoglycoprotein CD43, some of which are specific of Th17 cells,

and others more broad in the context of heart inflammation *in vivo*. Our results identify new CD43 regulated pathways involved in Th17 cell recruitment and in inflammation associated with cardiac dysfunction.

Acknowledgements

The PhD is not just a degree. It is an experience that trains us and shapes us, not just as scientists, but as human beings with much to give back to the community. It would not have been possible to complete this doctoral thesis without the support of all the kind people around me, particularly everyone I will try and name here.

I would like to start by thanking everyone with whom I have collaborated and worked with. Dr. Kevin Croce, Dr. William Luscinskas, Mark Aronovitz, and everyone who has given such amazing insight and feedback on this project. I would also like to thank everyone in the immunology program: Di, Stephen and Allen for their help sorting and all the faculty that have given me input throughout this work. Additionally, I would be remiss if I did not include my undergraduate University of Puerto Rico at Aguadilla and my professors which inspired me and pushed me forward, (Liza Jimenez, Jose Planas, Roberty Mayer, Jesus Lee).

I would also like to thank all my thesis committee members: Dr. Mercio Perrin, Dr. Honorine Ward and Dr. Thereza Imanishi-Kari, who have been incredibly supportive and provided critical insight into my project as it developed. I would of course like to thank and give my deepest appreciation to my advisor, Dr. Pilar Alcaide, for the support and your faith and trust in me. You have been an incredible mentor and teacher who has pushed me not just to excel, but to learn from everyone around me. I have always admired the way you run your lab and how you have achieved an amazing work/life balance that many would find enviable. Your lab has been like a second home to me. It goes without saying, that I must also thank my labmates: Tania, Ane and Jay. I can't stress enough, how for many experiments in this lab it is essential to have really good teamwork. I could always count and rely on you guys for anything I did. Every little question, no matter how silly I thought it could sound, was always received and answered with a smile. From checking math problems, to teaching me new protocols and guiding me through it, you guys have

been amazing. More importantly, I want to thank you all for all the laughs, the memories and your friendship. You guys are more than just a lab to me, you've become family. I am pretty sure I might never get to have a group in which my love of "quenepas" and mango, and coffee will ever be enjoyed as much.

I would also like to thank my friends. When I first came to Boston, and was left with making a decision of where to go to graduate school, a significant factor in deciding was the friendships of the students that made up the immunology program at Tufts. I honestly am not sure how I would have survived my first year at Tufts without my fellow first years, particularly Maria RePass who has become a best friend to me. I still remember when you invited me to Easter dinner with your family so I wouldn't be alone the first time I was here in Boston. I would also love to acknowledge old friends and new ones: Elizabeth, James Sampson, Dan Ram, Angel Leung, Meghan McPhillips, Abdo Slaybi, Vanessa Yanez, Arti Patel, Bina Julian, Becca, Giang, Basma and everyone else I might be momentarily forgetting at Sackler that made this journey worthwhile. Of course, I can't forget all the wonderful friends outside of Sackler as well, particularly Victor Cruz and Nianest Alers, who have been with me sharing laughs and memories all the way from out undergrad at UPRAg. Everyone's friendship has given me the strength and solidarity that pushes me forward when we are farthest from home.

Last, but certainly not least, I would like to express my deepest thanks to my family and Jocelyn. For all the unconditional support, motivation, love and the occasional moment of bringing me back to reality. Particularly I would like express my deepest thanks to my mother and sister to whom this thesis is dedicated. My mother has always been a fighter. I can learn from no one better to persevere and always keep on trying. To set no limit to my goals but more importantly, always be humble. My sister is perhaps the most compassionate person I know, whose kindness and love have always been something I

wish to emulate and has always had my back. No existen palabras con las que pueda expresar lo que siento cada vez que vuelvo a Puerto Rico y las veo. This journey would not have ever been possible if not for you guys and the lessons in life, kindness, perseverance and love that you have thought me. Gracias por creer en mí y haberme dado su apoyo, su amor y la fuerza para continuar adelante, sin la cual, nada de esto hubiese sido posible.

Table of Contents

Table of Contents

List of Tables

List of Tables

List of Figures

List of Figures:

List of Copyrighted Materials

Publication

Title: “CD43 Functions as an E-Selectin Ligand for Th17 Cells *In vitro* and is Required for Rolling on the Vascular Endothelium and Th17 Cell Recruitment during Inflammation *In Vivo*”

Authors: Francisco Velázquez, Anna Grodecki-Pena, Andrew Knapp, Ane M. Salvador, Tania Nevers, Kevin J. Croce and Pilar Alcaide

J Immunol February 1, 2016, 196 (3) 1305-1316; DOI: https://doi.org/10.4049/jimmunol.1501171

List of Abbreviations

List of Abbreviations

AKT: Protein Kinase B

APC: Antigen presenting cell

CAM: Cell Adhesion Molecule

CCL: Chemokine Ligand

CCR: C-C Chemokine Receptor Type

CD: Cluster of Differentiation

CHO-E-sel: Chinese hamster ovary cell line expressing E-selectin

CHO-Mock: Chinese hamster ovary cell line expressing mock vector

CLA: Cutaneous Lymphocyte Antigen + cell

Con A: Concanavalin A

CVD: Cardiovascular Disease

CXCR: C-X-C Chemokine Receptor Type

DAMP: Damage-Associated Molecular Patterns

DCM: Dilated Cardiomyopathy

EAE: Experimental Autoimmune Encephalomyelitis

EC: Endothelial Cell

EDD: End Diastolic Diameter

EDP: End Diastolic Pressure

ESD: End Systolic Diameter

EGF: Endothelial Growth Factor

ERK: Extracellular-signal Regulated Kinase

ERM: Ezrin/radixin/moesin complex

ESAM: Endothelial Selective Adhesion molecule

ESL: Endothelial Selectin Ligand

E-selectin: Endothelial selectin

FoxP3: Forkhead Box P3

FS: Fractional Shortening

GATA3: GATA binding protein 3

GPCR: G Protein Coupled Receptor

GTP: Guanosine Triphosphate

HF: Heart Failure

H&E: Hematoxylin and Eosin

IBD: Irritable Bowel Disease

ICAM-1: Intercellular Adhesion Molecule 1

IFNγ: Interferon Gamma

Ig: Immunoglobulin

IgG: Immunoglobulin G

IHC: Immunohistochemistry

IL: Interleukin

JAM: Junctional Adhesion Molecule

kD: Disassociation Constant

KO: Knockout

L-selectin: Leukocyte selectin

LFA1: Lymphocyte Function Associated Antigen 1

LV: Left Ventricle

Mac1: Macrophage antigen 1

MHC: Major Histocompatibility Complex

MI: Myocardial Infarction

MLN: Mediastinal Lymph Nodes

MS: Multiple Sclerosis

PKC: Protein Kinase C

P-Selectin: Platelet selectin

PAMS: Pattern Associated Molecular Signals

PSGL-1: Platelet Selectin Glycoprotein Ligand 1

PECAM1: Platelet and Endothelial Cell Adhesion Molecule

PMA: Phorbol Myristate Acetate

PO: Pressure Overload

Tbet: T box Transcription Factor

TCR: T Cell Receptor

TGFβ: Transforming Growth Factor Beta 1

Th: T helper

Treg: T regulatory

TM: Transmembrane

TNFα: Tumor Necrosis Factor Alpha

TEM: Transendothelial Membrane

TIM-1: T cell Immunoglobulin and Mucin Domain 1

RA: Rheumatoid Arthritis

Rhoa: Ras homolog gene family A

Rac1: Ras-related C3 botulinum toxin substrate 1

RORγT: Retinoic acid receptor related orphan receptor gamma-T

RORα: Retinoic acid orphan receptor alpha

SLE: Systemic Lupus Erythematosus

sLx: Sialyl Lewis X

sICAM-1: Soluble Intercellular Adhesion Molecule 1

STAT: Signal Transducer and Activator of Transcription

VCAM-1: Vascular Cellular Adhesion Molecule 1

VE-Cadherin: Vascular Endothelial Cadherin

VLA-4: Very Late Antigen 4

Chapter 1: Introduction

1.1. Inflammation

Inflammation is the body's response to injury or infectious agent. A critical step in this process is the recruitment of blood leukocytes into vascularized tissues. This protective response involves the immune system and the cardiovascular system, and molecular mediators such as cytokines and interferons. Primarily, inflammation is meant to eliminate the cause of harm or injury that is affecting the body, clearing dead tissue, and repairing damaged tissue. Classical signs of an inflammatory response are heat, pain, redness, swelling, and loss of function.

Inflammation can be classified into two categories: acute inflammation or chronic inflammation (Fig. 1.1). Acute inflammation is the earliest response; it occurs in minutes or hours and the leukocytes involved are mainly cells of the innate immune response. The process of acute inflammation is initiated by resident cells that are already present in the area of injury. These cells recognize pathogen associated molecular patterns (PAMP's) and damage associated molecular patterns (DAMP's), which are specific molecules that are associated with a pathogen or damage that has occurred to the host respectively promoting the innate immune response. Additionally, this causes vasodilation, which leads to increased blood flow and increased permeability of the vasculature. The vascular endothelium becomes "activated" by cytokines that have been released by the innate immune cells and undergoes a dramatic alteration in phenotype, including conversion to a pro-adhesive surface to recruit circulating leukocytes via interactions of endothelial cell adhesion molecules with their ligands expressed on the circulating leukocytes, in a process called the leukocyte recruitment cascade (1, 2). This allows immune cells to infiltrate the affected area to eliminate the infection or clear the injury.

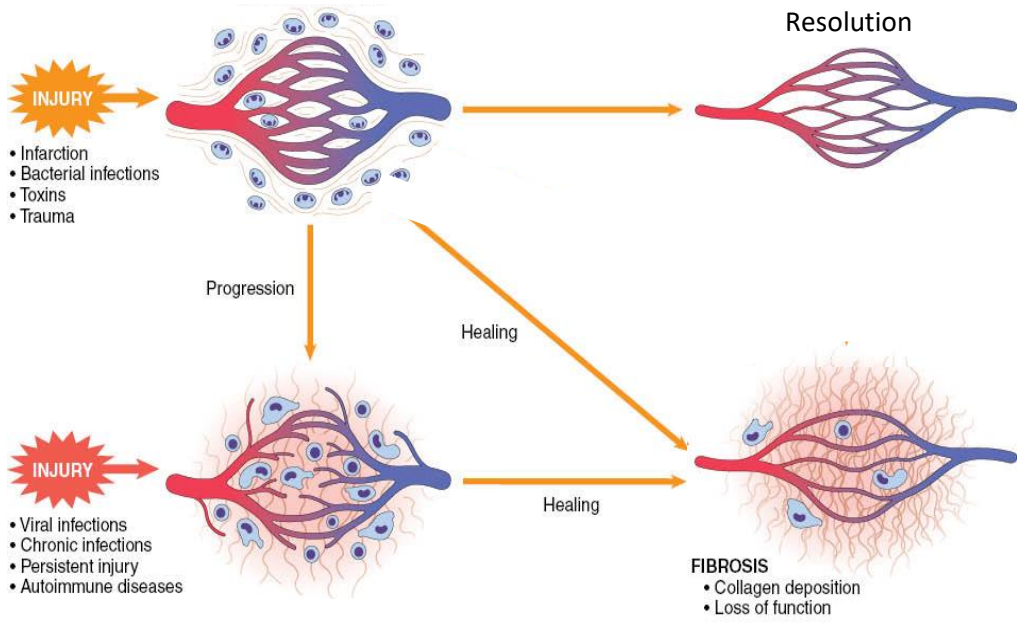

Figure 1.1: Acute and Chronic Inflammation.

A. In response to injury and an immune response, acute inflammation is followed by vascular changes, recruitment of leukocytes that promote healing and limited tissue injury resulting in resolution. **B.** Chronic inflammation is characterized by angiogenesis, leukocyte cell infiltrate and fibrosis. Figure adapted from Robbins and Cotran's Pathologic Basis of Disease, 1974. Edited by: Vinay Kumar, Abul K. Abbas and Jon C. Aster.

If the acute response does not resolve, the process evolves into chronic inflammation. This is characterized by sustained active inflammation that leads to endothelial cell dysfunction and constant recruitment of several types of leukocytes including neutrophils, monocytes and lymphocytes.

1.2. Leukocyte Recruitment

Leukocytes are recruited from the blood into the infected or injured tissue through a tightly regulated sequential process known as the leukocyte recruitment cascade that involves adhesion molecules on the leukocytes and the vascular endothelium and chemo-attractants produced during an immune response (Fig. 1.2)

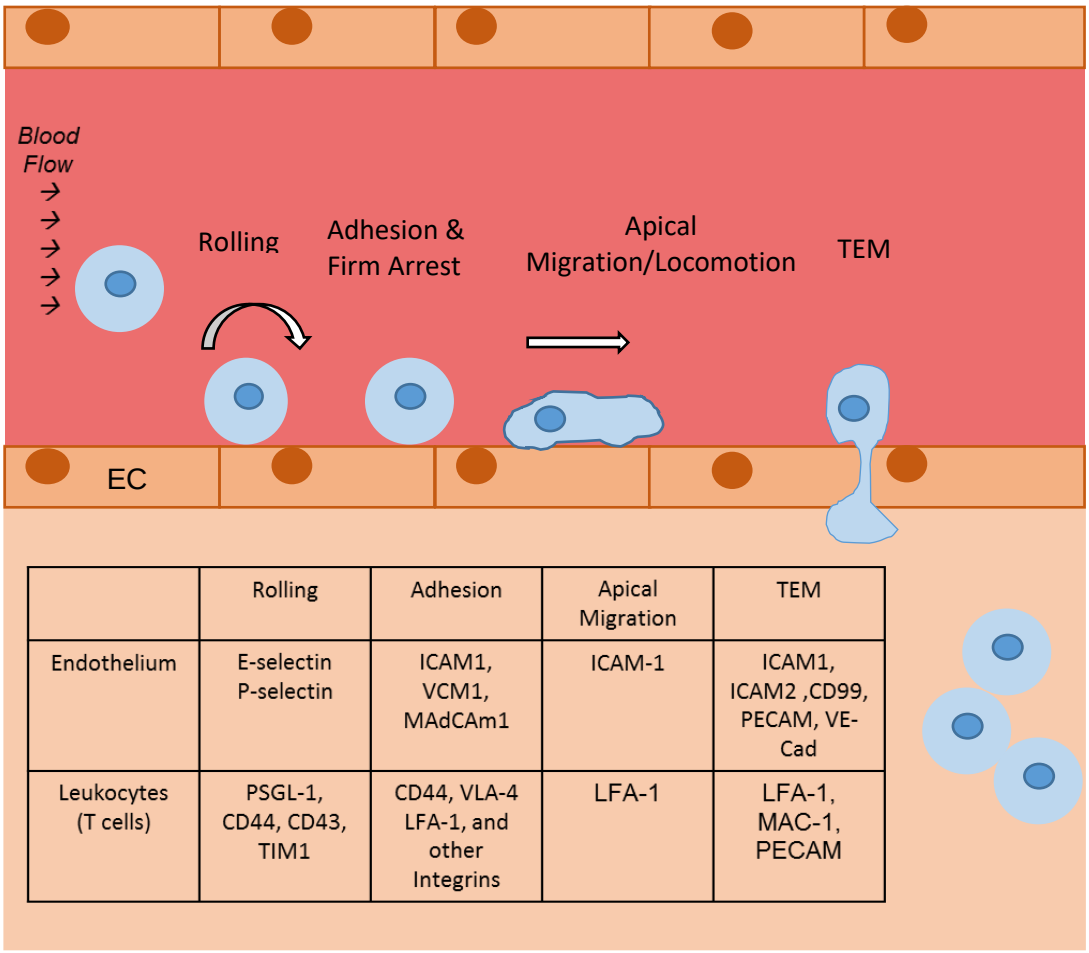

	Rolling	Adhesion	Apical Migration	TEM
Endothelium	E-selectin P-selectin	ICAM1, VCM1, MAdCAm1	ICAM-1	ICAM1, ICAM2 ,CD99, PECAM, VE-Cad
Leukocytes (T cells)	PSGL-1, CD44, CD43, TIM1	CD44, VLA-4 LFA-1, and other Integrins	LFA-1	LFA-1, MAC-1, PECAM

Figure 1.2: The leukocyte recruitment cascade.

The leukocyte recruitment cascade is a very tightly regulated sequential process. Upon inflammatory stimulation, the vascular endothelial cells (EC) upregulate adhesion molecules such as selectins and integrin ligands. This allows for leukocytes to interact with the endothelium through selectin ligands and integrins to infiltrate the tissues following the last step of transendothelial migration.

In the leukocyte recruitment cascade, the initial steps occur in response to an inflammatory stimulus. The endothelial cells that line the postcapillary venules at the affected tissue rapidly increase the surface expression of proteins known as selectins. Cytokines such as tumor necrosis factor (TNF-α) and interleukin-1 (IL-1) are among the top activators of the vascular endothelium. The recruitment of leukocytes occurs under low hemodynamic shear forces, and starts with the capture of free flowing leukocytes to

the vessel wall. This is followed by rolling along the vessel wall. Capture and rolling is mediated by endothelial selectins binding to carbohydrate determinants on selectin ligands (3). This is followed by the subsequent steps: firm adhesion, involving stable interactions between endothelial integrin ligands and leukocyte integrins in the presence of tissue-derived chemokines, and transendothelial migration (TEM), in which several endothelial and leukocyte molecules are involved to mediate the leukocyte passage from the blood stream, across the vascular endothelium and into the tissue (4).

1.2.1. Rolling

The capture and rolling of leukocytes is mediated by selectins that bind to carbohydrate components on selectin ligands (3). These selectins allow leukocytes to interact with the vascular endothelium under flow conditions. The initial rolling interactions of leukocytes with the vascular endothelium is crucial for cells to be slowed down and permit these cells to be firmly arrested and continue with later steps of the cascade. The rolling interactions involve constant binding and release between selectins and their counter-receptors that only occur under shear stress. This is due to the high on–off-rate nature of the bonds (5). These binding interactions between selectins and selectin ligands can become strengthened with higher sheer stress under physiological flow conditions (6). Besides the different selectins, leukocyte-expressed integrins are also capable of modulating leukocyte rolling.

1.2.1.1. Selectins and Selectin Ligands

In the selectin family, each selectin is composed of a single-chain transmembrane glycoprotein with a similar modular structure. The amino terminus, which is expressed extracellularly, is related to mammalian carbohydrate proteins that are known as C-type lectins. Like other C-type lectins, the selectin ligands bind in a calcium-dependent manner. The lectin domain is then followed by domains that are homologous to those

found in epidermal growth factors and in similar proteins in the complement system, with a hydrophobic transmembrane region (Fig 1.3).

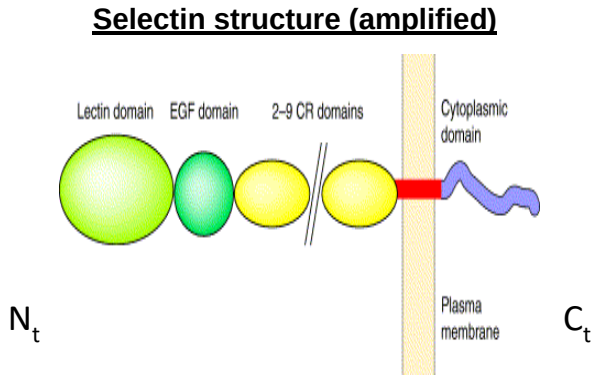

Figure 1.3: Structure of Selectin molecules.

Selectins have a basic structure that is very similar to C-type lectins. The extracellular portion possess a lectin domain, followed by an epidermal growth factor domain, and the constant repeat domains, which vary depending on the selectin. Figure modified from Ley, Trends Mol. Med, 2003.

There are two types of selectins that are expressed by the endothelium in response to inflammatory mediators (Table 1.1). Platelet-selectin (P-selectin), was first identified in the secretory granules known as Weibel-Palade bodies of platelets and later found to also be expressed in endothelial cells (7). It is rapidly redistributed to the surface in response to inflammatory mediators. Upon reaching the endothelial surface, P-selectin is essential in mediating the initial recruitment interactions of leukocytes that express its ligand P-selectin glycoprotein ligand-1 (PSGL-1) and T cell immunoglobulin and mucin-1 (TIM1) (8). Endothelial-selectin (E-selectin), in contrast, is transcriptionally regulated in response to inflammatory stimuli and takes hours to be expressed (with maximal expression at 6-12 hours) on the cell surface of the endothelium. E-selectin recognizes complex sialylated carbohydrate groups related to the Lewis X or Lewis A family, found on various surface proteins of leukocytes. E-selectin is important in the migration of leukocytes, neutrophils and effector and memory T cells to some peripheral sites of inflammation (9).

Selectin	Size	Distribution	Ligand
E-selectin (CD62E)	110 kD	Endothelium activated by cytokines	PSGL-1 CD44 CD43 ESL (in neutrophils)
P-selectin (CD62P)	140 kD	Storage granules and surface of endothelium and platelets.	PSGL-1 TIM-1
L-selectin (CD62L)	90-110 kD (varied with glycosylation)	Leukocytes (high expression on naïve T cells, low on memory and effector T cells)	Sialyl-Lewis X, GlyCAM-1, MadCAM-1, CD34

Table 1.1: Selectins.

Selectins expressed in the vascular endothelium in response to inflammation. TNFα and IL-1β induce the expression of P- and E-selectin.

Finally, Leukocyte-selectin (L-selectin) is expressed on most lymphocytes and other leukocytes. It serves as a homing receptor for naïve T cells into the lymph nodes. Leukocytes also express the carbohydrate ligands for P- and E-selectin, which facilitate interactions with the vascular endothelial cell surface. These carbohydrate ligands are

known as selectin ligands and they are of low affinity with a fast on and fast off rate along with a high tensile strength for them to occur (5, 10).

The physiological roles of selectins have been demonstrated by studies using gene deficient mice. L-selectin deficient mice have small, poorly formed peripheral secondary lymphoid organs and defective induction of T cell dependent immune responses and inflammatory responses. On the other hand, mice that lack E-selectin or P-selectin only develop mild defects in leukocyte recruitment, which suggest that these two molecules share functional redundancy. When both E-and P-selectin molecules are knocked out, there is significantly impaired leukocyte recruitment with increased susceptibility to infections. Additionally, mice that have defects in glycosyltransferase enzymes like fucosyltransferases, which make the carbohydrate ligands that bind to the selectins, have marked defects in T cell migration and cell mediated immune responses (11).

The molecules PSGL-1, CD44, and CD43 have been previously found to act as E-selectin ligands on both mouse and human T cells (12). PSGL-1, the most thoroughly characterized selectin ligand expressed on hematopoietic cells, is the main ligand for P-selectin and can also act as a major E-selectin ligand in Th1 cells and Neutrophils (13). CD44 is a glycoprotein that is involved in cell-cell interactions, cell adhesion and migration. It is also the hyaluronic acid receptor, expressed on hematopoietic and non-hematopoietic cells, and serves as an E-selectin ligand in neutrophils and can also function as an E-selectin ligand in mouse Th1 cells in combination with PSGL-1 (14). TIM-1 is a recently described P-selectin ligand that mediates tethering and rolling of Th1 cells and Th17 cells (8).

1.2.1.2. CD43

CD43 is also a glycoprotein, also known as syalomucin that lies in two states: a low and a high glycosylation state (Fig. 1.4). The high glycosylation state is often used as a marker for activation of T cells and is mediated by the enzyme Core 2 which only occurs when the T cell is activated, and happens to be the form that acts as an E-selectin ligand in mouse Th1 cells and skin human T cells (11, 15).

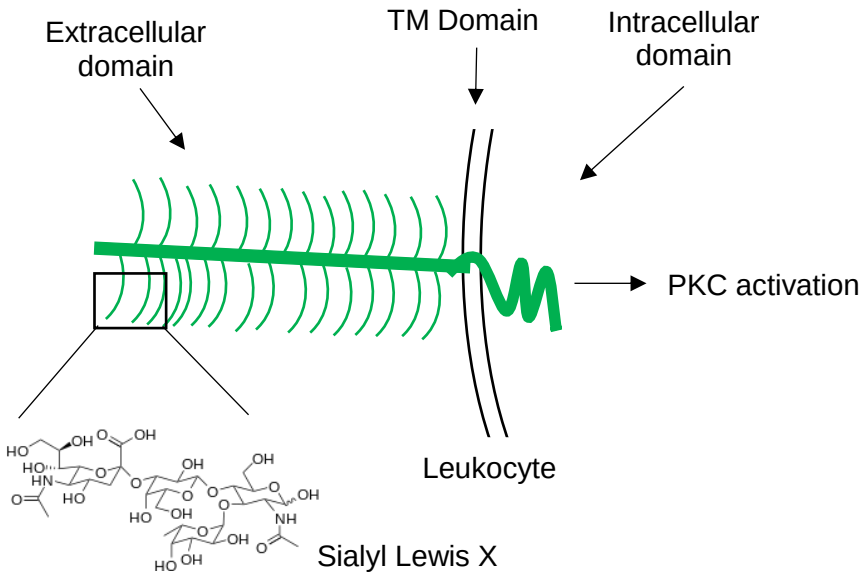

Figure 1.4: Structure of CD43.

CD43 is expressed in a low glycosylated form and a highly glycosylated form. It is composed of an extracellular domain (decorated in many carbohydrate modifications such as Sialyl Lewis X), a transmembrane domain and an intracellular domain which can signal in certain leukocytes and induce PKC activation.

CD44 and CD43 act as E-selectin ligands only in combination with PSGL-1, as seen in double and single knockout models that result in decreased leukocyte binding to E-

selectin. However, when knocked out in combination with PSGL-1, a further decrease in binding to E-selectin occurs, as compared with PSGL-1 knocked out alone. CD43 has been reported to be involved in various other functions apart from being a T cell E-selectin ligand. Indeed, CD43 has multiple ligands with which it can interact in different cells (Fig 1.5). CD43 has been reported to function as an adhesive or anti-adhesive molecule. Numerous experimental data demonstrate that CD43 participates in cell adhesiveness, functioning both as a physical barrier that controls cell activation and as a receptor that enhances intercellular contacts (16). In contrast some studies have demonstrated how the absence of CD43 might cause T cells to be more easily activated due to a lack of negative charges that would push antigen presenting cells away (17). Thus, CD43 has been reported to function in adhesion and anti-adhesion interactions that help regulate TCR signaling and the amount of time to which the T cell binds its receptor to another cell. In addition to this, CD43 has also been shown to have a role in signaling and activating PKC in leukocytes (11, 18). Given all of these functions, it is not surprising that CD43 plays a role in a number of diseases. In humans, defects in CD43 are associated with the development of Wiskott-Aldrich syndrome, and overexpression of the highly glycosylated form of CD43 has been reported to be critical in T cell lymphomas and myeloid tumors (19, 20). In mice, the absence of CD43 can impair Th2 immune responses in the lung, and has additionally been implied in autoimmunity as well as cardiovascular disease (21-24).

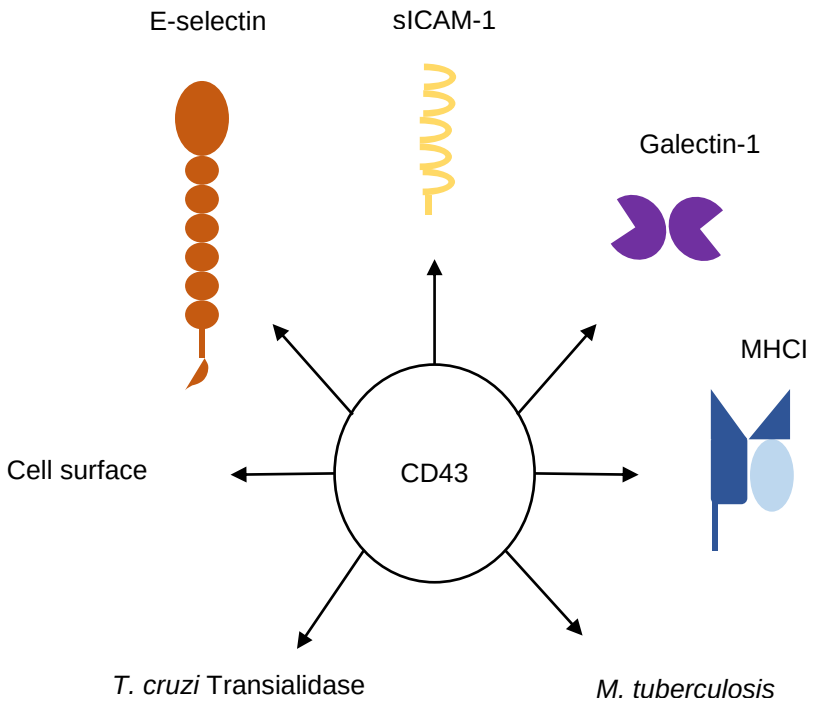

Figure 1.5: CD43 ligands.

CD43 has been implied in interacting with a number of different molecules in different models. These different cell-cell interactions demonstrate a complexity to CD43 expression and function in different cell types.

1.2.2. Adhesion and Firm Arrest

Once the leukocytes have been slowed down, they can recognize chemokines. Some of the chemokines that are produced at a site with an inflammatory response are transported to the luminal surface of the endothelial cells of the post-capillary venules, and are displayed at high concentrations. Not all chemokines however use motifs to bind to extracellular cell matrix. These chemokines can then bind to their chemokine receptors on the rolling leukocytes, activating their integrin ligands. Integrins are ubiquitously expressed heterodimeric cell surface receptors consisting of an α and a β subunit. After these initial rolling interactions there is adhesion and firm arrest. These integrins change from a closed state to an open state where they have an increased affinity and avidity and help stabilize the leukocytes to the vascular endothelium.

Vascular cell adhesion molecule-1 (VCAM-1) is the ligand for the integrin very late antigen-4 (VLA-4), and intercellular adhesion molecule-1 (ICAM-1) is the ligand for lymphocyte function-associated antigen (LFA-1) and macrophage-1 antigen (MAC-1). Both become highly expressed and allow for firm attachment of leukocytes to the vascular endothelium. Following selectin- and chemokine-induced integrin-dependent arrest, the adhesion needs to be strengthened and the cytoskeleton undergoes reorganization before the cell can continue on with the cascade. Not only integrin affinity but also the density of integrin heterodimers per area of plasma membrane is increased, improving adhesion of leukocytes to the underlying endothelium (25, 26).

1.2.2.1. Integrin and Integrin Ligands

Integrins are proteins that function mechanically by attaching the cell cytoskeleton to the extracellular matrix. The integrin family of proteins is composed of alpha and beta subtypes, which make a transmembrane heterodimer (Fig. 1.6). They serve as adhesion receptors for extracellular ligands and can transmit signals that result in cell movement. Interestingly they can function bi-directionally using outside-in (Signal produced by conformational change of integrin allowing binding to ligand) and inside-out signaling (Signals that are received by the cytoplasmic end of the integrin). For integrins to become functional they must undergo a process of activation, where they go from a closed state or conformation to an open state, in which their affinity and avidity to their ligands is increased. Once this occurs, adaptor proteins can bind to the integrin cytoplasmic domains connecting the molecule to the cytoskeleton. As this process occurs, the integrins cluster for efficient ligand binding. Different types of combinations between the alpha and beta subunits exert different *in vivo* effects of integrins depending on the cell type (27).

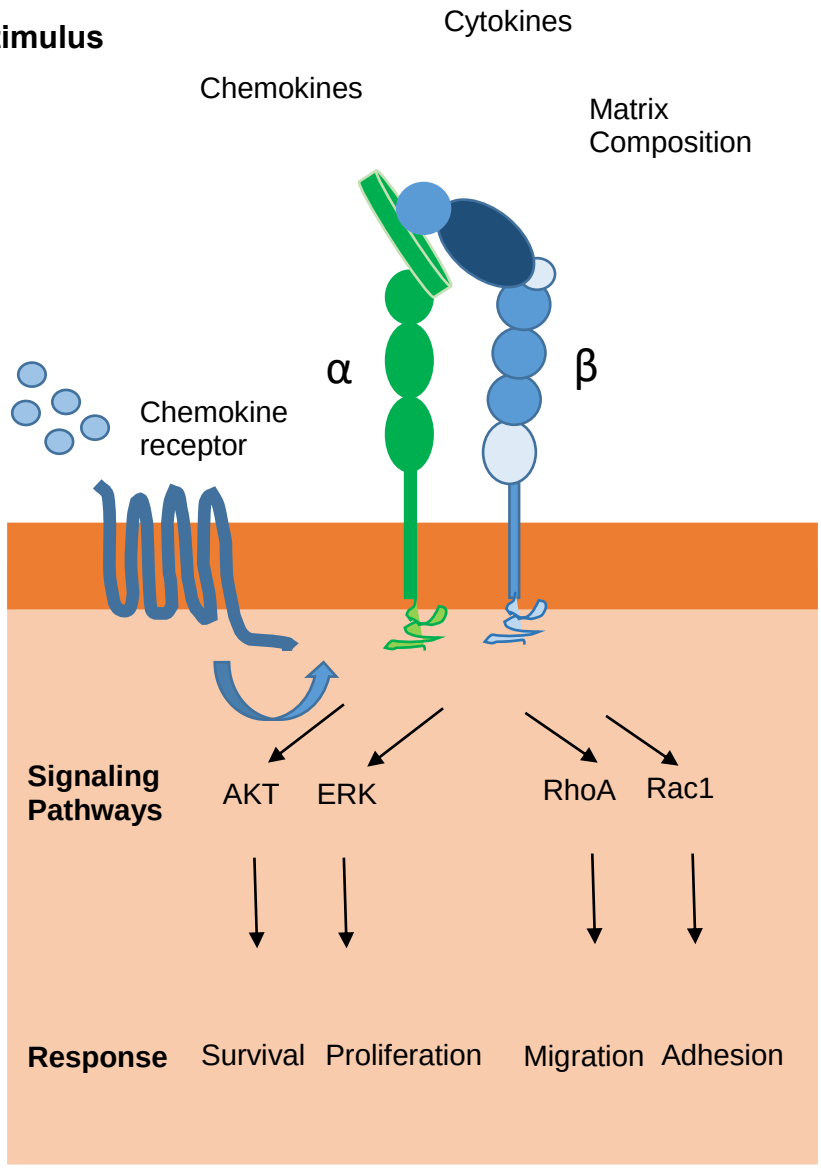

Figure 1.6: Integrins

In response to various different stimuli, integrins sense
Outside-in signaling and become activated. Depending on the type of stimuli and cell type, various types of responses can be achieved.

Different integrins have different ligands, including fibronectin, vibronectin, collagen, and various cell adhesion molecules (CAM's). Of these CAM's the most prevalent are ICAM-1 and VCAM-1, with much of the present thesis work focusing on ICAM-1. Both ICAM-1 and VCAM-1 play crucial roles in the leukocyte recruitment cascade by facilitating

counter receptors for the integrins on the leukocyte and allowing for firm arrest, apical migration and finally transendothelial migration (4, 28).

1.2.2.2. Chemokines and Chemokine Receptors

Chemokines are small proteins that serve chemotactic purposes and control the migratory phenotypes of immune cells. It is a critical component in immune cell movement and homeostasis. Chemokine receptors are the ligands for chemokines and these are differentially expressed across all leukocytes. Chemokine receptors can be divided into two groups: g-protein coupled receptors (Gpcr's) and the atypical chemokine receptors, which can shape the chemokine gradients and can dampen inflammation. While chemokines and their receptors are widely known for serving as guiding components of immune cell recruitment, they also play a major role in the development of T cells, by guiding naïve cells and antigen presenting cells, to their appropriate secondary lymphoid organs (29). Additionally, recent studies have begun to demonstrate how chemokines can also have an impact on T cell priming, differentiation and activation (30). Certain chemokine-chemokine receptor signaling can lead to integrin activation and T cell arrest to the endothelium (31).

1.2.3. Locomotion

Once the cells have become firmly adhered, they undergo a process of crawling on the endothelial surface. This was a process that was originally observed with monocytes and was called locomotion (32). This process is highly dependent on adhesion of LFA-1 to ICAM-1 as can be appreciated in studies in which blocking LFA-1 causes monocytes to not crawl and detach (33). Through the process of "outside-in-signaling" LFA-1 becomes activated, switching from its closed or bent, to its extended and then open conformation (34). This is an essential step that is crucial for T cell migration and the formation of immune synapses. At the same time, chemokine signals are also important

to direct the T cell and create T cell polarity that will result in apical migration. Much of this process is dependent on GTPases of the Rho family. These GTPases, which regulate the actin polymerization, coordinate the redistribution of LFA-1 to the leading edge of the cell, where pseudopods form, and thus allow for the T cell to locomote across the endothelial surface.

1.2.4. Transendothelial migration

The final step in the leukocyte recruitment cascade involves the transmigration of leukocytes across the endothelium. Once the leukocytes are firmly arrested on the endothelium, the chemokines can stimulate the cells to migrate through the inter-endothelial spaces along the chemical gradient. Transendothelial migration, also known as diapedesis, occurs either by the paracellular route (through endothelial junctions) or transcellularly (through the endothelial cell itself) (35, 36). It is a very complex process that involves a number of adhesion molecules expressed within the endothelial junctions that actively support transendothelial migration of leukocytes and cooperate during paracellular transmigration. Some of these molecules are: platelet/endothelial cell adhesion molecule-1 (PECAM1), ICAM-1 and -2, junctional adhesion molecule-A (JAM-A), JAM-B and JAM-C, endothelial cell-selective adhesion molecule (ESAM), CD99, CD99L2 and VE-Cadherin (28, 37-39). Adherent leukocytes have also been shown to induce transmigratory cups on endothelial cells composed of clusters enriched in VCAM-1 and ICAM-1 that support diapedesis of leukocytes (40).

The accumulation of leukocytes in tissues is a major component of chronic inflammation. There is some specificity in this process of leukocyte migration based on the expression of different combinations of the adhesion molecules and chemokine receptors on the leukocytes. One such example is how neutrophils will use LFA-1-ICAM-1 interactions along with the chemokine receptor CXCR1, while monocytes will mainly use VLA-4-

VCAM-1 interactions alone with the chemokine receptor CCR2 (41). Thus, different adhesion molecules and chemokines will affect the migration of different immune cells, depending on the type of inflammatory stimulus, and whether it is an acute or chronic inflammatory response.

A fundamental aspect of the differentiation of naïve T cells into effector cells, which occurs in the peripheral lymphoid organs, is a change in the expression of chemokine receptors as well as adhesion molecules that determine a cells migratory behavior. The expression of molecules that are involved in naïve T cell homing include L-selectin and CCR7. These molecules are downregulated as a T cell differentiates and prepares to migrate into an afflicted tissue. Some effector cells have an actual propensity to migrate into particular tissues. This selectin migratory phenotype is acquired during differentiation. In this way, the adaptive immune system can direct cells with specialized functions to locations where they are best suited to deal with different types of immune responses.

1.3. Naïve T cells and T helper cell subsets

The immune system is comprised of two separate branches, each with their own crucial roles in maintaining an adequate immune response. These branches are known as the innate and adaptive immune system. The innate immune system is the first responder after a tissue suffers an insult or infection. This rapid response, which causes an inflammatory reaction, then triggers the adaptive immune system. This part of the immune system is specialized to target the specific cause of injury and creates a response that will leave the host with memory of the infectious pathogen encountered. The adaptive immune system is comprised by lymphocytes. Among the lymphocytes we can find B cells and T cells, and within those T cells we can find $CD4^+$ and $CD8^+$ T cells. The present thesis focuses on $CD4^+$ T helper cells, and their subsets (Fig 1.7).

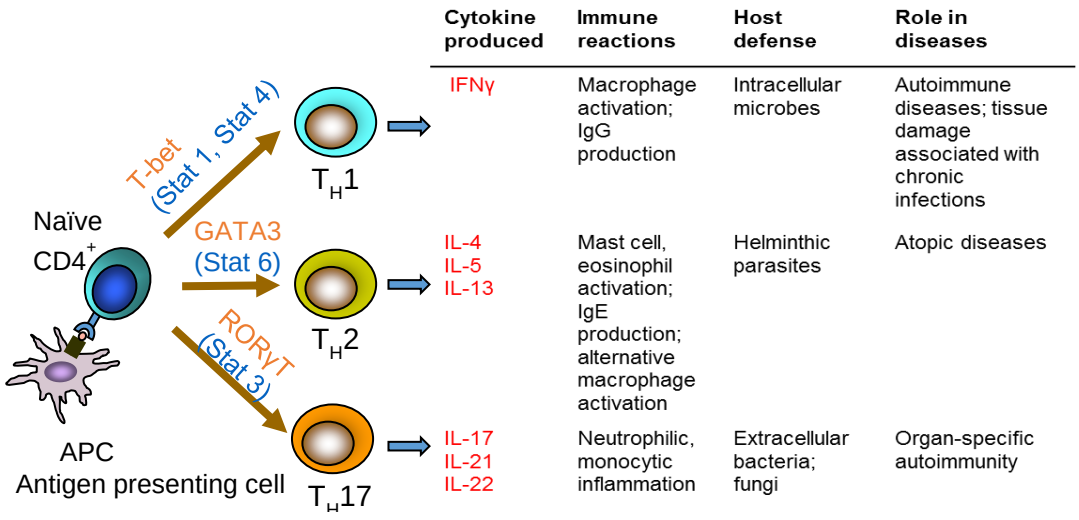

Figure 1.7: T cell subsets.

T cells can differentiate into a wide variety of different effectors. Each of which have their own specific function in the immune system.

T helper cells (Th) are the mediators of cellular immunology and are so named after their development in the thymus. Th cells are known for their key role in helping other immune cells effectively carrying out their functions, including cytotoxic T cell activation, cytokine production by innate cells, recruitment of other immune cells and antibody production by B cells. They are also key players that characterize chronic inflammation by being recruited once inflammation has failed to resolve (42).

1.3.1. Naïve T cells

T cell subsets arise from naïve $CD4^+$ T cells upon antigen stimulation in the presence of specific cytokines that activate different transcription factors, which drive T helper cell differentiation towards different T cell subsets in secondary lymphoid organs (16, 18, 21, 43, 44). Those subsets include Th1, Th2, Th17, T regulatory cells, each expressing the signature transcription factors Tbet, GATA 3 RORγt and Foxp3, and producing the signature cytokines such as IFNγ, IL-4, IL17 and IL-10 respectively. These are

necessary to perform their own specific immune functions, promote lineage specific differentiation and prevent the differentiation of other subsets (42).

1.3.2. Th1 Cells

The Th1 subset was first described in the 1980's through studies of large panels of cloned cell lines derived from antigen-stimulated mouse $CD4^+$ T cells. Its phenotype, mechanisms of differentiation, and contribution to both protective immunity and disease have been extensively characterized (18). Th1 cells are involved with the elimination of intracellular pathogens and are also associated with organ-specific autoimmunity. The major transcription factor that regulates Th1 cell differentiation is Tbet. Th1 cells produce IL12 and mainly IFNγ which further promotes cells towards Th1 cell differentiation and inhibits the proliferation of other T cell subsets. Additionally, IFNγ production is vital for the activation of IFNγ response genes (45).

1.3.3. Th2 Cells

Th2 cells were discovered at the same time as Th1 cells and are also very well characterized and defined. Th2 cells are more suited and prepared for generating responses towards extracellular parasites and helminths. They play a key role in the induction of allergies and asthma, as well as in maintaining their persistence. Some key cytokines these cells generate are IL4, IL5, IL9, IL10 and IL25. IL4 is critical for their differentiation and the signature transcription factor that controls their lineage differentiation is GATA3. Th2 cell differentiation and cytokine production can also inhibit Th1 cells differentiation (45).

1.3.4. Th17 cells

Another subset of T cells known as Th17 cells were more recently discovered. Th17 cells emerged more recently when experimental models of autoimmune disease, previously thought to be mediated by Th1 cells, were exacerbated in animal models

lacking a Th1 response (43). Th17 cells are a distinct subset of $CD4^+$ T cells with IL-17 as their major cytokine, orchestrating the pathogenesis of inflammatory and autoimmune diseases. They are primarily involved in maintaining mucosal barriers and contributing to pathogen clearance at mucosal surfaces. They are also involved in immune-mediated inflammatory diseases. Two particular transcription factors, retinoic acid-related orphan receptor γ-t (RORγT) and retinoic acid, related orphan receptor-α (RORα) induce the expression and differentiation of Th17 cells. IL-1 signaling is crucial for the programing of Th17 cells and for Th17 cells that are involved in autoimmunity. In Th17 cells, IL-1 synergizes with IL-6 and IL-23 to regulate Th17 cell differentiation and survival, which is similar in humans and in mice (46). The main focus in this thesis work is on Th17 cells.

1.3.5. T regulatory cells (Tregs)

T regulatory cells are a subset of T cells that modulate the activation of the immune system. They are responsible for maintaining tolerance to self-antigens and preventing the development of autoimmunity. In order to achieve their function, Tregs are immunosuppressive and downregulate induction and proliferation of effector T cells. The master transcription factor for Tregs is FOXP3 and they are believed to be derived from the same lineage as $CD4^+$ T cells. There are two types of Tregs. The first originates at the thymus and helps with T cell development. The second, known as inducible Tregs, arise from naïve $CD4^+$ T cells in the periphery that differentiate into Tregs in response to antigen presentation in the presence of TGFβ. Tregs mainly produce IL10 which helps in immunosuppression of other T cells, and also produce TGFβ and IL35 (42).

1.3.6. Mechanisms of T cell migration

The activation of T cell subsets and their differentiation into different effector T cells has an impact on the adhesion molecules that are expressed on the T cell surface. This is turn causes very unique migratory phenotypes for each T effector cell (Table 1.2). This

involves the transcription factor-specific induction of glycosyltransferases that are required for the synthesis of the carbohydrate moieties to which the selectins bind. Similarly, this transcription factor stimulation will result in the expression of chemokine receptors. Different T cells have different expression of these adhesion molecules and glycosylation, hence creating different migratory phenotypes for each cell. Th1 cells are perhaps one of the best characterized T cell subsets, and, for instance, Th1 cell migration has been demonstrated to be very strong into areas with an immune response and this correlates with a high expression of E-selectin ligands, in contrast to Th2 cells, with low expression of properly glycosylated selectin ligands and lower extravasation potential. Th17 cells on the other hand are strong responders in migrating to sites of immune responses, some of which are also populated by Th1 cells. It has been previously shown that Th17 cells have a high affinity to E-selectin as compared to Th1 cells, however, their migratory phenotype and selectin ligand expression is not known (47).

	Th1	**Th2**	**Th17**
Transcription Factor	*Tbx21*	*GATA3*	*Rorc*
Cytokines	IFNγ, IL2	IL4, IL13, IL5	IL17, IL21, IL22
Ligands for endothelial selectins	+++ (48, 49)	+/-	Investigated in this thesis dissertation
Migration into sites of strong	+++ (43, 50, 51)	+/-	+++

innate immune responses			

Table 1.2: T cell migratory phenotype.

T cells have unique migratory phenotypes that contribute to their effectiveness to migrate to an area of an immune response.

1.4. T helper 17 cells in inflammation and immunity

Th17 cells have been associated with the development of inflammation and autoimmunity. They participate in several human immune inflammatory diseases that are strongly associated with chronic inflammation and organ specific autoimmunity. Because of this, Th17 cells and how these cells regulate inflammation and disease are of central interest in the field of autoimmunity and chronic inflammatory diseases. Up until now, Th17 cells have been implicated in participating in several chronic inflammatory diseases like Crohn's disease, Multiple Sclerosis (MS), and Psoriasis as demonstrated in human patients and replicated in animal models of such diseases (Fig 1.8).

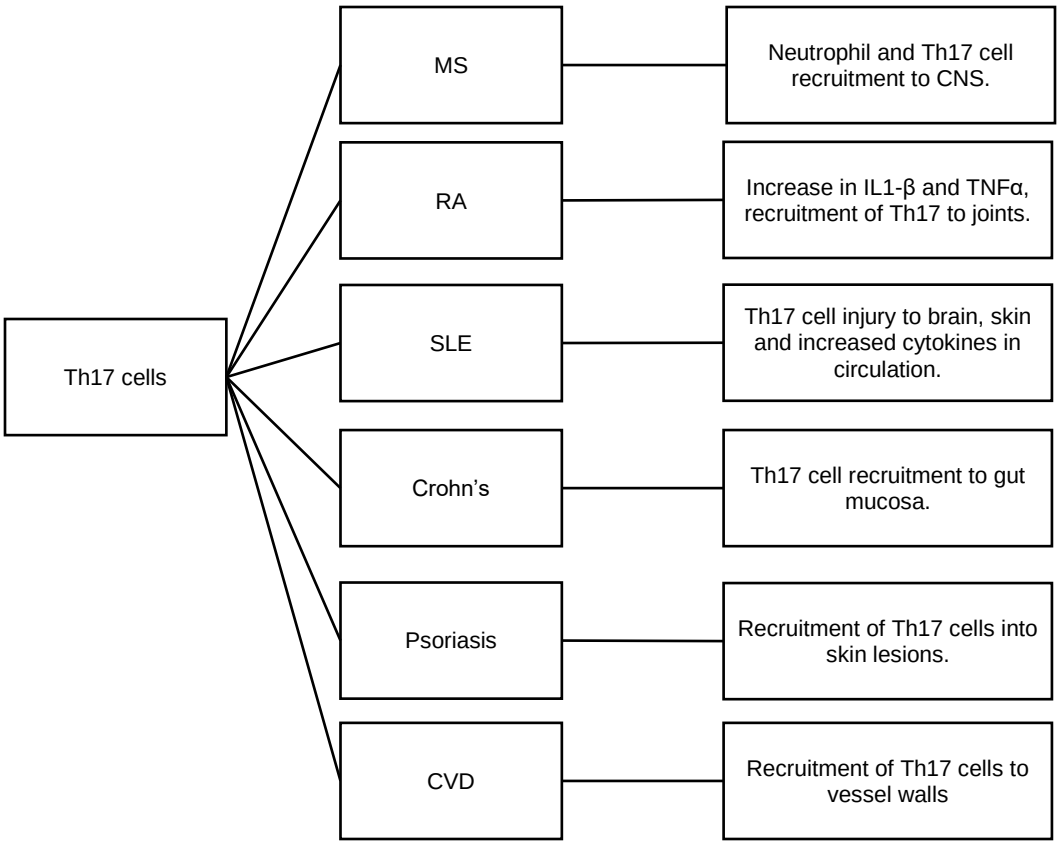

Figure 1.8: Role of Th17 cells in various diseases.

Th17 cells have been demonstrated to play a role in a number of autoimmune and inflammatory diseases found both in human and mice. MS = multiple sclerosis, RA = Rheumatoid Arthritis, SLE, Systemic Lupus Erythematosus, CVD = Cardiovascular Disease.

Multiple studies have shown, that Th17 cells are involved in inflammation. Cytokines that are expressed by Th17 cells play a role in the pathogenesis of inflammation. IL-17 is over expressed in inflamed lung endothelial cells. In rheumatoid arthritis (RA), as well as other autoimmune diseases, there is also upregulation of IL-17. Meanwhile, IL-23, the cytokine that stabilized Th17 cell lineage, has also been shown to heavily drive inflammation (52). In Crohn's disease, this cytokine promotes inflammation, and aids in maintaining the stability of Th17 cells, promoting the production of cytokines such as IL-6 and IL-17. IL-22 has been shown to promote the pathogenesis of autoimmune

diseases through the IL-22R, inducing Janus kinase-signal transducer and activators of transcription. This is more commonly observed in cancer, where IL-22 induces tumor growth and inhibition of apoptosis (53). Additionally chemokines like CCL20 and the expression of CCR6 induces the recruitment of Th17 cells to the inflammatory sites. Studies where CCL20 and CCR6 are neutralized lead to a decreased susceptibility to experimental autoimmune encephalomyelitis (EAE) in mouse models (47, 54). The MAP kinase p38 has also been shown to regulate IL-17 synthesis and production (55).

In autoimmunity, down regulation of Th17 cells decreases inflammation and the severity disease. In the model of EAE, IL-17$^{-/-}$ mice exhibit suppressed autoimmunity (56). Consistent with this, IL-9 deficiency also correlates with the absence of IL-17 and IFNγ expression in the central nervous system and reduced susceptibility to EAE (57). The ratio of Th17/Th1 cells also plays an important role in inflammation. A disproportion of Th17 to Th1 cells, with Th17 cells outnumbering Th1 cells, leads to an increase in disease severity and in EAE affects the levels of inflammation in the brain parenchyma. Additionally, the ratio of Th17/Th1 cells is important in bone maintenance (58). Th17 cells are also involved in inflammatory bowel disease (IBD), where the balance of Th17 cells to T regulatory (Tregs) cells plays a role in deciding whether the inflammation is sustained or resolved (59). Lastly, IL-17 deficiency has been reported to be protective in some models of cardiovascular disease, such as atherosclerosis and autoimmune myocarditis, however these studies could not define whether this was exclusively by suppressing Th17 cell responses of other immune cells producing IL-17 (60, 61). Recent advances on research in Th17 cells has substantially allowed for the understanding of the pathogenesis of various immunological diseases: from how the cytokines produced by Th17 cells participate in sustaining this T helper cell subset, to affecting the tissue being afflicted, to the plasticity and balance of Th17 cells with other T helper cells. However, the migratory phenotype of these cells is not completely understood.

1.5. T cell mediated inflammation in Heart Failure

Heart failure (HF) is a complex clinical syndrome that can result from any structural or functional cardiac disorders that impair the ability of the ventricle to fill or eject blood. It is a serious condition and there is no cure for this disease. Heart failure is a chronic, progressive condition where the heart fails to pump enough blood to meet the body's demands. Under normal conditions the heart is a healthy, strong muscular pump that is composed of four chambers. The two upper chambers are known as the atria, while the lower chambers are called the ventricles. The right atria takes in oxygen-depleted blood from the rest of the body and sends it back out into the lungs through the right ventricle, where the blood can become oxygenated again. The heart tries to overcompensate in response to left ventricular pressure overload during HF by becoming larger (myocyte hypertrophy and increase in ventricle wall thickness), the deposition of collagen (cardiac fibrosis resulting in less efficient muscle contraction), and by attempting to pump blood faster (increasing heart rate). Thus, cardiac hypertrophy and cardiac fibrosis in response to increased pressure overload in the heart, can lead to cardiac dysfunction that impacts the ability of the heart to pump blood efficiently to the tissues. Recent emerging data indicates that inflammation is also associated with pathological cardiac remodeling (Fig. 1.9).

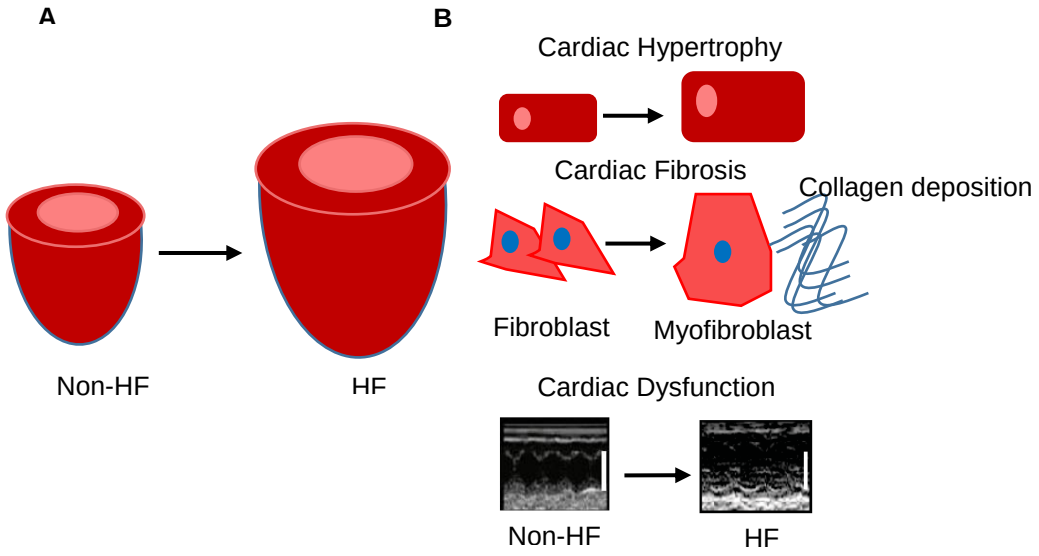

Figure 1.9: Cardiac hypertrophy in pressure overload induced heart failure.

Pathological remodeling of the heart **(A)** results in the inability to pump enough blood throughout the body, and is characterized by cardiac myocyte hypertrophy, increase in wall thickness, cardiac fibrosis, increased heart rate all leading to cardiac dysfunction **(B).**

Heart failure (HF) is a major health problem and has a prevalence of over 5.8 million people in the USA and over 23 million people worldwide (62, 63). In 1997, HF was singled out as an emerging epidemic(64). HF involves a number of factors, such as inflammation, the interplay of myocardial factors, renal dysfunction, and neurohormonal activation (65, 66) (Fig 1.10). Given the complexity of HF and all the factors that are involved, it is very difficult to delineate the respective responsibility and contribution that each of these factors have in HF. It has been observed that in patients that have HF there is increased circulation of pro-inflammatory cytokines, and this correlates with disease stage and mortality. Indeed, clinical trials were launched targeting TNFα; these trials, however, were unsuccessful and were ended prematurely due to lack of both improvement of survival and the hospitalization rate (67, 68). Most of the studies done in HF have focused heavily on the activation of the immune system, particularly focusing

on the innate immune response. Particularly, more is known of ischemic HF than non-ischemic. In humans, recent studies have shown a positive correlation between inflammatory cytokines that are potentially being produced by T cells and left ventricle (LV) dysfunction. Indeed, T cells can infiltrate into the heart and negatively affect cardiac function (69-73).

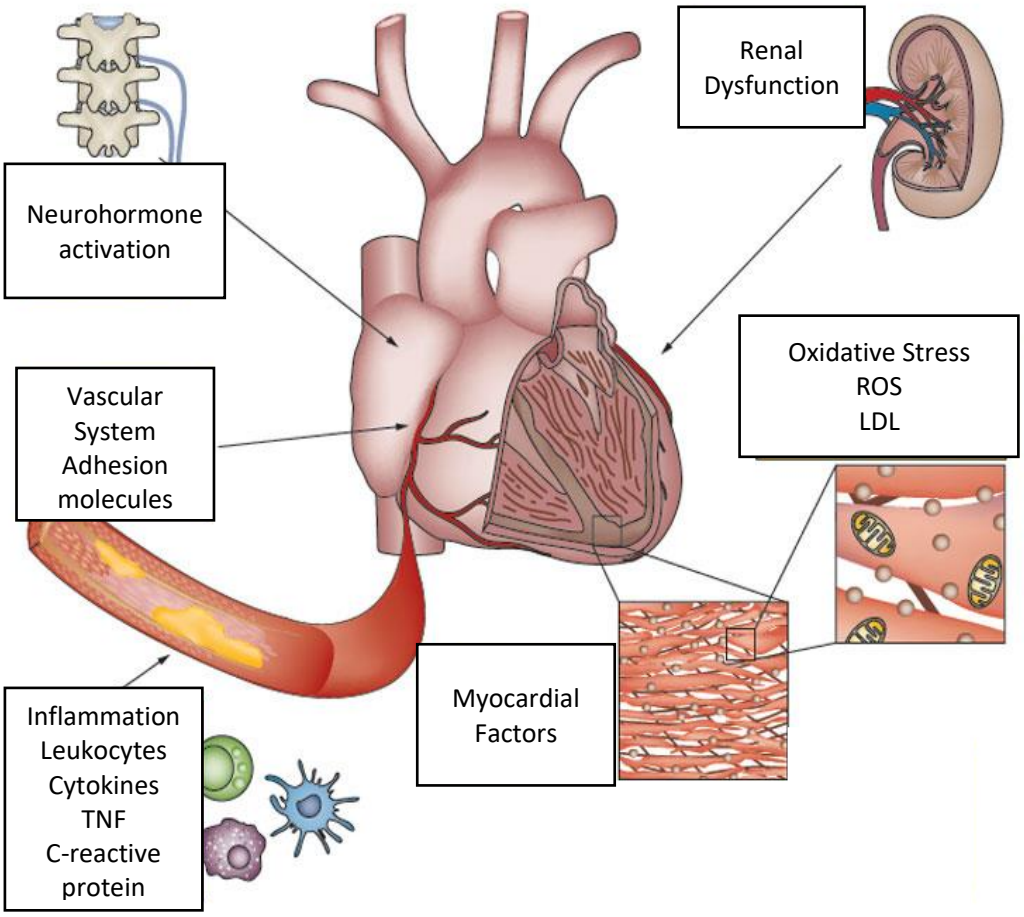

Figure 1.10: Heart Failure is a complex syndrome.

HF is a systematic illness that involves the interplay of various myocardial factors, inflammation, renal dysfunction, and neurohormonal activation. Figure modified from Ahmad, Tariq et al, Nature Reviews Cardiology 2012.

Thus, T cells are critical regulators of pathological cardiac remodeling in non-ischemic HF. The absence of T cells not only prevents the development of fibrosis and

pathological hypertrophy in the LV in HF, but also preserves cardiac function (74). Additionally, we have observed that adhesion molecules such as ICAM-1 are essential in the recruitment of leukocytes into the LV in the setting of HF in PO (75).

CD43 has been recently implicated in in two mouse models of cardiovascular disease, including abdominal aortic aneurysm, and atherosclerosis. In both studies absence of CD43 is protective by mechanisms involving CD8 IFNy production by CD8+ T cells and cholesterol efflux in macrophages, respectively (23) (22). However, the role of CD43 in heart failure, and potential mechanisms related with leukocyte recruitment have never been studied, and it is the focus of Chapter 3.3 in the present thesis.

1.6. Specific Aims

1.6.1. Determine the expression and functionality of CD43 and other E-selectin ligands on Th17 cells and their role *in vitro* and *in vivo.*

This aim, presented in Chapter 3.1, demonstrates that known E- selectin ligands expressed on mouse and human T cells are all expressed in mouse Th17 cells. Specifically we show a unique high uniform expression for CD43 on Th17 cells as compared to Th1 cells. Our findings demonstrate that CD43 is a crucial regulator of Th17 cell recruitment *in vitro* and *in vivo* via the use of real time viodeomicroscopy, the air pouch model of leukocyte recruitment and intravital microscopy.

1.6.2. Investigate the role of CD43 in the context of autoimmune disease using the mouse model of Experimental Autoimmune Encephalomyelitis (EAE), and whether CD43 specifically regulates Th17 cell trafficking and/or differentiation in EAE.

Th17 cells were first discovered and characterized in the model of EAE. We evaluated the role of trafficking of antigen-specific Th17 cells in EAE and their mechanisms as determined *in vitro*. The findings of this aim are presented in Chapter 3.2.

1.6.3. Determine the role of CD43 in cardiovascular disease (CVD) using the *in vivo* mouse model of Thoracic Aortic Constriction (TAC).

Recent evidence associates T cell recruitment to the heart with CVD. In the context of TAC, we have demonstrated that T cells play a crucial role in pressure overload induced Heart Failure (HF). This is an optimal model to evaluate the role of CD43 in the recruitment of T cells in response to TAC.

Chapter 2: Materials and Methods

2.1. Mice

All mice used were bred in the pathogen free facility at Tufts University School of Medicine Ziskind Building, in accordance with the guidelines of the committee of Animal research at Tufts University School of Medicine, Tufts Medical Center and the NIH Animal research guidelines. C57Bl/6 (WT) mice were purchased from Jackson Laboratory (Bar Harbor, Maine) or used as littermates from heterozygous crosses. Double knock out (DKO) CD44$^{-/-}$/PSGL-1$^{-/-}$ and CD43$^{-/-}$/PSGL-1$^{-/-}$ mice were obtained from Dr. Rodger McEver (OMRF, Oklahoma city, OK). Strain matched mice deficient in CD43 (CD43$^{-/-}$), PSGL-1 (PSGL-1$^{-/-}$) were generated from intercrosses of CD43$^{-/-}$PSGL-1$^{-/-}$ DKO and PSGL-1$^{-/-}$CD44$^{-/-}$ DKO mice with C57Bl/6 (WT) mice. Triple knock out (TKO) CD43$^{-/-}$CD44$^{-/-}$PSGL-1$^{-/-}$ were generated by crossing CD43$^{-/-}$PSGL-1$^{-/-}$ DKO mice with CD44$^{-/-}$PSGL-1$^{-/-}$ DKO mice. Mice were sacrificed at 7-12 weeks of age for harvest of naïve T cells, or used between 8-10 weeks of age for Air pouch experiments. The genotypes were determined by PCR and null mutations were also confirmed by FACS analysis of spleen cells. Double and triple KO animals were viable, fertile and displayed significant increase in circulating leukocytes as previously described (51, 76, 77)

2.1.1. DNA isolation for CD43 mice

Mouse tail clips from pups generated for the CD43$^{-/-}$ colony were incubated in lysis buffer containing 4% of proteinase K at 60ºC overnight, precipitated with an equal volume of cold isopropanol, and pelleted by centrifugation. The DNA pellet was washed with 200 µL of 70% ethanol, air dried, and resuspended in Tris-EDTA buffer pH8.

2.1.2. Genotyping for CD43

DNA isolated from mice generated was amplified using Taq Master mix and the primer pairs listed in Table 1. According to cycling conditions. All PCR reactions were run on a 1% agarose gel for 1h at 100V to visualize the products.

Table 2.1: reaction components for genotyping PCR

Reaction Components	Volume (µL)	Final Concentration
DNA template	1	-
Forward Primer	0.5	20 uM
Reverse Primer	0.5	20 uM
Taq master mix	10	1X
Water	8	-

Table 2.2: CD43 genotyping PCR program

Cycle steps	Temperature (ºC)	Time	
1	94	8 min	
2	94	30 sec	40 cycles
3	60	30 sec	
4	72	30 sec	
5	72	5 min	
6	4	hold	

Table 2.3: Primers for genotyping E-selectin ligand deficient mice

Gene	Forward	Reverse	Neo
PSGL-1	5'-GCT TCC TTG TGC TGC TGA C-3'	5'-CCT CTG TGG ATG CTG GTT G-3'	5'-GTC CGG TGC CCT GAA TGA ACT GC-3'

CD44	5’-GCA GCC CCC AGC CAG TGA CAG 3’	5’-AGA GGC TGC GGG CAT CCA AGA GTA-3’	5’-GTC CGG TGC CCT GAA TGA ACT GC- 3’
CD43	5’-CGG AAC TGC AGC ATC TAC AT-3’	5’-GCA TGG GCA CCA GTA ACA TG-3’	5’ GTA CAG AGA GGG GAC AGG TCA C-3’

2.2. Cell Culture

2.2.1. Preparation of effector T cells

$CD4^+$ cells were isolated from spleen and lymph node cell suspensions of WT mice using positive selection by immunomagnetic beads (Invitrogen, Carlsbad, CA). Th1 cells were derived from the naïve T cells by anti-CD3 and anti-CD28 stimulation in the presence of IL-12 and IFN□, as previously described (47). To achieve Th17 differentiation, naïve T cell were stimulated with anti-CD3 in the presence of human TGF-β (3ng/ml), mouse IL-6 (30ng/ml), mouse IL-23 (20ng/ml), plus anti-IFN-□ (10ug/ml), anti-IL-4 (10µg ml), and anti-IL-2 (10µg/ml) mAb. On day 3, Th1 and Th17 cultures were diluted 1:1 with fresh medium containing IL-2 (25U/ml) and IL-23 (20ng/ml), respectively. Cells were harvested on day 4 and immediately used in experiments as illustrated in Fig. 2.1.

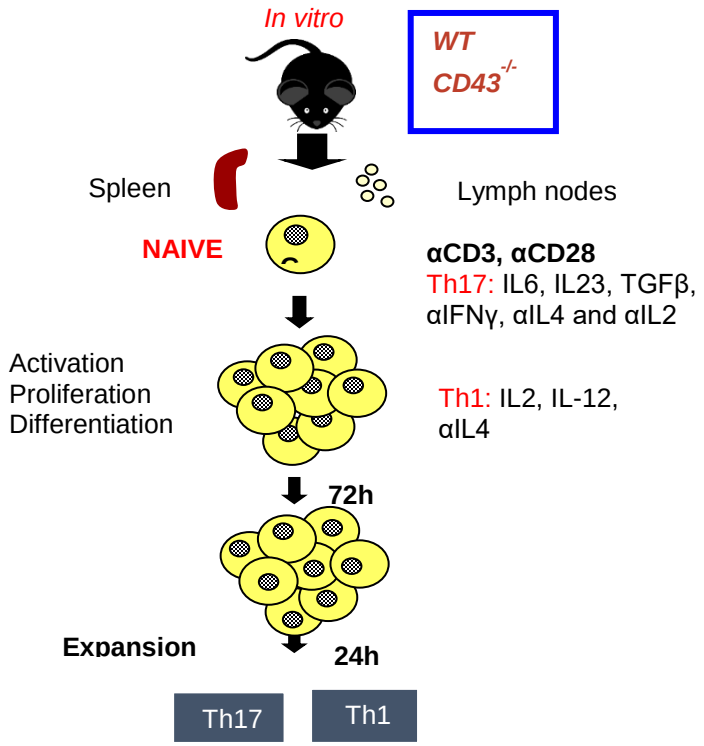

Figure 2.1: T cell differentiation.

Naïve CD4 T cells are isolated from the spleen and lymph nodes of mice. They are cultured *in vitro* in plate bound αCD3 and soluble αCD28 in the presence of cytokines and blocking abs for 3 days. The cells are split using IL23 for Th17 cells and IL2 for Th1 cells, and then harvested 24 hrs later

2.2.2. Re-stimulation of cells isolated from lymph nodes

Mice immunized with emulsified MOG in CFA were sacrificed at day 7 and inguinal, axial, and cervical lymph nodes were isolated. Lymph nodes were smashed on a 70 um filter and centrifuged at 1500 rpm for 5 minutes. Cells were resuspended in RPMI media with IL2 (50 U/mL) and IL23 (20 ng/mL) and cultured for three days. On the third day, cells were harvested and stained for IL-17A and IFNγ flowing the established protocol for flow cytometry.

2.3. RNA

2.3.1. RNA Isolation

RNA isolation of *in vitro* cultured cells, was achieved using 1 mL of TRIzol LS Reagent (Thermofisher 10—296-028) with the sample and allowed to sit for 5 mins at room temperature. When RNA from a tissue was harvested, 500 µL of TRIzol were added to each sample and crushed using a pestle until the sample was ground up. Samples were allowed to sit for 5 minutes before proceeding. All samples were then added 200 µL of chloroform per 1 mL of TRIzol. Samples were then vortexed vigorously for 15 seconds, incubated at room temperature for 2-3 minutes and centrifuged at 12500 rpm at 4ºC for 20 minutes. Once phases were separated, the upper aqueous phase was collected and placed in a fresh tube, and added equal volume of ispropyl alchohol. Samples were incubated at room temperature for 10 minutes and then centrifuged at 12500 rpm for 10 mins at 4ºC. Precipitated RNA (white pellet) would form after this. Carefully removing the supernatant, the pellet was resuspended in 75% ethanol and centrifuged at 9500 rpm for 5 mins at 4ºC. After spin supernatant was removed and pellet was air-dried for 10 minutes at room temperature. Pellet was resuspended in 30 µL of RNase Free water (DEPC-treated water) and incubated for 10 minutes at 60ºC. Quantification of RNA was determined using ThermoScientific NanoDrop 2000c UV-Vis Spectrophotometer. RNA concentration and purity was determined via optical density of 260 nm and 280 nm. Ratios of optical density (260/280) from 1.8-2.0 were considered adequate to use.

2.3.2. Reverse Transcription

For synthesizing complementary DNA (cDNA) from RNA, the following volumes of each reagent was added per 1 µg of template RNA listed below. The cDNA was synthesized using Applied Biosystems protocol based on 10 minute cycle at 25ºC, 20 minutes cycle at 42ºC, 5 minutes at 99C, finalized holding the samples at 4ºC.

Table 2.4: Reverse transcription reaction components

Component	Volume (µL)	Final concentration	Manufacturer	Reference
25 mM $MgCl_2$	4	5mM	LifeTechnologies	361691
10X PCR buffer II	2	1X	LifeTechnologies	4486218
DEPC Water	Variable	-	Thermofisher	R0601
dNTP's (10mM)	2	1mM	LifeTechnologies	362275
RNase Inhibitor	1	1 U/mL	LifeTechnologies	100021540
Random Hexamers	1	2.5 µM	Invitrogen	100026484
MµLV RT	1	2.5 U/mL	LifeTechnologies	100023379
RNA template	(Max is 9µL)	1µg	-	-

2.3.3. qRT-PCR

Gene expression through mRNA levels, 3 µL of each in 1/10 dilution of cDNA sample was mixed with 1.25 µL of 10uM forward primer, 1.25 µL of 10 µM reverse primer, 12.5 µL of SYBR Green (QuantiTect SYBR Green Master Mix, Quiagen 1020722) and 8 µL of RNase Free water. Reaction was run in 384 well plates using the 7900HT Fast Real-Time PCR System (Applied Biosystems).

Table 2.5: qPCR primers

Gene	Forward	Reverse
Icam1	5'-GCT GTG CTT TGA GAA CTG TG-3'	5'-GTG AGG TCC TTG CCT ACT TG-3'
Esel	5'-TGA CCA CTG CAG GAT GCA T-3'	5'-ATC CAA CGA ACC AAA GAC TCG-3'
Tbx21	5'-CAA CAA CCC CTT TGC CAA AG-3'	5'-TCC CCC AAG CAG TTG ACA GT-3'
Rorc	5'-CCG CTG AGA GGG CTT CAC-3'	5'-TGC AGG AGT AGG CCA CAT TAC A-3'
Foxp3	5'-CAC CC GGA AAG ACA GCA ACC-3'	5'-GCA AGA GCT CTT GTC CAT TGA-3'
Gapdh	5'-ACC ACA GTC CAT GCC ATC AC-3'	5'-TCC ACC ACC CTG TTG CTG TA-3'
Bactin	5'- TCC TTC GTT GCC GGT CCA-3'	5'- ACC AGC GCA GCG ATA TCG TC-3'

2.4. Flow Cytometry and Cell Sorting

Flow cytometry was performed to corroborate the differentiation of Th17 cells as described, the expression levels of E-selectin ligands on Th1 and Th17 cells (47), and Th17 cells and Th1 cells production of cytokines and infiltration into various tissues. To detect intracellular IL-17A and IFN-γ. Intracellular staining of signature cytokines was performed, cell suspensions were initially incubated for 3-5 hours at 37 C with RPMI T cell media containing 1X of ionomycin (Sigma Aldrich I0634), brefeldin A (BioLegend 420601), and monensin (BioLegend 420701) and 50 ng of PMA (Phorbol Myristate Acetate, Sigma Aldrich P8139). This mixture would allow for the accumulation of secretory proteins in the endoplasmic reticulum of highly activated cells. After incubation, surface staining was performed with antibody of choosing at a 1:50 dilution in FACS buffer (PBS without Ca/Mg with 2% FBS). This was followed by cell fixation for 15 minutes at RT protected from light, and then samples were washed 2x with FACS buffer. Immediately after, cells were permeabilized with was/perm buffer (10X diluted in water to 1X) and stained with intracellular antibodies at 1:50 dilution for 20 minutes at RT protected from light. Cells were then washed and acquired on a BD LSRII and analyzed using FlowJo.

For sorting of Th17 and Th1 cells, cells were stained with the CD43 activation-associated glycoform Ab (clone 1B11) from BioLegend and separated based on expression of CD43 based on histogram analysis using a MoFlo Astrios EQ (Beckman Coulter). The data were acquired on a FACS LSRII flow cytometer (BD Biosciences, San Jose, CA) and analyzed using FlowJo software (Tree Star, Ashland, OR).

Table 2.6: Flow cytometry antibodies

Antibody	Clone	Manufacturer
Anti-mouse CD45.2-PE	104	Biolegend
Anti-mouse CD45.2-APC	104	BioLegend
Anti-mouse Ly6C-APC-Cy7	HK1.4	BioLegend
Anti-mouse CD4-FITC	GK1.5	BioLegend
Anti-mouse CD4-APC-Cy7	GK1.5	BioLegend
Anti-mouse CD3e-FITC	145-2C11	BioLegend
Anti-mouse CD11b- PerCP	M1/70	BioLegend
Anti-mouse CD44-APC-Cy7	IM7	BioLegend
Anti-mouse CD62L-PE	MEL-14	BioLegend
Anti-mouse LFA-1-FITC	H155-78	BioLegend
Anti-mouse MAC1- APC	M1/70	BioLegend
Anti-mouse CD43-PE	1B11	BioLegend
Anti-mouse PSGL1-PE	KPL-1	BioLegend
Anti-mouse CD11a-FITC	2D7	BioLegend
Anti-mouse-IFNy-PE	XMG1.2	BioLegend
Anti-mouse IFNy-APC	XMG1.2	BioLegend
Anti-mouse IL17-PE	TC11-18H10.1	BioLegend
Anti-mouse IL17-APC	TC11-18H10.1	BioLegend

2.5. Western Blots, Immunoprecipitation, and blot rolling assays

The preparation of cell lysates with 1% N-octylglucoside (Roche, Indianapolis, IN), reducing SDS-PAGE, and immunoprecipitation and western blotting techniques were all performed as previously described (47). Protein concentrations were determined with the

BCA kit (Thermo Fisher Scientific, Rockford, IL). Immunoprecipitation reactions used anti-PSGL-1 antibody (2PH1), anti-CD43 glycoform antibody (1B11) plus anti-CD43 antibody (sc-7054), or antiCD44 (clone IM7). Briefly, aliquots of lysate from Th17 cells (300–450 mg) were incubated with 6 mg of the indicated mAb or with isotype control mAb and 30–45 mL of protein A-G PLUS Agarose beads (Santa Cruz Biotechnology) with rotation overnight at 4°C. Agarose bead immune complexes were collected by centrifugation, washed with 1% N-octylglucoside lysis buffer and the process repeated once more. Each sample was subjected to SDS-PAGE and western blotting under standard conditions. The blot rolling assay allows for real-time observation of selectin-mediated interactions with cellular glycoproteins separated by molecular mass or immunoprecipitated from total cellular lysates and immobilized on membrane used in Western blot. The parallel flow chamber system, maintenance and processing of E- or P-selectin transfected CHO cells and use of the blot rolling assay have been described in detail (43, 51).

2.6. Flow Adhesion Assays

The system utilized for flow adhesion assay is demonstrated in Fig. 2.2. It is a flow chamber (designed by Dr. Jian Shen and Forbes Dewey at MIT). The chamber is compose of two non-oxidizing plates separated via a plastic gasket controlling directionality of the flow. The upper plate has an entrances on the top and on the sides, as an added measure to prevent bubbles from getting in. This upper plate has an added section that can be heated up, with an insert for a thermometer to keep the temperature at 37ºC. The bottom plate of the chamber has circle cut into it, where we can place glass coverslips above a thin silicone gasket to create a sealed chamber. We use 25mm coverslips from Carolina Glass that have been prechosen to fit on the chamber. The chamber can be sealed by using 4 screws with spacers causing the gasket placed on the upper plate of the chamber to have the only space through which liquid can enter and exit.

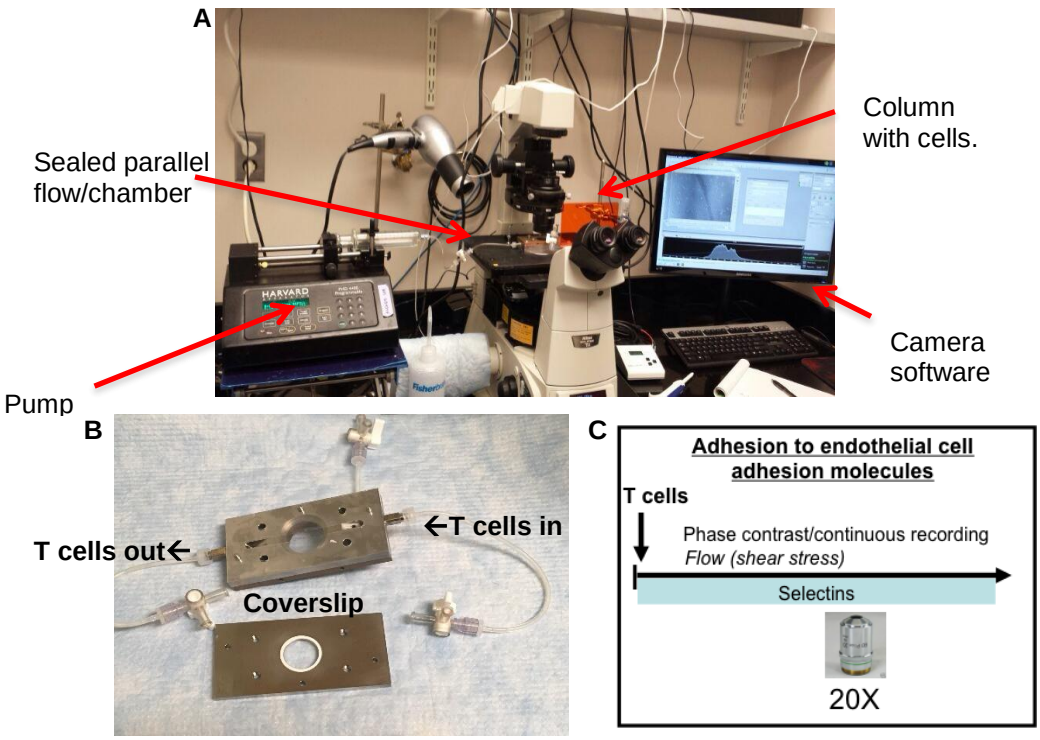

Figure 2.2: Video microscopy set up.

A. Inverted microscope with parallel sealed flow chamber, pump and column cell set up**. B**. parallel flow chamber is demonstrated with upper plate and lower plate separated. Cells flow in on indicated section with arrow, passing through the allowed space in the gasket and exit at indicated section as the pump pulls the cells through. This layer is placed over the coverslip before sealed. **C**. Representative image of flow of cells over coverslip.

2.6.1. Coverslip preparation

Coverslips were prepared overnight, by being washed with sodium bicarbonate pH 9.2 for 3 times, before being washed with PBS and incubated with our protein of interests. To observe better ICAM-1 adhesion, coverslips were treated with anti-human IgG (Abcam) for 30 minutes at RT, washed with PBS 2x and then ICAM-1 was placed on coverslip. This would allow for better orientation of the ICAM-1 chimera for the T cells. Coverslips were kept in 6 well plates and a moist No.1 Whatman filter paper was placed over the coverslips before the cover to prevent evaporation of liquid during incubation at 4ºC overnight. Coverslips were washed with PBS 5 times the next morning and blocked

for 1 hour at room temperature with PBS with 2% Bovine Serum Albumin. Before the coverslip was sealed in the chamber prior to perfusion of T cells, 100 µL of 0.1% Tween 20 in PBS was added to the coverslip.

Table 2.7: Chimeric adhesion molecules for adhesion assays

Chimera	Concentration on coverslip (µg/mL)	Reference	Manufacturer
Mouse-E-selectin	5	575-ES-100	R&D Systems
Mouse-P-selectin	10	737-PS-050	R&D Systems
Mouse ICAM-1	20	553006	BioLegend

2.6.2. Adhesion Assays

The adhesion assays consist of perfusing flow buffer (2% bovine serum albumin in 100 mL of PBS with Calcium and Magnesium, and 100 mL of PBS without Calcium and Magnesium) that contains 1 x 10^6 cells in a bolus of 2 mL connected to the chamber. The bolus containing the cells will be pulled by a Harvard apparatus pump (Model 4400) which will be programmed to run through different shears. The program for adhesion is as follows: 3' at 1 dyne/cm^2 (0.56 mL/mn refill rate), 2' at .8 dyne/cm^2 (0.36 mL/mn refill rate), 2' at .5 dyne/cm^2 (0.26mL/mn refill rate). T cells will be perfused over coverslips coated with our protein of interest such as E-selectin chimera (purchased at R&D 5 µg/mL), P-selectin chimera (purchased at R&D 10 µg/mL) or ICAM-1 chimera (Biolegend 20 µg/mL). For any T cells being perfused over ICAM-1, T cells were first stimulated with 50 ng of PMA for 5 mins at 37ºC before being perfused. Once perfused, the program was paused for 5 mins to allow T cells to form firm arrest on ICAM-1 and shear stress was commenced once again. We record 1 min per each shear stress at 20X magnification using an

inverted microscope with phase (Nikon Eclipse TE200U) using Nikon Elements NIS software. A minimum of 6 fields of vision were analyzed per each recorded video.

Table 2.8: Antibodies used for function blocking

Antibody	Clone	Manufacturer
Anti-mouse LFA1	M17/4	BioLegend
Anti-mouse ICAM-1	YN1/1.4	BioLegend

2.6.3. Detachment Assays

Detachment assays use the same flow buffer as in method 3.2, with 2 $x10^6$ T cells activated with 50 ng of PMA for 5 minutes at 37ºC before being perfused in a 100 µL bolus. To ensure that no air bubbles enter the chamber, 10 mL of flow buffer are added immediately as cell bolus has been pumped in. Cells are perfused at 1 dyne/cm^2. Shear stress will be maintained for 30 seconds, before increased to 2 dyne/cm^2. This will continue until 10 dyne/cm^2 of shear stress has been achieved. Each recording will be the remaining 15 seconds of the 30 second shear stress to allow cells to adjust, while imaging the same area. Below is a diagram representing how Th17 cells are perfused into the chamber with increases in shear stress in Fig. 2.3.

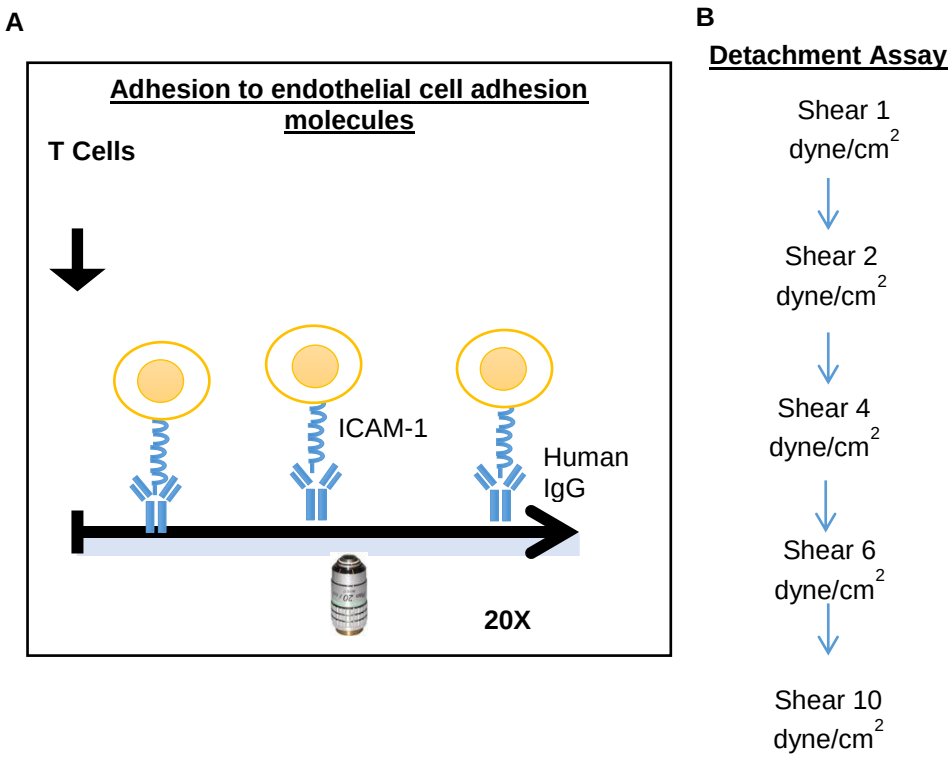

Figure 2.3: Detachment Assay of Th17 cells on ICAM-1 under physiological shear flow.

A. WT and CD43$^{-/-}$ stimulated Th17 cells are perfused over coverslips coated with an ICAM-1 chimera. Once the cells have been perfused, the flow program will be stopped for 5 mins to allow for firm arrest of cells before commencing the shear flow program and recording. **B**. representation of shear flow program.

2.6.4. Locomotion Assay:

Locomotion assays use the same flow buffer as in method 3.2, with 1 x10^6 cells [after PMA (50 ng/100 µL) activation at 37ºC for 5 min] being perfused into the sealed flow chamber in a 100 µL bolus, followed immediately by 10 mL of flow buffer as the sample is pumped into the chamber. Cells were perfused at 1 dyne/cm^2 and the programed was paused for 5 minutes, before restarting the flow program. One area was recorded for 20 minutes with 15 seconds interval imaging. Quantification of each recording, was done

using ImageJ and tracking each cell per individual frame that moved after being bound for an average of 10 frames as demonstrated in Fig. 2.4 below.

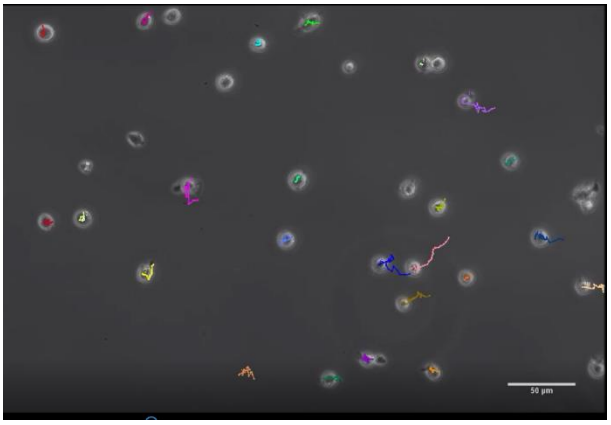

Figure 2.4: T cell migration tracking.

T cells were tracked after confirming that they were adhered after 10 frames using ImageJ. Values of pixels were converted to um by obtaining the conversion of um/pixel of Zyla camera software.

2.7. Chemotaxis Assay

T cells were generated by differentiating Naïve T cells into Th17 cells for 4 days as established (See method 2.1). On day 3, transwells were coated with 20 µg/mL of ICAM-1 and incubated at 4ºC overnight. On day 4 T cells were harvested and stained with CFSE (Thermo Fisher Scientific, C34554) for 30 minutes at 37ºC and washed with PBS before being resuspended in T cell media. Transwells were then washed with PBS 5 times on the fourth day before T cells were placed in well that contained media with or without 100 ng/mL of CCL20 (Peprotech and 250-27B).

2.8. *In vivo* Models

2.8.1. Air Pouch Model of Inflammation

Air pouches were created in the dorsal side of the back of aged matched WT and the indicated selectin ligand deficient mice as previously described (47, 78). PBS, TNFα (500ng/mouse) of CCL20 (400ng/mouse) were injected in the air pouch, and 20h later, cell infiltrates were harvested by repeated washes with PBS (Fig. 2.5). Single cell suspensions were permeabilized and stained for intracellular IL-17 or IFNγ and analyzed by flow cytometry.

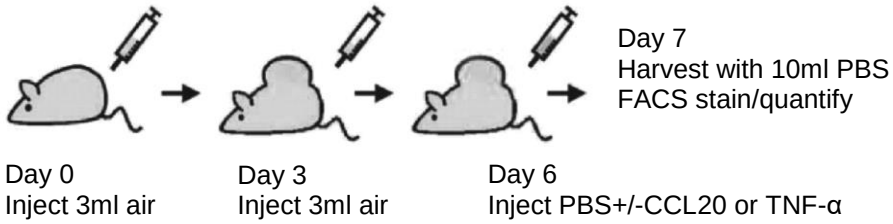

Figure 2.5: Air pouch model.

Mice are injected with 3 ml of air on day 0. 3 days later, the mice are injected again with 3 ml of air to stabilize the air pouch and make a solid structure. After 3 more days the mice are injected with 400 ng of CCL20 or PBS. 24 hours later the cells are collected by pouch lavage and quantified and stained for FACS analysis.

2.8.2. Competitive rolling assay for T cell adhesion *in vivo* in the cremaster muscle.

Intravital microscopy studies of the mouse cremaster muscle microcirculation were performed as described (13, 47). Mouse recombinant TNF-α (500 μg in 200 μL saline/mouse) was injected intrascrotally 1.5 hours prior to cremaster exteriorization. Mice were anesthetized and a microcatheter was introduced to the right femoral artery to enable retrograde injection of fluorescently labeled Th17 cells. Where indicated, 90 μg IgG or anti–E-selectin Ab (clone 9A9) was injected via the jugular vein right before

injection of the T cells. Transmitted light and fluorescence cremaster imaging was performed with an Olympus FV1000 confocal intravital microscope using a ×20 water immersion objective (Olympus). Fluorescence imaging was done sequentially at 473 and 635 nM to reduce the potential for channel crosstalk (Fig 2.6). CFSE- and Alexa Fluor 680–labeled Th17 WT and CD43$^{-/-}$ Th17 cells or Th1 cells were suspended at 33 × 10^7 cells/ml and small boluses (3 × 10^6 of each type) of a mixture of both were injected retrograde into the femoral artery catheter to visualize their adhesion in the postcapillary venules. Microvessel images were analyzed off-line using Imaris software (Imaris, South Windsor, CT).

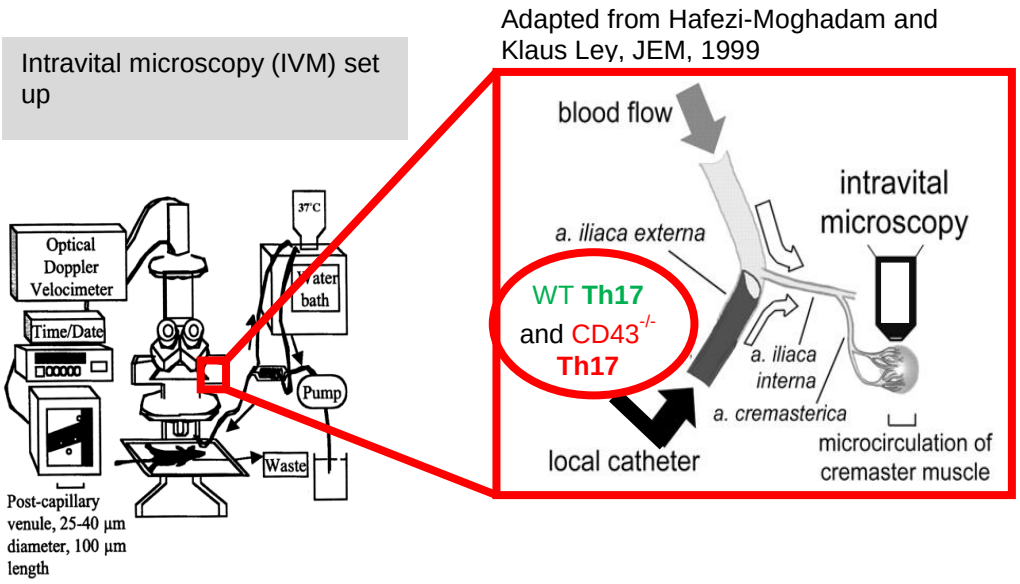

Figure 2.6: Intravital microscopy set up

Labeled T cells are retrograde injected into the femoral artery of 7 week old mice and recorded via confocal intravital microscopy. 33 x10^6 cells/mL are injected per each vessel imaged with equal number of WT and CD43$^{-/-}$ Th17 cells.

2.8.3. Experimental Autoimmune Encephalomyelitis

WT and CD43$^{-/-}$ mice were immunized using 100 µg MOG emulsified 1:1 in CFA. Mice were also given 200 ng pertussis toxin to permeabilize the blood–brain barrier. Mice were clinically scored using the following criteria: 0, no disease; 1, flaccid tail; 2, hindlimb weakness; 3, hindlimb paralysis; 4, forelimb weakness; 5, moribund. The spinal cords were harvested at day 16 postinjection, and cells were isolated using Ficoll gradient and stained for CD4, IL-17A, and IFN-γ by flow cytometry. Lymph nodes were harvested at day 8 postimmunization, passed through a cell strainer, and the cells were cultured ex vivo with MOG (10 µg/mL), IL-2 (25 U/mL), and IL-23 (25 ng/mL). Cells were harvested 72 hours later and stained for flow cytometry.

2.8.4. CNS Isolation

Isolation of the spinal cord was completed using Pino P. A. et al 2011 protocol (79). Mice were euthanized and perfused with 10 mL of PBS into the heart to flush out blood. The spinal cord was carefully dissected and dislodged from the spinal column. Spinal cord was then homogenized through a 70 um strainer with stock isotonic percoll (G&E health sciences) at gradients of 30% and 70%. After centrifugation, the interphase is carefully removed from between the 30% and 70% stock isotonic percoll and centrifuged a final time, before resuspending the pellet in 1X HBSS

Table 2.9: Reagents for spinal cord isolation digest

.

Component	Concentration	Manufacturer
Percoll	-	G&E Health Sciences
Stock Isotonic Percoll	9:1 (Percoll: 10XHBSS)	-
HBSS without Ca/Mg	10X	Thermo Fisher Scientific

2.9. Transverse Aortic Constriction

Left ventricular (LV) pressure overload was induced via the constriction of the transverse aorta of 8-10 week old male mice. 2.5% Isoflurane carried in 100% oxygen was used to induce anesthesia and to maintain the anesthesia while the mice were on the respirator. The mice were placed in supine position and then the chest cavity was accessed through the intercostal space. TAC was performed between the two common carotid arteries through the ligation of a 7-0 nylon suture material against a 27-gauge needle (80). Sham operated mice underwent the same procedure but without ligation. 1.0 mg/kg buprenorphine sustained release (SR) was administered subcutaneously with a 20-gauge needle using a Hamilton micro syringe as post-operatory analgesia. After 4 weeks of TAC, mice were euthanized and tissue was harvested for further analysis.

2.9.1. Isolation of Left Ventricle

The LV was separated from the RV, after the heart was perfused with 10 mL of PBS. LV's were chopped with razors until they were thoroughly minced and collected in 10 mL digestion buffer containing collagenase type II (0.895mg/mL) and protease XIV (0.5mg/mL). Cell suspensions were incubated at 37ºC in a water bath for 30 minutes with intermittent shaking and triturated with a cannula. The digests were then filtered through a 40 µm cell filter followed by centrifugation at 1500 rpm for 5 minutes. Pellets were then resuspended in 200 µL of FACS buffer (PBS without Ca/Mg with 2% FBS) and then stained for flow cytometry.

Table 2.10: Reagents for LV digestion buffer

Chemical	**MW**	**nmoL/L**	**g/mg for 1L dH_2O**
NaCl	58.44	120	7.0128g
KCl	74.55	5.4	402.57mg
NaH_2PO_4	120	1.2	144mg
$NaHCO_3$	84.01	20	1.6802g
Glucose	180.2	5.6	1.0091 g
Taurine	125.15	5	625.75 mg
$MgCl_2$	95.21	1.6	152.336 mg
2,3- butanodione monoxime	101.1	10	1.011g

2.10. Histology

Samples of TAC and Sham mice were excised and the LV was separated from the right ventricle. The LV was immediately embedded in OCT or Fixed in 10% Formalin, embedded in paraffin, and cryostat cut into 5um LV sections.

2.10.1. Immunohistochemistry

ABC elite peroxidase method was used for immune cell and adhesion molecules staining of OCT embedded frozen LV sections. Samples were thawed, fixed with acetone for 6 minutes and incubated with 10 % goat serum in PBS (corresponding to the species in which the secondary antibody was produced). Avidin and Biotin (Vector SP-2001) mediated blocking was performed by incubating the sections for 10 minutes with each solution. After blocking, samples were incubated with 100µL of primary antibody (1:500

in PBS without Ca/Mg) for 1 hour at RT, followed by a 40 minute incubation at room temperature with the goat-anti-rat biotinylated secondary antibody (1:300 in 6 µL of 2% mouse serum and 300 µL PBS without Ca/Mg per secondary antibody µL). After the antibody incubation, sections were washed with 1% H2O2 in PBS without Ca/Mg for 10 minutes at RT to inactivate endogenous non-specific peroxidase activity of the tissue. After, 30 µL of ABC complexes per section were added and incubated for 40 minutes at RT protected from light (100 µL of PBS without Ca/Mg with 1 µL of solution A and 1 µL of solution B, and allowed to incubate for 30 minutes before use. Vectastain Elite ABC HRP kit PK-6100). After incubation, sections were washed with 0.1M acetate buffer for 4 minutes at RT followed by a 10 minute incubation with AEC buffer (300 mL acetate buffer pH 5.2 + 15 mL AEC stock solution + 150 µL 30% H2O2, filtered through No.1 Whatman Filter paper). Samples were then washed again in 0.1M acetate buffer for 3 minutes, followed by a wash in distilled water. Samples were incubated in filtered Gill's hematoxylin solution for 1 minute. Samples were then washed thoroughly with warm water and covered with glycerin and capped with a glass coverslip.

Table 2.11: 0.1 M acetate buffer (500 mL)

Chemical	**MW**	**Molarity**	**Volume**
$CH_3COONa_3H_2O$	136.08	0.2M	197.5mL
CH_3COOH glacial	60.08	0.2M	52.5 mL
Distilled Water	-	-	250 mL

Table 2.12: 3-Amino-9-ethylcarbazole (AEC) solution (100 mL)

Chemical	MW	Molarity	Volume
3-amino-9-ehtylcarbazole	210.27	0.02M	0.4g
N,N-Dimethylformamide	73.09	-	100

Table 2.13: Immunohistochemistry antibodies

Antibody	Clone	Manufacturer
Anti-mouse CD54	YN1/1.7.4	BioLegend
Anti-mouse CD4	GK1.5	BioLegend
Anti-mouse CD11b	M1/70	BioLegend

2.10.2. Hematoxylin and eosin staining and picrosirius staining

Hematoxylin and Eosin dyes were used for staining the nucleus and cytoplasm of 5um LV sections that were embedded in paraffin. The staining was initiated by heating sections for 20 minutes at 60ºC, followed by washes with xylene, 100% alcohol, 95% alcohol and water. Hematoxylin (Richard-Allan Scientific Signature Series Hematoxylin 7211, Thermo Fisher Scientifc) staining was done for 2 minutes, followed by water washes. 1 minute incubation with Clarifier 2 was done to remove the background staining, bluing to enhance the color of the nuclei after hematoxylin staining and 30 second wash with 95% alcohol. Alcoholic Eosin staining was done for 2 minutes, providing delineation of cytoplasmic components. Several washes of 95% and 100% alcohol, and xylene were done before placing coverslip on section. Cardiomyocyte area was determined in H&E stained LV sections by measuring the area of 10-20 myocytes per mouse using ImageJ and tracing the area around the myocyte. Percent of leukocyte

infiltration was determined using ImageJ and dividing 20X image sections and dividing the section into 30 grids. Grids were counted and the number of grids containing leukocytes infiltrated were considered as positive. (% = positive grids/30 x 100)

For picrosirius red staining, staining was commenced by heating sections of LV's of TAC and Sham mice for 40 minutes at 60C, followed by washes with xylene, 100%, 95% and 85% alcohol. Sections were then incubated in 0.2% phosphomyobdic acid for 5 mins, followed by deionized water rinsing. Picrosirius red staining was done by incubating the sections with 0.1% picrosirius solution (Direct Red 80, Sigma Aldrich 365548) for 60 minutes. After tissues were rinsed with deionized water, air dried and placed in xylene, they were covered with a glass coverslip. Collagen deposition was determined by intensity of staining in 5-7 representative fields per LV using ImageJ

2.11. Cardiac function parameters

2.11.1. Transthoracic echocardiography

Transthoracic echocardiography was performed under light sedation with 1.5% isoflurane administered via nose cone while the core body temperature was maintained at 37C. M Mode and 2-dimensional images were obtained from the short axis view, as described previously (81, 82) . Left Ventricular end-diastolic and end-systolic diameters (EDDs and ESDs) and heart rate were measured by averaging values obtained from 5 cardiac cycles. Fractional shortening was calculated using the following standard equation: % FS = [(EDD-ESD)/EDD] x 100. Investigators were blinded to genotype during data acquisition analysis.

2.12. Statistical Analysis

Data are represented as the mean ± SEM or SD where indicated. Statistical analysis was done by unpaired T Test or non-parametric Mann-Whitney Test where indicated using GraphPad Prism Software. When unpaired T test was used, confirmation was achieved by looking at normal distribution. Differences were considered statistically significant at $p \leq 0.05$ and indicated with ***.**

Chapter 3: Results

Chapter 3.1

3.1. Determine the role and functionality of CD43 mediating Th17 cell interactions with E-selectin and the activated vascular endothelium.

Rationale: Leukocyte recruitment is of essential importance in the inflammatory response. The process by which leukocytes are recruited from the blood stream into tissues during an immune response is known as the leukocyte recruitment cascade, is tightly regulated and consists in sequential steps that slow down circulating cells to facilitate interactions with the vascular endothelium. We can summarize this process into the following sequential steps: 1. Leukocyte rolling and capture; 2. Leukocyte firm arrest; 3. Leukocyte apical migration; and 4. Leukocyte transmigration. As indicated in the introduction of the present thesis dissertation, a number of adhesion molecules are involved in the leukocyte recruitment cascade. This chapter will focus on the first initial rolling interactions, involving endothelial selectins and their selectin ligands expressed in leukocytes. Previous studies have identified E-selectin ligands such as PSGL-1, CD44 and the highly glycosylated form of CD43 in mouse and human neutrophils, and in mouse Th1 cells and human skin T cells (43, 83). In contrast, E- selectin ligands are differentially expressed and function differently in Th2 cells, which, as a result, have a lower extravasation potential to sites of strong immune responses. This chapter focuses on Th17 cells, which are known to be recruited to sites of autoimmune reactions and in response to inflammatory cytokines similarly as Th1 cells, but adhere to E-selectin in higher numbers (47). In this chapter, we characterize the expression and functionality of E-selectin ligands in Th17 cells and identify their relevance during Th17 cell recruitment and inflammation *in vivo*.

3.1.1. Th17 cells express all known E-selectin ligands expressed in CD4+ T cells, with PSGL-1 and CD43 supporting major E-selectin dependent rolling under flow conditions *in vitro*.

We generated Th17 cells *in vitro* from primary CD4+ T cells isolated from C57/BL6 Wild Type (WT) mice. We first examined the expression levels of the three candidate scaffold proteins known to be functional E-selectin ligands expressed on $CD4^+$ T cells, PSGL-1, CD43 and CD44 (15). Using flow cytometry we found that an E-selectin chimeric protein bound to Th17 cells with higher affinity than to Th1 cells, suggesting higher expression of E-selectin ligands in Th17 cells (Fig 3.1A). Th17 cells express all three proteins, PSGL-1, CD43 and CD44. The levels of PSGL-1 and CD44 were expressed similarly in Th17 and Th1 cells (Fig 3.1C-D). However, Th17 cells showed a more robust expression of CD43 and a loss of the typical bimodal expression of highly glycosylated CD43 observed in Th1 cells (Fig 3.1C).

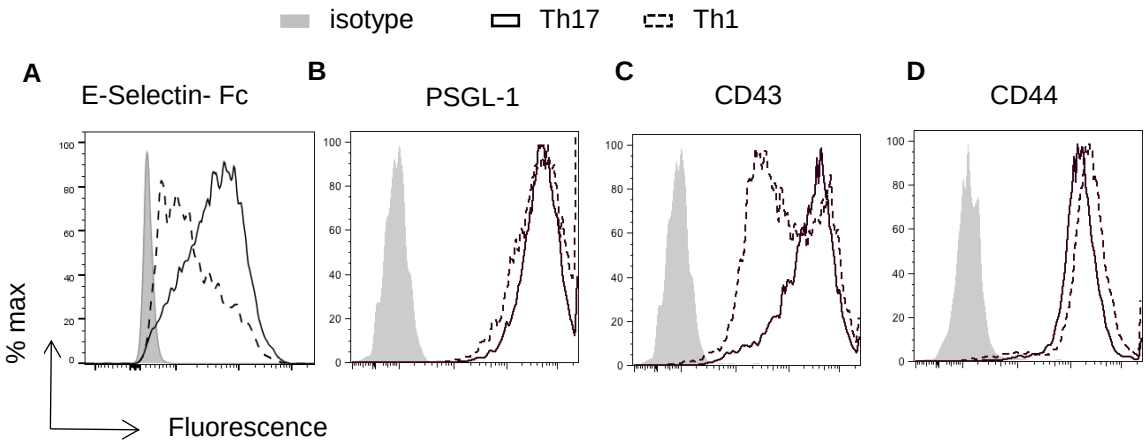

Figure 3.1: Th17 cells express CD43 uniformly and at higher levels than Th1 cells.

WT Th17 and Th1 cells were generated from naïve isolated $CD4^+$ T cells using cytokine cocktails and stained with an E-selectin Chimera **(A)**, PSGL-1 **(B)**, CD43 **(C)** and CD44 **(D)** and assessed by flow cytometry. Data is representative of 3-5

While these studies demonstrated expression of selectin ligands in Th17 cells and differential expression of CD43 between Th17 and Th1 cells, the functionality of the ligands had yet to be addressed. To measure the function of these scaffold proteins in Th17 cells we used blot rolling assays under flow conditions. This assay can detect E-selectin–dependent rolling on CD43, CD44, and PSGL-1 immunoprecipitated from WT *in vitro*–generated Th17 cell lysates and immobilized on Western blots. As expected, PSGL-1 migrated at a band of ~220 kDa, CD43 at a band of ~130 kDa, and CD44 at a band of ~90 kDa (Fig. 3.2A-C). PSGL-1 and CD43 immunoprecipitated from Th17 cells supported significant rolling of CHO cells overexpressing E-selectin (CHO-E cells) (Fig. 3.2D-E). Interestingly CD44, a reported E-selectin ligand for neutrophils and Th1-cells (14, 77, 84), supported very little E-selectin rolling (Fig. 3.2F). To ensure that the rolling of CHO-E cells on the scaffold proteins was E-selectin dependent, we used CHO-MOCK cells and a $Ca2^+$ chelator EDTA since these interactions are calcium dependent. The observed rolling activity was E-selectin specific because the immunoprecipitated proteins did not support rolling of control CHO-MOCK cells under the same conditions, and the CHO-E rolling activity was abolished in the presence of EDTA (Fig 3.2D-F). These data indicate that Th17 cells express all E-selectin ligands, with the highly glycosylated form of CD43 being expressed more robustly and uniformly than in Th1 cells, and that PSGL-1 and CD43 support major E-selectin mediated rolling *in vitro*.

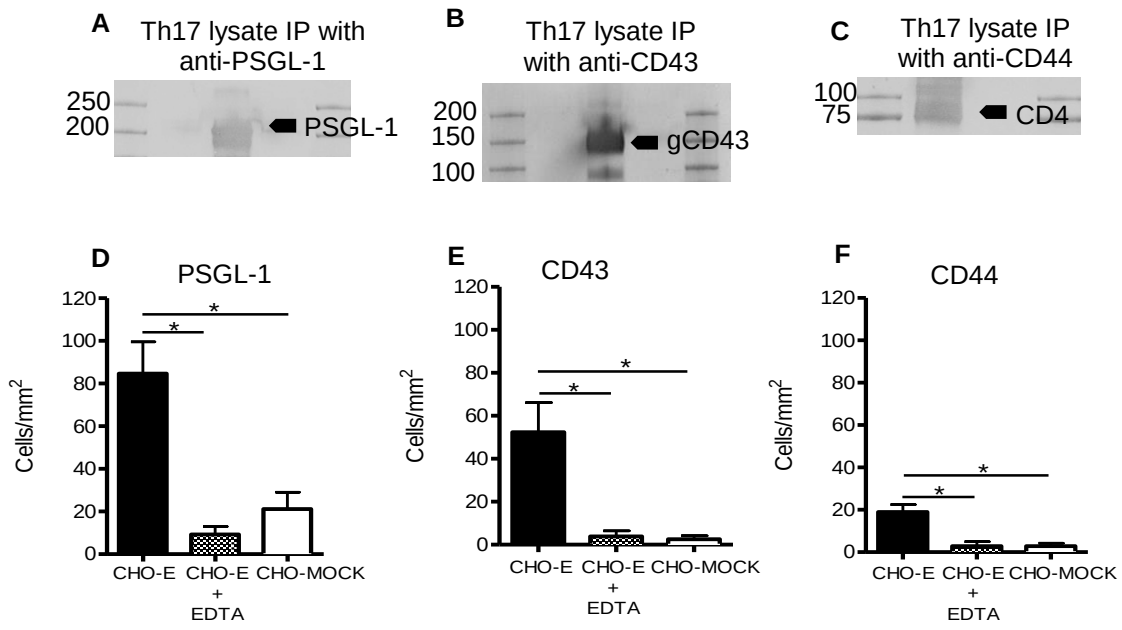

Figure 3.2: Immunoprecipitated PSGL-1 and CD43 from Th17 cells support E-selectin dependent rolling under flow conditions *in vitro*.

Aliquots of lysate from Th17 cells were immunoprecipitated with the indicated Abs using A/G Plus-agarose beads. Immunocomplexes were subjected to SDS-PAGE and Western blotting for the indicated Abs under standard non-reduced conditions. Molecular mass markers are included in the flanking lanes of the blot. A representative Western blot is shown for each ligand PSGL-1 **(A)**. CD43 **(B)** and CD44 **(C)**. CHO-MOCK and CHO-E cells were drawn in the flow chamber at a shear stress of 0.6 dyne/cm^2 in the presence or absence of EDTA across Th17 cells PSGL-1 **(D)**, CD43 **(E)**, and CD44 **(F).** Data show the mean 6 SD values. *p, 0.05.

These results, led us to hypothesize that CD43 may function differently in Th17 cells as compared to Th1 cells. To address this hypothesis, we generated a CD43$^{-/-}$ colony, by backcrossing PSGL1/CD43 double deficient mice in the C57/BL 6 background, to WT C57/BL6 mice for at least 6 generations (Fig 3.3A-B).

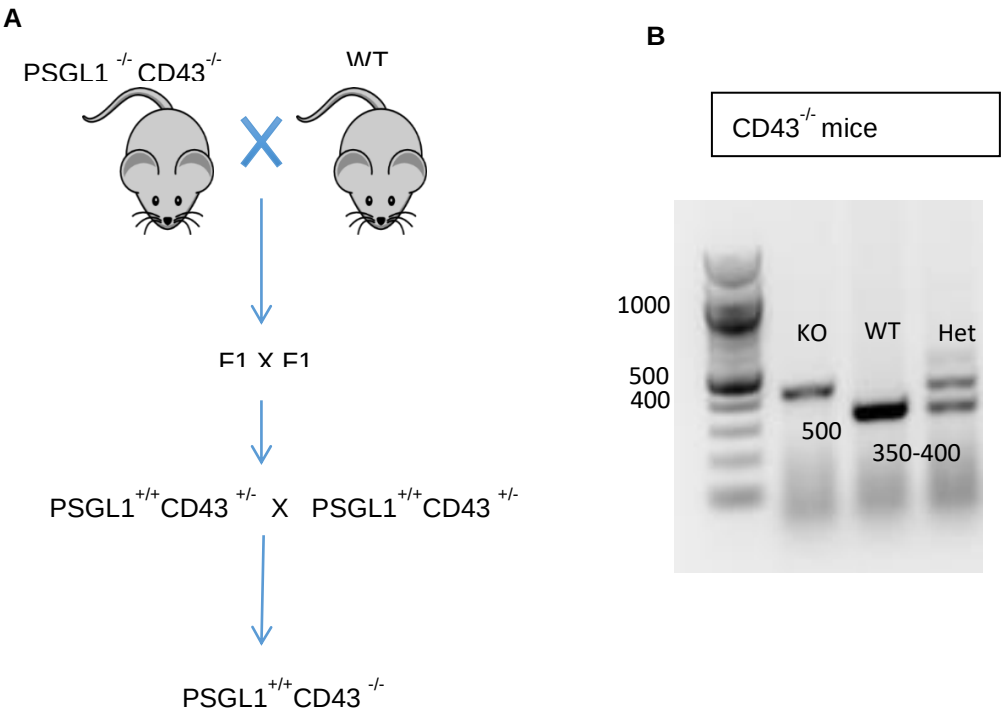

Figure 3.3: Generation of CD43$^{-/-}$ mice.

A. PSGL1$^{-/-}$CD43$^{-/-}$ double knock out mice were bred with WT C57/BL6 mice. Resulting heterozygous mice were further crossed with one another until we acquired PSGL-1$^{+/+}$CD43$^{-/-}$ mice (CD43$^{-/-}$ mice). These mice were used or back crossed again with WT C57/BL6 to generate WT and CD43$^{-/-}$ litter mate mice. **B.** Agarose gel demonstrating genotyping for CD43 knock out, WT and Heterogeneous bands.

3.1.2. Absence of PSGL-1, CD43, or both molecules results in severe impairment of Th17 cell adhesion to E-selectin under flow conditions *in vitro*.

To determine how each selectin ligand contributes to Th17 cell adhesion to E-selectin, we generated Th17 cells from isolated CD4$^+$ T cells from different E-selectin ligand deficient mice. CD4$^+$ cells isolated from each selectin ligand knock out under study differentiated similarly into Th17 cells as CD4$^+$ cells isolated from WT mice, indicating that the lack of these molecules does not result in impaired Th17 cell differentiation *in vitro* (Fig 3.4). Additionally, we generated mice that lacked all E-selectin ligands by crossing PSGL1$^{-/-}$

CD43$^{-/-}$ with CD44$^{-/-}$ knock out mice (TKO) as a control and for future studies on novel glycoproteins (section 3.1.4 of this thesis).

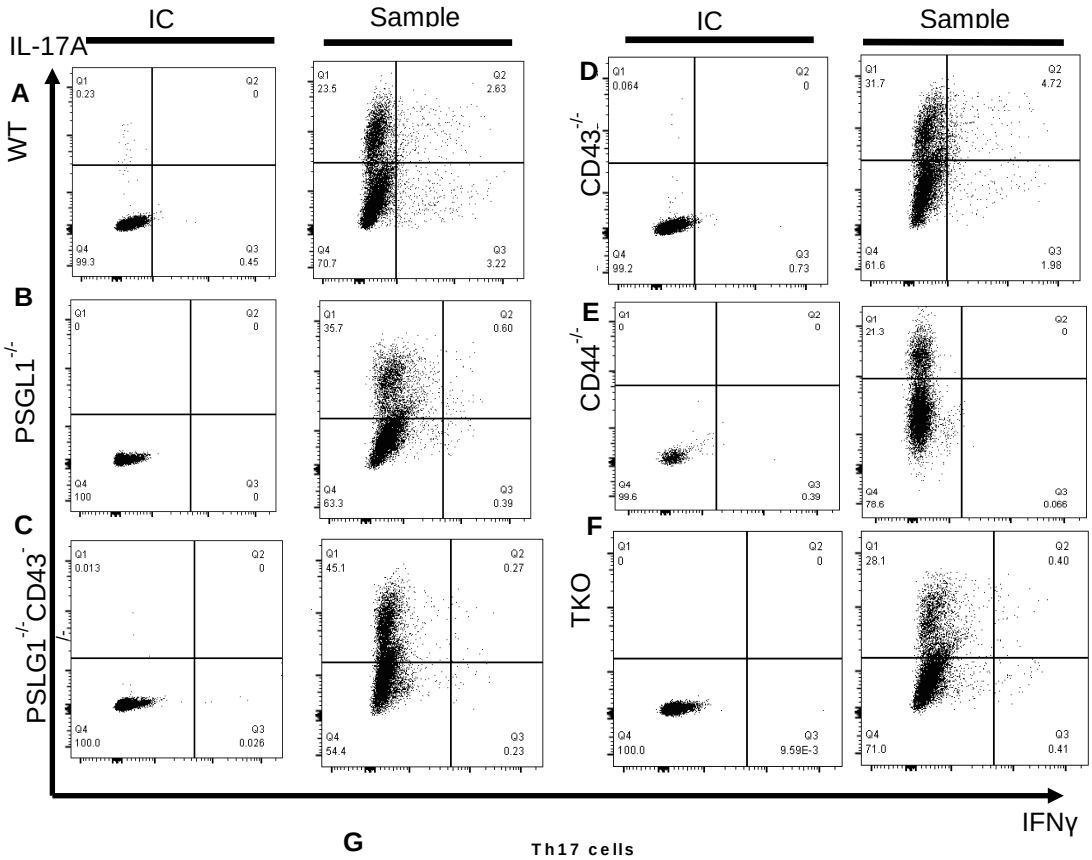

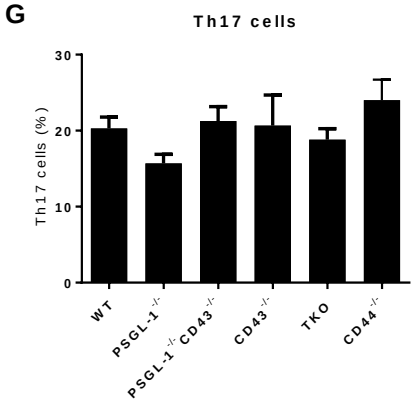

Figure 3.4: Th17 differentiation in the indicated candidate scaffold molecules deficient mice.

Naïve $CD4^+$ T cells from WT **(A)**, PSGL-1 **(B)**, PSGL-$1^{-/-}$$CD43^{-/-}$ DKO (**C**), $CD43^{-/-}$ (**D**) $CD44^{-/-}$ **(E)** and TKO (**F**) mice were polarized to Th17 cells as described in methods and assessed by flow cytometry for IL17-A staining. Quantification of the percentages of $IL17A^+$ cells among the different preparations for the indicated mice. A representative FACS plot is shown from 3-6 independent experiments quantified in **G.**

We next evaluated the ability of Th17 cells generated *in vitro* from WT or PSGL-$1^{-/-}$ mice to accumulate on E-selectin under flow conditions. Because both CD43 and CD44 have been reported to function as E-selectin ligands on Th1 cells only in cooperation with PSGL-1 (50, 51, 77), we also evaluated the ability of Th17 cells generated from PSGL-$1^{-/-}$$CD44^{-/-}$ and PSGL-$1^{-/-}$$CD43^{-/-}$ DKO mice to accumulate on E-selectin. This methodology allowed us to determine if CD43 and CD44 contributed to the adhesion of E-selectin in the absence of PSGL-1 or if both molecules were required for adhesion to E-selectin. Removal of PSGL-1 alone resulted in a 42% decrease in Th17 cell accumulation on E-selectin as compared with WT Th17 cells.

The removal of CD43 in combination with PSGL-1 in the DKO PSGL-$1^{-/-}$$CD43^{-/-}$ Th17 cells, resulted in significantly reduced E-selectin interactions as compared with both WT and single PSGL-$1^{-/-}$ mice (66% reduction PSGL-$1^{-/-}$$CD43^{-/-}$ versus WT, and 41.5% reduction on PSGL-$1^{-/-}$$CD43^{-/-}$ versus PSGL-$1^{-/-}$). This additional drop in level of adhesion in the Th17 cells indicates that CD43 does indeed contribute to E-selectin adhesion in Th17 cells. In contrast, Th17 cells lacking CD44 and PSGL-1 (PSGL-$1^{-/-}$$CD44^{-/-}$) showed no further significant decrease in binding to E-selectin compared with PSGL-$1^{-/-}$, suggesting that the reduction in E-selectin binding compared with WT cells was attributable to the absence of PSGL-1 (Fig. 3.5A). Our findings so far indicated a unique expression of CD43 in Th17 cells versus Th1 cells (Fig. 3.1), functionality of CD43 isolated from Th17 cells in mediating E-selectin–dependent rolling (Fig. 3.2), and decreased

adhesion of PSGL-1$^{-/-}$CD43$^{-/-}$ versus PSGL-1$^{-/-}$ Th17 cells to E-selectin under flow conditions. Therefore, we hypothesized that CD43 functions as an E-selectin ligand for Th17 cells that is sufficient to mediate E-selectin adhesion and does not require cooperation with PSGL-1. Interestingly, CD43$^{-/-}$ Th17 cells showed significant impairment in binding to E-selectin (63.4% reduction versus WT), similar to PSGL-1$^{-/-}$CD43$^{-/-}$ DKO Th17 cells, and further decreased as compared with PSGL-1$^{-/-}$ Th17 cells (Fig. 3.5A). Indicating to us that CD43 by itself is an essential E-selectin ligand without the cooperation of PSGL-1. Additionally we perfused the same E-selectin ligand deficient T cells over P-selectin, and observed that lack of PSGL1 or both molecules in the DKO mice abrogated interactions with P-selectin (Fig 3.5B).

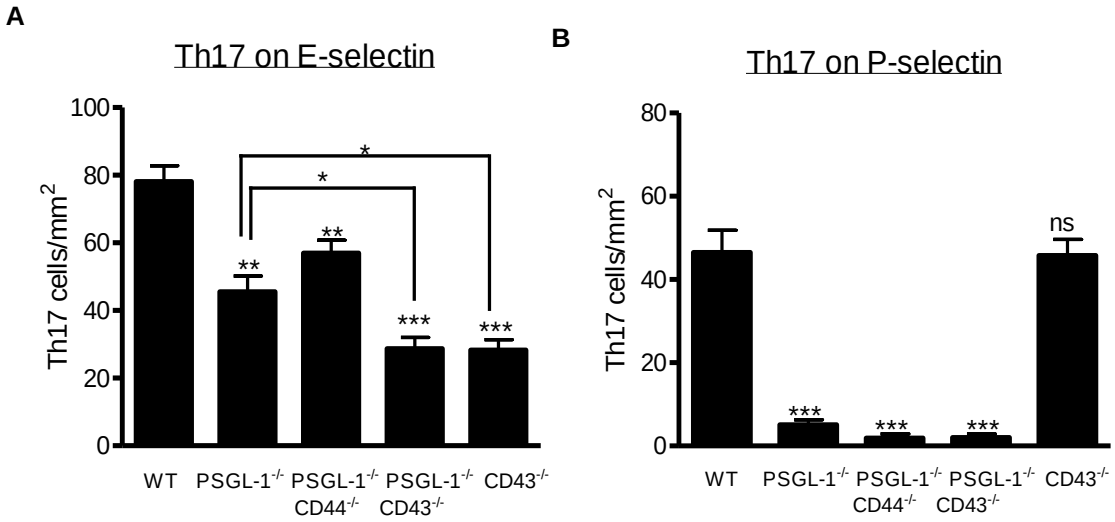

Figure 3.5: Absence of CD43 in Th17 cells impairs adhesion to E-selectin.

Th17 cells from WT or E-selectin ligand deficient mice were perfused at (1 x 10^6 cells/ml) over E-Selectin **(A)** and P-Selectin **(B)** at 1 dyne/cm^2. CD43 and PSGL-1, but not CD44, function as Th17 cell E-selectin ligands under shear flow conditions in vitro. N = 8 independent WT Th17 cell preparations, N = 5 independent cell preparations for PSGL1$^{-/-}$, CD43$^{-/-}$ DKO and PSGL1$^{-/-}$CD44$^{-/-}$, DKO mice; N = 4 independent cell preparations for CD43 mice. Data show the mean 6 SD values. *p, 0.05.

To determine if this was a specific subset event between Th1 and Th17 cells, we used Th1 cells from all E-selectin ligand deficient mice. We observed a similar effect in decrease of adhesion to E-selectin of PSGL-1 and PSGL-1$^{-/-}$CD43$^{-/-}$ DKO Th1 cells and no difference in adhesion of single CD43$^{-/-}$ Th1 cells adhered to E-selectin as compared to WT cells, as we and others have previously described (51) (Fig 3.6A-B). The absence of CD44 alone did not impact the adhesion of either Th17 cells or Th1 cells to E-selectin under the same conditions (Fig 3.7) nor did it impact their differentiation *in vitro* (Fig 4).

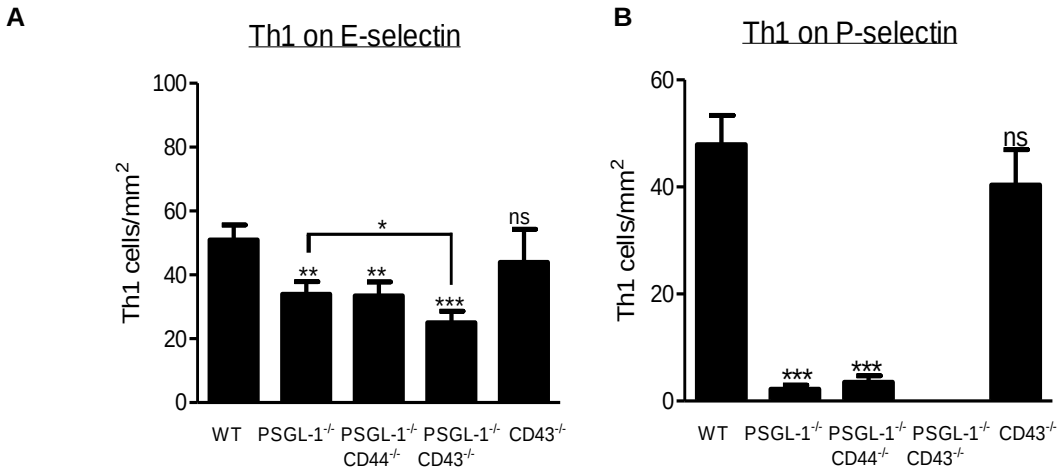

Figure 3.6: CD43 by itself does not impact Th1 cell adhesion to E-selectin.

Th1 cells from WT or E-selectin ligand deficient mice were perfused at (1 x 10^6 cells/ml) over E-Selectin **(A)** and P-Selectin **(B)** at 1 dyne/cm^2. CD43 by itself did not impact adhesion to E-Selectin. N = 8 independent WT Th17 cell preparations, n = 5 independent cell preparations for PSGL1$^{-/-}$, CD43$^{-/-}$ DKO and PSGL1$^{-/-}$CD44$^{-/-}$, DKO mice; N= 4 independent cell preparations for CD43$^{-/-}$ mice. Data show the mean 6 SD values. *p, 0.05.

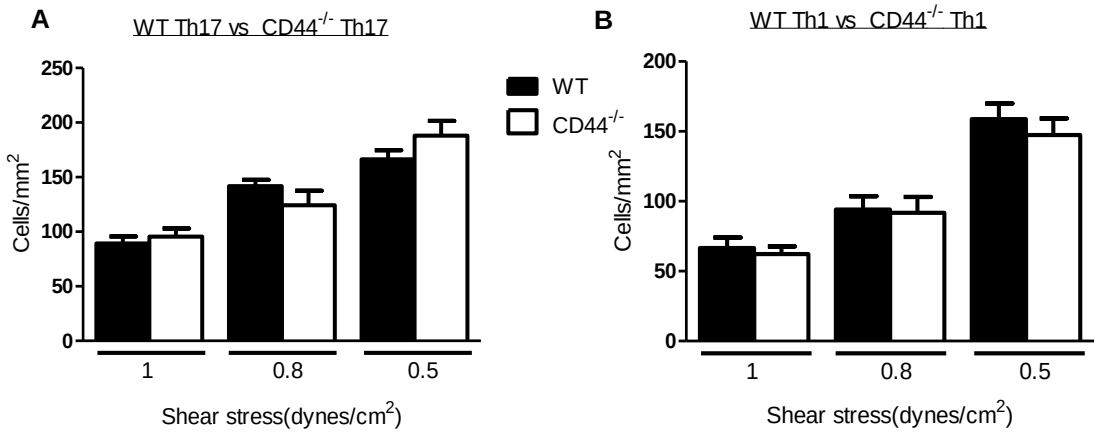

Figure 3.7: CD44 does not play a role in Th17 cells adhesion to E-selectin.

Naïve $CD4^+$ T cells from WT and $CD44^{-/-}$ mice were polarized to Th17 **(A)** and Th1 cells **(B)** and perfused over E-selectin coated coverslips at the indicated shear stress. $CD44^{-/-}$ and WT naïve T cells adhere to E-Selectin similarly. Representative FACS plots and quantification **(C-D).** Data shown from 3 individual T cell preparation per cell subset.

Taken together, our results indicate that CD43 functions as a major ligand for E-selectin on Th17 cells but not on Th1 cells under shear flow conditions *in vitro*.

3.1.3. CD43 glycosylation and expression contribute to differences in adhesion of Th17 and Th1 cells to E-selectin.

Our data indicated that Th17 cells expressed a unique uniform and more robust expression of the highly glycosylated form of CD43 in Th17 cells as compared to the bimodal expression observed in Th1 cells (Fig 3.1). Additionally $CD43^{-/-}$ Th17 cells had severely impaired adhesion to E-selectin as compared to $CD43^{-/-}$ Th1 cells. We then sought to test if the Th1 cells that highly expressed glycosylated CD43 were not being masked in their adhesion to E-selectin by the Th1 cells expressing lower levels of CD43, and if these two subpopulations functioned mechanistically different. Th17 and Th1 cells were sorted based on the levels of expression of CD43 on Th17 cells (uniformly expressing high levels of CD43), Th1 cells expressing intermediate levels of CD43

(CD43M), and Th1 cells expressing high levels of CD43 (CD43H) (Fig. 3.8A-B). Sorted cells were perfused into the flow chamber to evaluate their adhesion to E-selectin. CD43M Th1 cells showed significantly decreased adhesion to E-selectin as compared with Th17 cells, indicating that the difference in expression of CD43 and its glycosylation contribute to decreased adhesion to E-selectin. Moreover, CD43H Th1 cells also had impaired adhesion to E-selectin as compared with Th17 cells, suggesting that CD43 can also function differently in both cell subsets (Fig 3.8C). Some Th17 and Th1 cells were perfused into the flow chamber before being sorted based on the expression of CD43 to control that the sorting process was not altering the ability of Th17 and Th1 cells to adhere to E-selectin. We observed that 91 ± 7 Th17 cells/mm^2 adhered to E-selectin under flow conditions, whereas 80 ± 4 Th17 cells/mm^2 adhered after sorting. For Th1 cells we observed that 50 ± 6 cells/mm^2 (including a mixed population of CD43H and CD43M before sorting) adhered to E-selectin, whereas 25 ± 2.8 CD43H cells/mm^2 and 19 ± 2.3 CD43M cells/mm^2 did so after sorting. These data additionally indicate that sorting of Th1 and Th17 cells does not impair cell adhesion to E-selectin under physiological flow conditions.

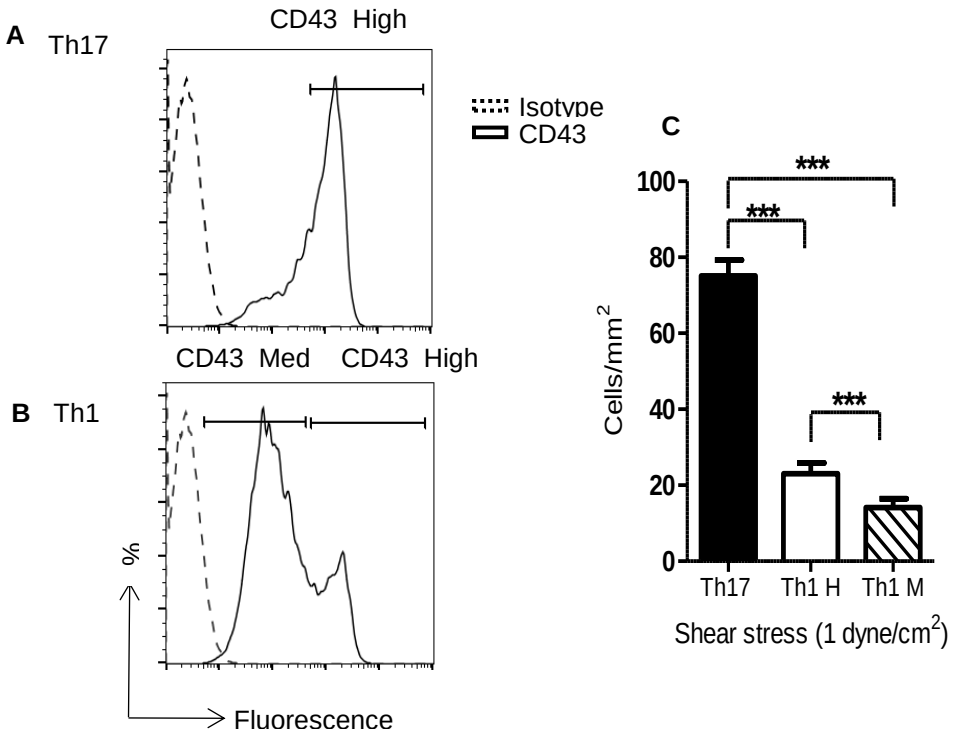

Figure 3.8: Th1 cells expressing similar highly glycosylated levels of CD43 as Th17 cells adhere significantly less than Th17 cells.

(A) Th17 and **(B)** Th1 cells were sorted based on the level of CD43 expression in three groups: CD43high for Th17 cells, and CD43int (CD43M) or CD43high (CD43H) for Th1 cells. **(C)** Th17 cells, Th1 CD43M, and Th1 CD43H were perfused at a shear stress of 1 dyne/cm^2 over E-selectin–coated coverslips. N = 3 independent experiments with three different T cell subset preparations. Data show the mean 6 SD values. *p, 0.05, **p, 0.01, ***p, 0.001 as compared with WT or as indicated.

3.1.4. Screening of alternative novel functional glycoprotein E-selectin ligands on Th17 cells.

Our results demonstrate that depletion of PSGL-1 or CD43 results in severe impairment in Th17 cell adhesion to E-selectin. However, the lack of both ligands (PSGL-1$^{-/-}$CD43$^{-/-}$) did not completely abolish Th17 cell adhesion to E-selectin. Additionally, CD44 supported low levels of E-selectin–dependent rolling, but it did not mediate Th17 cell adhesion to E-selectin in our assays on immobilized E-selectin. To evaluate the possibility that Th17 cells

express novel functional E-selectin ligands besides CD43 and PSGL-1, we generated Th17 cells *in vitro* from WT and PSGL1$^{-/-}$CD43$^{-/-}$CD44$^{-/-}$ (TKO) mice and performed adhesion assays on immobilized E-selectin under flow conditions. Th17 cells from WT and TKO mice, differentiated similarly (Fig. 3.4E). To our surprise, Th17 cells generated from TKO mice showed residual interactions with E-selectin, and these were abolished in the presence of an anti–E-selectin function–blocking Ab, but not in the presence of an IgG control Ab, demonstrating that these residual interactions are E-selectin–dependent (Fig. 3.9A). These data suggested the existence of potential novel functional E-selectin ligands to be identified in Th17 cells. Because E-selectin ligands are generally proteins that require post-translational glycosylation to be functional, we next evaluated whether the residual E-selectin binding activity observed in TKO Th17 cells (Fig. 3.9A) was mediated by a glycoprotein by treating TKO cells with the cysteine protease bromelain (85).

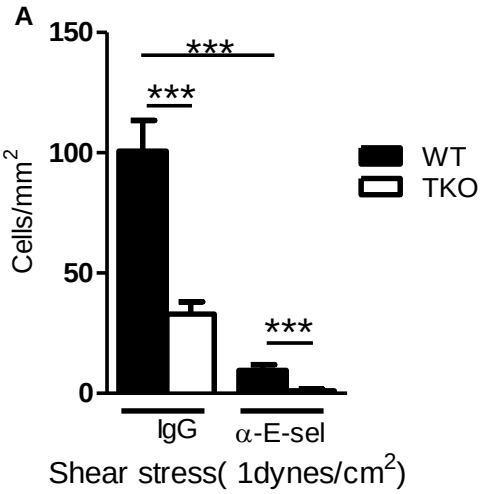

Figure 3.9: Th17 cells lacking E-selectin ligands have residual interactions with E-selectin.

(A) Th17 cells generated from WT and PSGL-1$^{-/-}$CD44$^{-/-}$CD43$^{-/-}$TKO were perfused at 1 dyne/cm^2 over glass coverslips coated with recombinant E-selectin. Coverslips were treated with anti–E-selectin Ab (clone 9A9) or rat IgG isotype control (20 mg/ml) for 20 min prior to the perfusion of the cells. Data show the mean 6 SD values. *p, 0.05, **p, 0.01, ***p, 0.001 as compared with WT or as indicated.

Treatment of WT Th17 cells with bromelain resulted in complete cleavage of PSGL-1, CD43, and CD44 from the cell surface and of other Th17 cell surface proteins that are not E-selectin ligands, such as CD4, also completely removed from the cell surface (Fig. 3.10A). As expected, bromelain treatment of WT Th17 cells resulted in abrogated adhesion to E-selectin, even when double amounts of Th17 cells ($2x10^6$ cells/ml) were perfused. In contrast, bromelain treatment of TKO Th17 cells did not result in further abrogation of Th17 cell adhesion to E-selectin, with the number of Th17 cells that accumulated on E-selectin being similar between vehicle- and bromelain-treated TKO Th17 cells (Fig. 3.10B). Because TKO mice lack PSGL-1, CD43, and CD44, and bromelain cleaves additional surface proteins in TKO Th17 cells, these results suggest that the observed remaining Th17 cell adhesion to E-selectin is not mediated by glycoproteins and may likely be due to glycolipids acting as E-selectin ligands, as it has previously been postulated for human T cells (86).

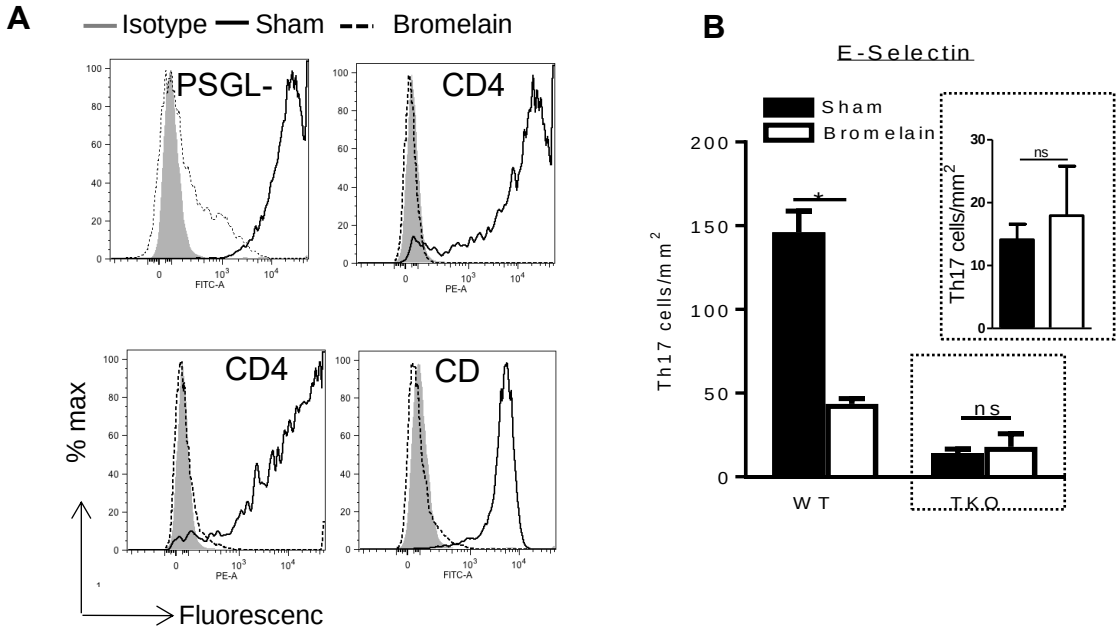

Figure 3.10: Residual adhesion of E-selectin ligand deficient Th17 cells is not dependent on glycoproteins.

(A) WT Th17 cells were treated with the protease bromelain (1 U/ml) 30 min at 37˚C, fixed, stained for the indicated markers, and analyzed by flow cytometry. Histograms from one representative experiment are shown from three separate experiments performed. **(C)** WT and TKO Th17 cells were treated with bromelain as in **(B)** and 2 x10^6 cells/ml were perfused at 1 dyne/cm^2 over glass coverslips coated with recombinant E-selectinTh17 cells generated from WT and PSGL-$1^{-/-}$$CD44^{-/-}$$CD43^{-/-}$ TKO were perfused at 1 dyne/cm^2 over glass coverslips coated with recombinant E-selectin. Coverslips were treated with anti–E-selectin Ab (clone 9A9) or rat IgG isotype control (20 mg/ml) for 20 min prior to the perfusion of the cells. Data show the mean 6 SD values. *p, 0.05, **p, 0.01, ***p, 0.001 as compared with WT or as indicated.

To confirm this observation, we prepared lysates of WT and TKO Th17 cells and performed blot rolling assays to screen for potential glycoproteins that support Th17 cell E-selectin rolling. As expected, CHO-E cells, but not CHO-MOCK cells, rolled on the regions corresponding to PSGL-1 (220 kDa) and to CD43 (130 kDa) in WT Th17 cell lysates (Fig. 3.11). In contrast and consistent with our prediction, we did not observe any E-selectin–dependent cell rolling activity in lysates of TKO Th17 cells (Fig. 3.11). Taken together, these data support the idea that Th17 cells most likely do not express alternative glycoproteins to PSGL-1 and CD43 as E-selectin ligands. The residual adhesion to E-selectin observed in TKO Th17 cells is most likely due to glycolipids, which run with the dye front in an SDS-PAGE gel and cannot be detected by blot rolling assays.

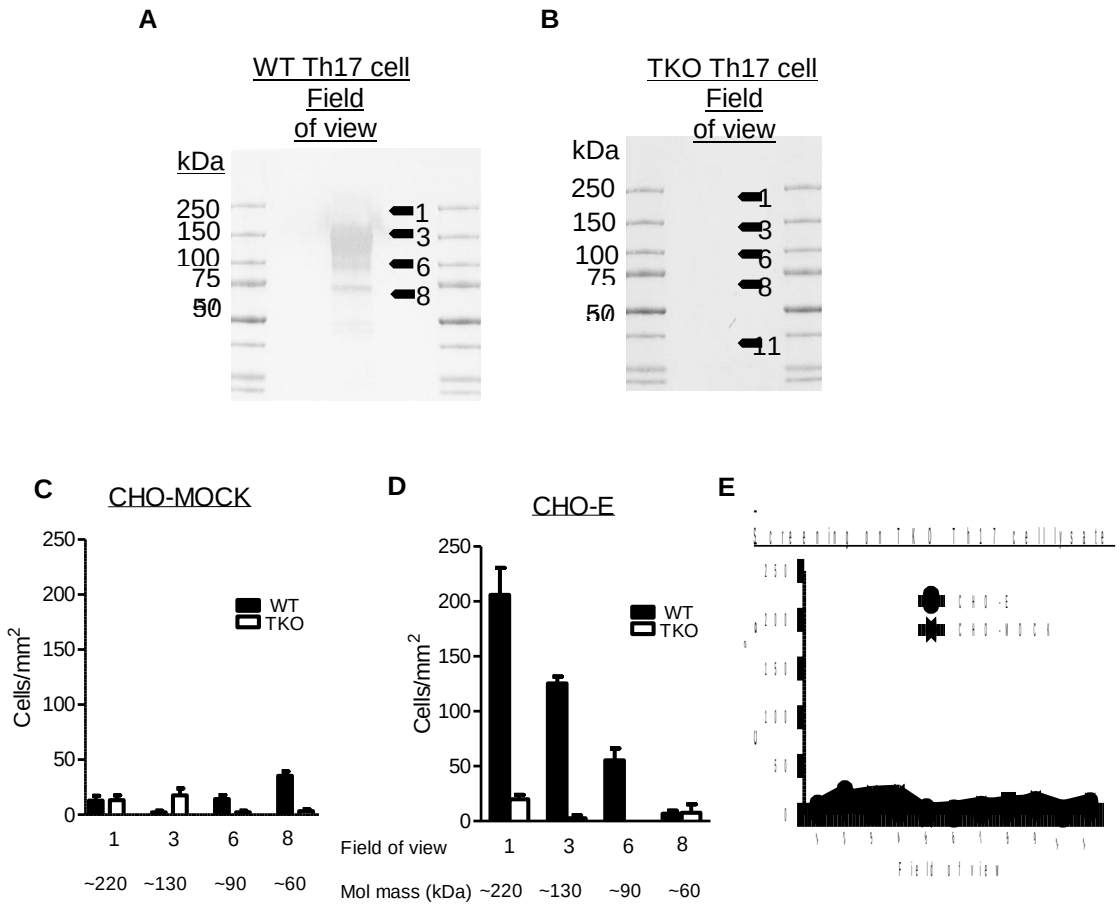

Figure 3.11: Proteins immunoprecipitated from Th17 cells lacking CD43, PSGL-1 and CD44 do not support E-selectin dependent rolling under flow conditions.

(A-E) WT **(A)** or TKO **(B)** Th17 cell lysates (50 mg) were separated by molecular mass under non-reducing conditions and immobilized on Western blots. The blot was assayed for functional E-selectin ligand activity by blot rolling analysis perfusing CHO-MOCK **(C and E)** or CHO-E **(D and E)** cells at the necessary shear of 0.6 dyne/cm^2 to avoid the turbulence created by the membrane surface at higher shears. Data show the mean 6 SD values from three independent experiments, in which 6–10 fields were recorded at each indicated molecular mass. Data show the mean 6 SD values. *p, 0.05, **p, 0.01, ***p, 0.001 as compared with WT or as indicated.

3.1.5. CD43 mediates Th17 cell recruitment into the air pouch in response to CCL20 and TNF-α *in vivo*.

Our data demonstrates that both CD43 and PSGL-1 isolated from Th17 cells mediate functional E-selectin rolling, but only on Th17 cells did CD43 function as a major E-selectin–dependent adhesion molecule in contrast to PSGL-1, which functioned as an E-selectin ligand, and also as a P-selectin ligand on both Th17 and Th1 cells (Fig. 3.5). To determine the role of CD43 as an essential recruitment molecule on Th17 cells *in vivo* we used the air pouch model of leukocyte recruitment. We created a dermal air pouch model in WT and $CD43^{-/-}$ mice. This model allows us to create a small compartment to which cells are recruited using a chemokine or a pro-inflammatory cytokine of preference. We injected CCL20 as an inflammatory stimulus that triggers $CCR6^{+}$ cells, the receptor for CCL20, which efficiently recruits Th17 cells *in vitro* and *in vivo*. Blood leukocyte counts were normal in $CD43^{-/-}$ mice as previously described (17). We found that CCL20 recruited leukocytes in WT and $CD43^{-/-}$ mice as compared with PBS control (Fig. 3.12A). The recruitment of $CD4^{+}$ T cells into the air pouch was significantly impaired in $CD43^{-/-}$ mice versus WT mice, suggesting that CD43 mediates recruitment of $CD4^{+}$ T cells *in vivo* (Fig. 3.12B-C).

Because CCL20 injection into the air pouch results in robust recruitment of Th17 cells but not Th1 cells, as previously described (47), we investigated the presence of Th17 cells within the $CD4^{+}$ population and whether their recruitment was dependent on CD43. As expected, injection of CCL20 into the WT air pouch resulted in enhanced Th17 cell recruitment as compared with PBS (Fig 3.13A-B). In contrast, CCL20 did not induce Th17 cell recruitment in $CD43^{-/-}$ mice, and the frequency and number of Th17 cells recovered in $CD43^{-/-}$ mice were severely impaired versus WT mice (Fig. 3.13C).

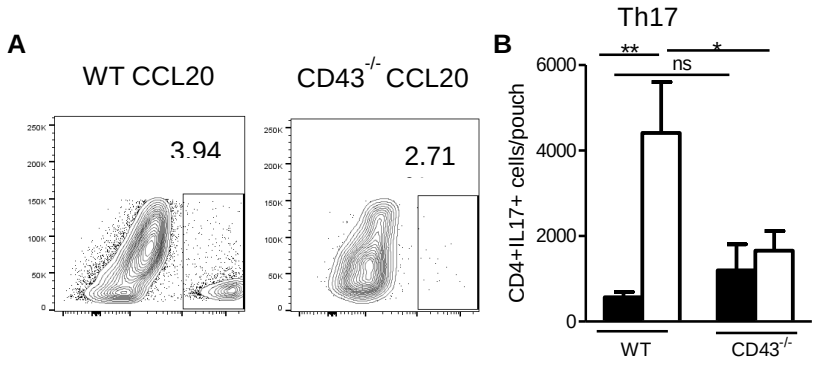

Figure 3.12: CD43$^{-/-}$ mice have impaired Th17 cell recruitment into the Air Pouch in response to CCL20.

The indicated mice (five per group in three independent experiments) received PBS or 400 ng CCL20 (four to seven mice per group in three independent experiments) into the air pouch, and recruited cells were harvested 24 h post-injection and analyzed by flow cytometry **(A)** and cell counting **(B)**. Representative dot plots indicate IL-17A staining in WT or CD43$^{-/-}$ **(A)** air pouches. *p, 0.05, **p, 0.01.

To determine if CD43 mediated Th17 cell recruitment *in vivo* under a more robust general pro-inflammatory response we injected WT and CD43$^{-/-}$ mice with TNF-α. This results in recruitment of mainly Gr1^{+} neutrophils as well as both Th17 cells and Th1 cell subsets (47, 87). TNF-α injection into the air pouch resulted in increased leukocyte recruitment as compared with PBS in both WT and CD43$^{-/-}$ mice (Fig. 3.13A); however, CD43$^{-/-}$ mice showed significantly reduced recruitment of total CD4^{+} T cells as compared with WT mice (Fig 3.13B-C).

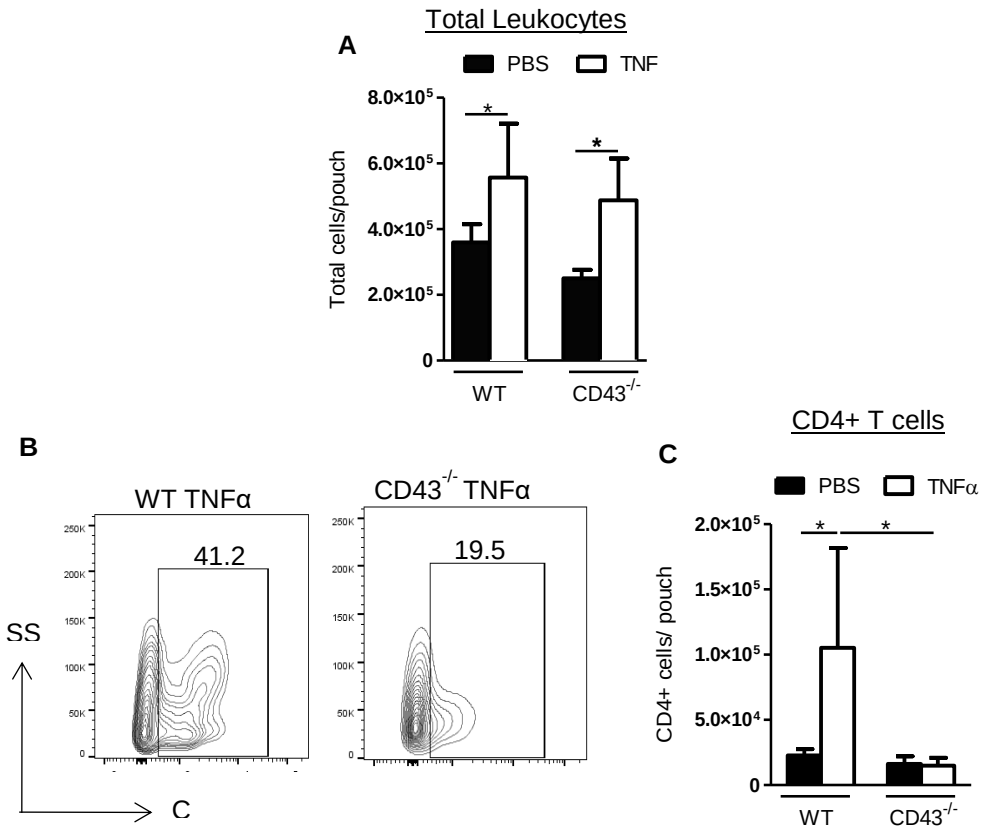

Figure 3.13: CD43$^{-/-}$ mice have impaired CD4 cell recruitment into the Air Pouch in response to TNF-α.

The indicated mice (five per group in three independent experiments) received PBS or 500 ng TNF-α (four to seven mice per group in three independent experiments) into the air pouch, and recruited cells were harvested 24 h post-injection and analyzed by cell counting **(A and C)** and flow cytometry. Representative dot plots indicate CD4 staining in WT or CD43$^{-/-}$ **(B)** air pouches. *p, 0.05, **p, 0.01.

From those CD4^{+} T cells that were recovered in the CD43$^{-/-}$ air pouch, only Th1 cells were identified in the air pouch (Fig. 13.4A-B), with Th17 cell recruitment being significantly impaired. Both Th1 and Th17 cells were identified in the lavage from WT mice (Fig. 3.14C-D).

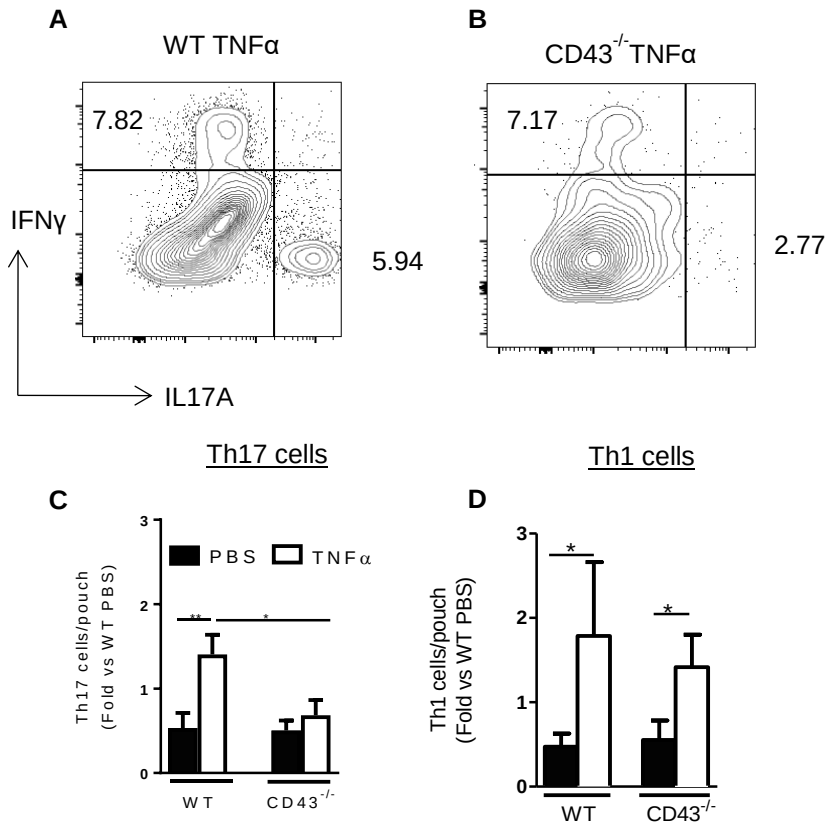

Figure 3.14: CD43$^{-/-}$ mice have impaired CD4 cell recruitment into the Air Pouch in response to TNF-α.

The indicated mice (five per group in three independent experiments) received PBS or 500 ng TNF- α (four to seven mice per group in three independent experiments) into the air pouch, and recruited cells were harvested 24 h post-injection and analyzed by flow cytometry **(A-B)** and cell counting **(C-D).** Representative dot plots indicate IL-17A and IFNγ staining in WT **(A)** or CD43$^{-/-}$ **(B)** air pouches. *p, 0.05, **p, 0.01.

In conclusion, our data demonstrate that CD43 plays an essential role in Th17 cell recruitment in response to CCL20 and TNF-α–induced inflammation in the air pouch *in vivo*

3.1.6. CD43 regulates specific Th17 cells rolling on the cremaster microvasculature *in vivo.*

Our air pouch data indicates that CD43 is a regulator of Th17 cell recruitment *in vivo*; however, the observed defect cannot exclusively be attributed to CD43 regulating Th17 cell rolling interactions with E-selectin given the broad expression of CD43 in hematopoietic cells and its role in T cell function, signaling, and neutrophil emigration(16, 18). We therefore sought to evaluate directly the interactions of Th17 cells from WT and $CD43^{-/-}$ mice with the activated vascular endothelium using confocal intravital microscopy.

When the mouse cremaster muscle is exposed to the mild trauma induced by surgical tissue preparation, leukocytes undergo rolling interactions on the vessel wall that are mediated by P-selectin and L-selectin (88). Pre-exposure of the cremaster muscle to TNF-α for 2 hours additionally induces local E-selectin expression and further elevates leukocyte adhesion (13, 47, 88). This is an ideal model to study whether CD43 mediates Th17 cell rolling interactions with the vascular endothelium *in vivo* in an E-selectin–dependent manner and allows us to view competitive rolling interactions between WT and $CD43^{-/-}$ Th17 cells on the same microvasculature. WT and $CD43^{-/-}$ Th17 cells were similarly differentiated *in vitro* for every independent experiment and expressed IL-17A and *Rorc* (RORɣT), but not *Tbx21* (T-bet) (Fig. 3.15).

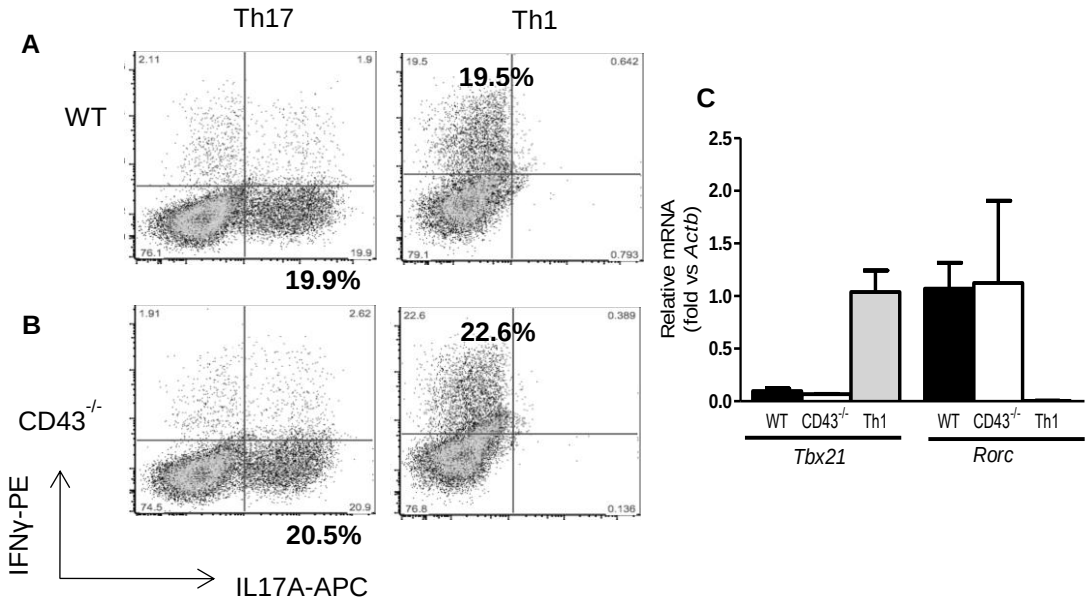

Figure 3.15: Th17 and Th1 cell differentiation from WT and CD43$^{-/-}$ mice used in competitive rolling intravital microscopy studies.

A. WT and **B.** CD43$^{-/-}$ Th17 and Th1 cells were generated using cytokine cocktails for Th17 or Th1 cells as described in methods. FACS plots are representative of 3 separate experiments. **C**. Quality of T cell preparations was also verified by qPCR. qPCR data is representative of 3-5 independent experiments. Th1 cells were used as control.

We counted and resuspended WT and CD43$^{-/-}$ Th17 cells in equal numbers before labeling with different fluorescent dyes. Cells were then mixed in a 1:1 ratio, and injected via the femoral artery after exteriorization of the TNF-α–stimulated cremaster muscle, thus enabling comparison of WT and CD43$^{-/-}$ Th17 cell interactions in the same vessels by competitive rolling analysis. WT Th17 cells interacted with a significantly higher frequency compared with CD43$^{-/-}$ Th17 cells (5.95 ± 1.03 rollers/min WT, 2.68 ± 0.42 rollers/min CD43$^{-/-}$) (Fig. 3.16A-B). In contrast, this effect was not observed in similar studies comparing WT and CD43$^{-/-}$ Th1 cells (1.79 ± 0.26 rollers/min WT, 2.95 ± 0.38 rollers/min CD43$^{-/-}$) (Fig. 3.16C) or CD43$^{-/-}$ Th1 cells (3.22 ± 0.31 rollers/min) versus CD43$^{-/-}$ Th17 cells (2.68 ± 0.42 rollers/min) (Fig. 3.16D). Additionally the rolling ratio between WT and

CD43$^{-/-}$ Th17 cells was significantly higher than the rolling ratio between WT and CD43$^{-/-}$ Th1 cells and between CD43$^{-/-}$ Th17 and CD43$^{-/-}$ Th1, which both remained close to 1 (Fig. 3.16E).

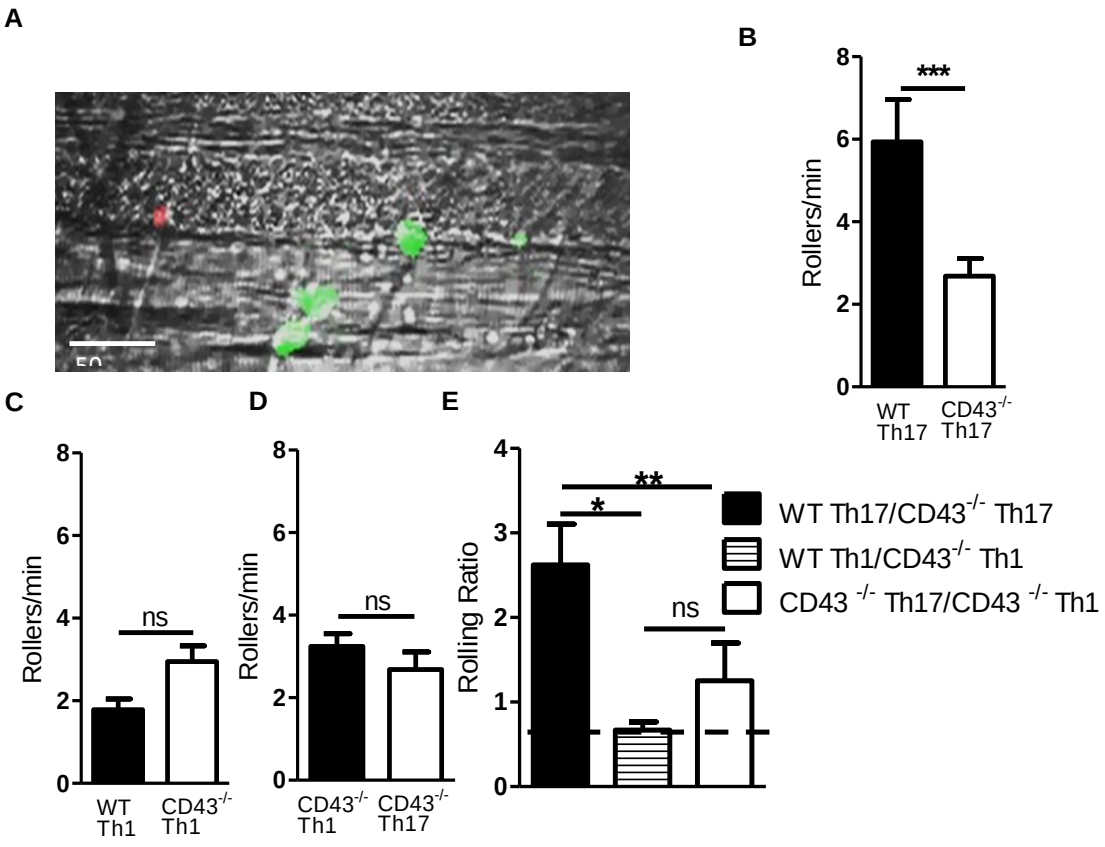

Figure 3.16: CD43$^{-/-}$ Th17 cells rolling on the cremaster microvasculature is decreased as compared to WT Th17 cells.

A. Representative image of microvasculature in the cremaster muscle with WT Th17 cells (Green) and CD43$^{-/-}$ Th17 cells (Red) rolling. Cells were quantified and resuspended at 33x10^{6} cells/mL before being stained with CFSE or Alexa 680 Fluor dyes and mixed in a 1:1 ratio for injection into the femoral artery **(B-D).** **B**. Quantification of CD43$^{-/-}$ Th17 cells vs WT Th17 cells rolling interactions with the cremaster microvasculature. **C**. Quantification of WT and CD43$^{-/-}$ Th1 cells and CD43$^{-/-}$ Th1 and Th17 cells **(D)** in competitive rolling. **E**. Rolling ratio of WT Th17 cells vs CD43$^{-/-}$ Th17 cells compared Th1 cells or CD43$^{-/-}$ Th17 and Th1 cell rolling ratios. Representative captions of microvasculature treated with anti–E-selectin or IgG (six mice, 15 vessels, and three independent T cell preparations). *p, 0.05, **p, 0.01.

We also evaluated the rolling velocities of CD43$^{-/-}$ and WT Th17 cells. The average rolling velocities were not different with CD43$^{-/-}$ Th17 cells rolling 42.63 ± 1.75 mm/s and WT Th17 cells rolling 41.80 ± 2.16 mm/s (Fig. 3.17A). These values also fall in the range of what has been described for T cells before (47).

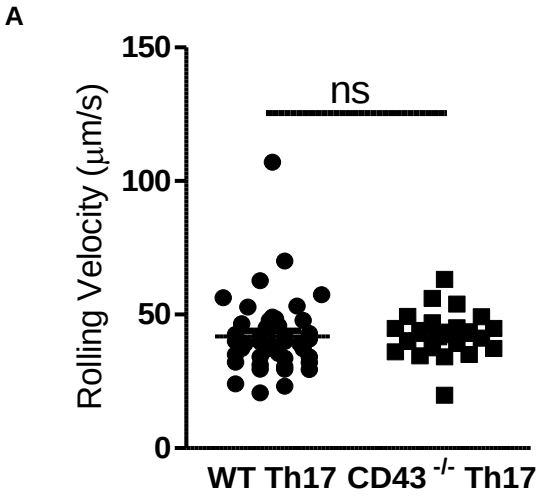

Figure 3.17: CD43$^{-/-}$ Th17 cells rolling velocity on the cremaster microvasculature is similar to WT Th17 cells rolling velocity.

A. The rolling velocity of high-velocity cell (Vcell) was calculated to ensure that these qualified as rolling leukocytes, defined as Vcell critical velocity (Vcrit). Velocities of WT Th17 cells and CD43$^{-/-}$ Th17 cells from three independent preparations (44 WT cells and 25 CD43$^{-/-}$ cells were analyzed).

Similar results were obtained when WT Th17 or CD43$^{-/-}$ Th17 cells were stained with a CFSE or with an Alexa Fluor 680 dye (Fig. 3.18).

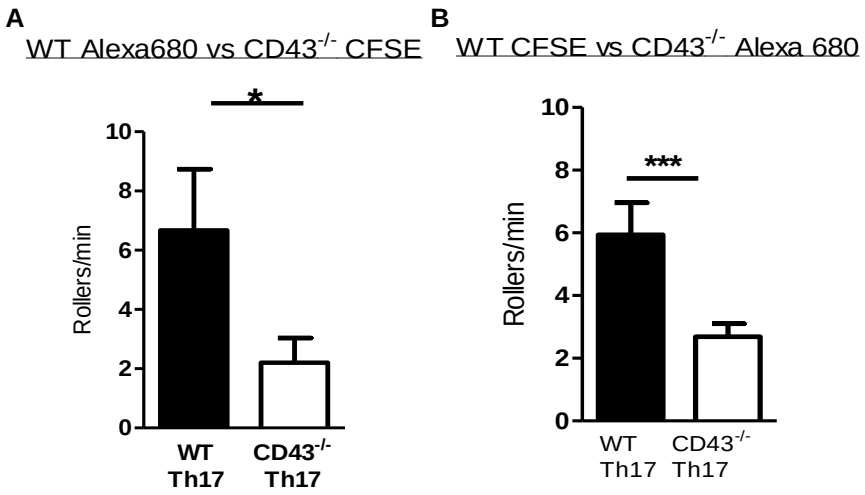

Figure 3.18: Less number of CD43$^{-/-}$ Th17 cells roll on the cremaster microvasculature as compared to WT Th17 cells, regardless of the dye used for Th17 cell labeling.

A. Equal amounts of WT Th17 cells stained with Alexa 680 and CD43$^{-/-}$ Th17 cells stained with CFSE were injected via the femoral artery into the cremaster muscle. This phenotype was confirmed when the dyes were inverted **(B)**. Data shown from 3 individual experiments using independent T cell preparations and imaging 305 vessels per experiment. *p<0.05, ***p<0.005.

To demonstrate that the difference between WT Th17 cell and CD43$^{-/-}$ Th17 cell rolling interactions with the endothelium was due to E-selectin, we performed similar assays in the presence of an anti–E-selectin function–blocking Ab or an isotype control. As expected, the number of WT and CD43$^{-/-}$ Th17 cells rolling on the vasculature was similar in the presence of anti–E-selectin, but significantly more WT Th17 cells rolled in the presence of an IgG control Ab. The remaining rolling interactions observed in the presence of anti–E-selectin are probably due to Th17 cell interaction with other endothelial cell adhesion molecules such as P-selectin (Fig. 3.19). These data confirm the role of CD43

as a critical mediator of Th17 cell rolling with the vascular endothelium *in vivo* in an E-selectin–dependent manner.

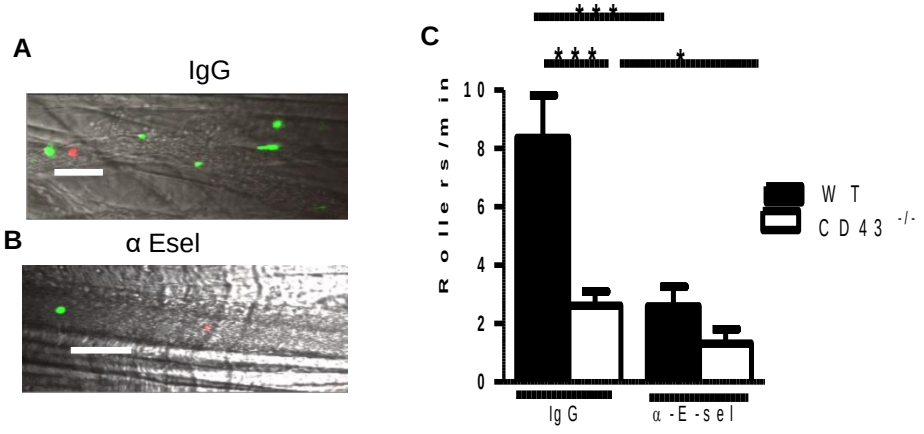

Figure 3.19: CD43$^{-/-}$ Th17 cells rolling velocity on the cremaster microvasculature is similar to WT Th17 cells rolling velocity.

A. Representative image of cremaster microvasculture treated with Isotype control IgG **(A)** or function blocking anti-E-Selectin **(B),** perfused with WT (Green) and CD43$^{-/-}$ (Red) Th17 cells **(A-B). C.** Mice were treated with 500 ng of TNF- α for 2 hours and injected with Isotype or function blocking anti-E-Selectin at 90 µg/mL, prior to injection of WT and CD43$^{-/-}$ *p , 0.05, **p , 0.01.

In summary, our data demonstrates a crucial unique role for CD43 in regulating Th17 cell rolling interactions with the cremaster micrvasculature, that is E-selectin dependent. This is a subset specific event, given that Th1 cells from CD43$^{-/-}$ mice and WT mice roll and interact similarly with the microvasculature.

3.1.7. Conclusion

In this chapter, we have characterized the expression and functionality of E-selectin ligands in Th17 cells, and further investigated the role of CD43 as an E-selectin ligand and a mediator of Th17 cell recruitment in vivo. We have demonstrated that Th17 cells express

the E-selectin ligands previously described for other T cell subsets, PSGL-1, CD43 and CD44. Particularly we have discovered that Th17 cells have a unique uniform and highly robust expression of the highly glycosylated form of CD43, which is unlike the classical bimodal expression described in the literature for Th1 cells. Using $CD43^{-/-}$ mice, we have demonstrated that Th17 cells have a high affinity to E-selectin, and absence of CD43 severely impairs adhesion of Th17 cells to E-selectin *in vitro*. Interestingly we observed, that unlike in Th1 cells where CD43 functions as an E-selectin ligand only in cooperation with PSGL-1, CD43 functions by itself in Th17 cells. To ensure that our *in vitro* observations occur also *in vivo* we employed two models of inflammation. The air pouch model of recruitment, which allows us to study endogenous leukocyte recruitment, and intravital confocal microscopy of the cremaster muscle allowing us to observe direct T cell subsets interactions with the microvasculature. We report that absence of CD43 impairs CD4 and Th17 cell recruitment into the air pouch in response to CCL20 and TNF-α. Interestingly, Th1 cells from both WT and $CD43^{-/-}$ mice were recruited in similar numbers in response to TNF-α. Using a model of intravital microscopy of the cremaster muscle, we demonstrated that CD43 is an essential molecule that mediates E-selectin dependent vascular endothelial rolling interactions of Th17 cells. This too was a subset specific event since Th1 cell rolling was not affected by the presence or absence of CD43. These data demonstrates that Th17 cells have a unique migratory pattern that can be attributed to the uniform expression of the highly glycosylated form of CD43 as an E-selectin ligand.

Chapter 3.2

3.2. Investigate the role of CD43 in the context of autoimmune disease using the mouse model of Experimental Autoimmune Encephalomyelitis (EAE), and evaluate CD43 mediated Th17 cell interaction with ICAM-1.

Rationale: T cell migration mechanisms are both shared as well as different among T cell subsets. For instance, Th1 cells and Th2 differ in their migratory phenotype in their ability to express properly glycosylated E-selectin ligands (89), whereas Th17 and Th1 share expression of some E-selectin ligands but differ in others such as CD43 (see Chapter 3.1 (90)). In chapter one we characterized the expression and functionality of E-selectin ligands in Th17 cells, and demonstrated that Th17 cells and Th1 cells can both be recruited to sites of inflammation *in vivo* and that CD43 regulates this process uniquely in Th17 cells. Th17 cells were first discovered in the mouse model of EAE, in which they play a crucial role in the development and progression of the disease. Immunization with myelin oligodendrocyte glycoprotein (MOG) results in differentiation, activation and recruitment of both Th17 and Th1 cells to the spinal cord, where T cells, activate glial cells, monocyte recruitment to destroy the myelin sheath, and activate macrophages that contribute to myelin destruction in EAE (90). However the contribution of T cell subset specific adhesion molecules remains largely unexplored. Interestingly, others demonstrated that CD43 contributes to EAE pathogenesis, as $CD43^{-/-}$ mice had reduced pathology. These findings however, were before the knowledge of the existence of Th17 cells (24). This chapter focuses in determining the role of CD43 in Th17 cell recruitment in the context of EAE, and evaluates potential novel adhesion pathways regulated by CD43 in Th17 cells in several *in vitro* studies.

3.2.1. CD43 regulates Th17 cell recruitment to the spinal cord in EAE.

To determine the role of CD43 in the recruitment of antigen specific Th17 cells *in vivo*, we used the EAE mouse model, in which Th17 cells are generated *in vivo* in response to MOG peptide immunization and are known to be recruited into the spinal cord as early as 10 days post-immunization and reach a peak directly associated with the highest clinical score of disease 16 days post immunization. This results in induction of multiple sclerosis like symptoms (91, 92) that can be scored clinically based on paralysis. These symptoms are scored as follows: 0 Normal mouse, no overt signs of disease; 1 Limp tail or hind limb weakness; 2 Limp tail and hind limb weakness; 3 Partial hind limb paralysis; 4 Complete hind limb paralysis; 5 Moribund state; death by EAE. We found that while WT mice started developing symptoms at day 11 post immunization, the clinical symptoms were more prominent by day 11-14, and peaked at 16 days post immunization. The $CD43^{-/-}$ mice however did not really show clinical symptoms until day 11 post-immunization, and these never rose above a clinical score of 1. $CD43^{-/-}$ mice remained protected from EAE (Fig. 3.20).

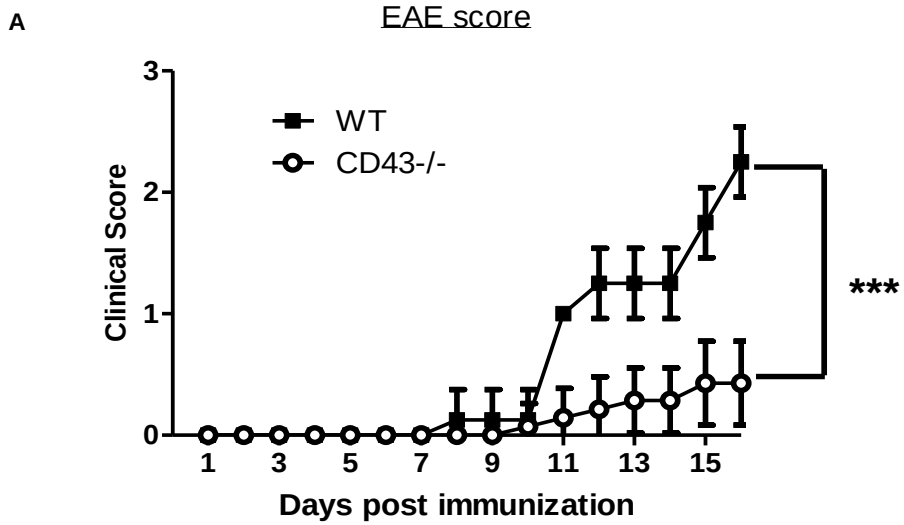

Figure 3.20: CD43$^{-/-}$ mice have decreased EAE clinical score.

A. CD43$^{-/-}$ mice were immunized with MOG peptide and pertussis toxin and followed for 16 days post-immunization. Mice were judged on the following clinical scores ***p, 0.001

To determine whether this protection was due to the lack of Th17 cell infiltration in the spinal cord, we isolated spinal cords of immunized WT and CD43$^{-/-}$ mice at the peak of disease and performed quantitative flow cytometry for CD4^{+} T cells, Th1 cells and Th17 cells. We observed a decreased infiltration of CD4^{+} T cells in the spinal cord, and more specifically Th17 cells in CD43$^{-/-}$ mice as compared with WT mice (Fig. 23.1 A-B). The number of Th1 cells recruited in the spinal cord at this time point was similar between WT and CD43$^{-/-}$ mice (Fig. 3.21C).

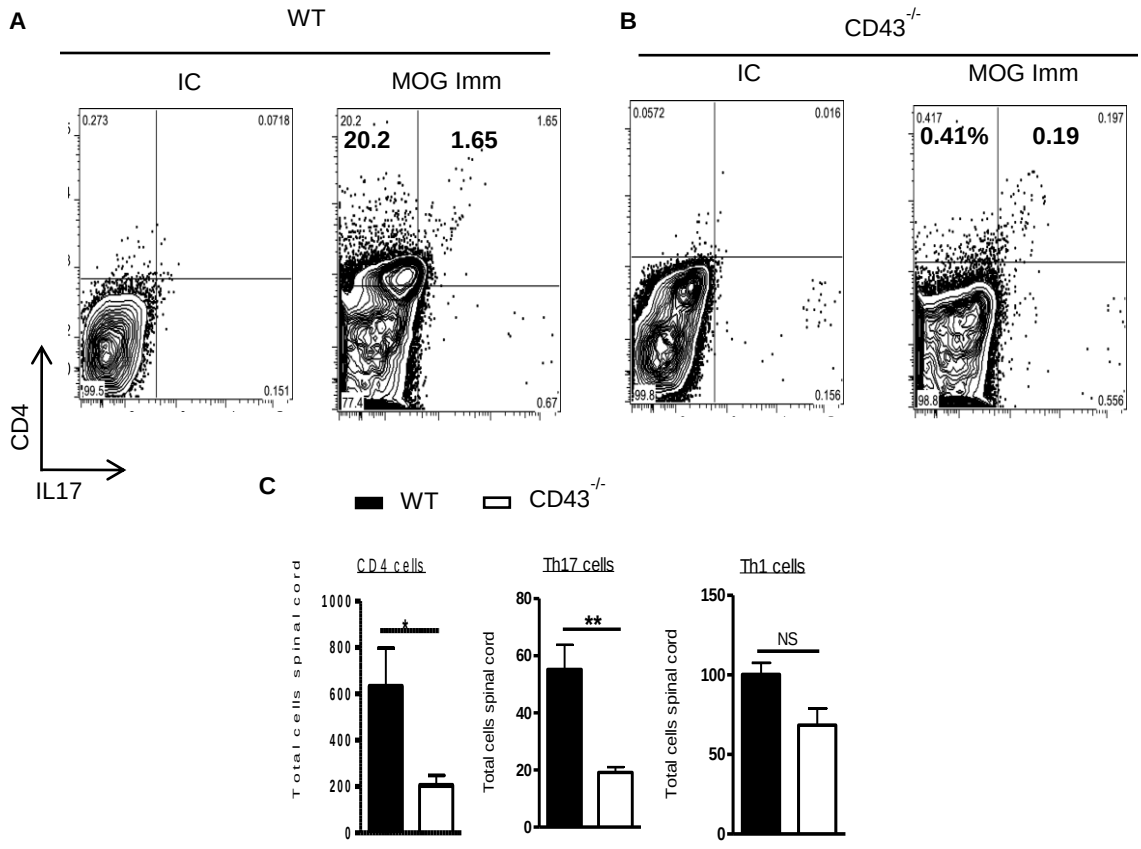

Figure 3.21: CD43$^{-/-}$ mice have significantly less CD4 and Th17 cell infiltrates into the spinal cord.

A. WT and CD43$^{-/-}$ **(B)** mice were immunized with MOG peptide and pertussis toxin at followed for 16 days post-immunization. Spinal cords were isolated and cells were stained for CD4, IL17A and IFNγ for assessment by flow cytometry. **C.** Total number of events were calculated from whole acquired sample from spinal cord. Data is representative of 3-5 independent experiments. . *p 0.05, **p, 0.01

We next tested whether CD43 was regulating T cell differentiation in response to MOG. To determine this, WT and CD43$^{-/-}$ mice were immunized with MOG and the lymph nodes were harvested at day 7 post-immunization, the time point where T cell activation and differentiation occurs prior to the development of disease symptoms (92). We found that the lack of CD43 did not impair Th17 or Th1 cell differentiation in the lymph nodes in response to MOG immunization, suggesting that CD43$^{-/-}$ T cells respond to MOG but have a defect in being recruited into the spinal cord (Fig. 3.22A-C).

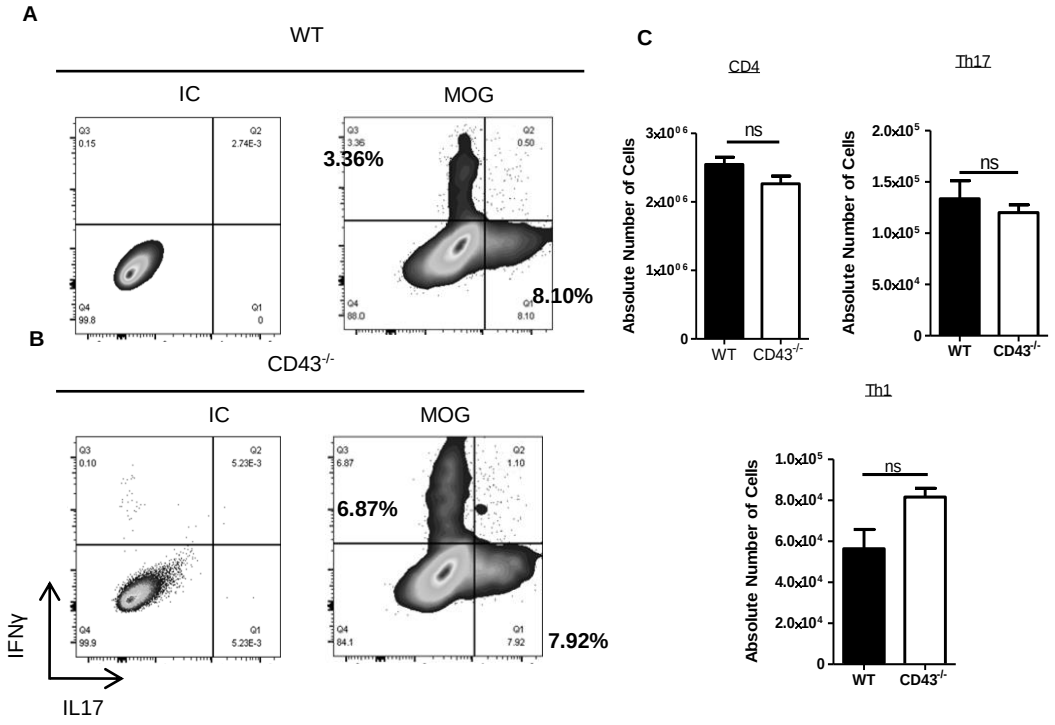

Figure 3.22: WT and CD43$^{-/-}$ mice respond similarly to MOG immunization.

(A-B) Representative FACS data. **A.** WT and CD43$^{-/-}$ **(B)** mice were immunized with MOG peptide and lymph nodes were harvested at 7 days post immunization. CD4 T cells were isolated and stained for IL17A and IFNγ for assessment via flow cytometry. **C**. Total number of cells was calculated by referring the percentages of CD4^{+}/cytokine^{+} cells to the total amount of cells harvested in the lymph nodes by cell counting and back calculated to percentages from FACS. Data is representative of 3-5 independent experiments. *p, 0.05, **p, 0.01, ***p, 0.001

Taken together, these data indicate that CD43 does not regulate T cell MOG antigen recognition and differentiation to Th17 cells, but it is critical in antigen specific Th17 cell recruitment *in vivo*.

3.2.2. ICAM-1, but not E-selectin, is expressed in the spinal cord in EAE, and CD43$^{-/-}$ Th17 cells have impaired adhesion to ICAM-1 under physiological flow conditions.

In Chapter 3.1 we demonstrate that CD43 functions as an E-selectin ligand on Th17 cells *in vitro* and in different models of inflammation *in vivo*. Additionally, we demonstrate CD43$^{-/-}$ mice have decreased Th17 cell recruitment in the spinal cord and are protected from EAE. However, several studies indicate that E-selectin is not required for T cell infiltration and the development of EAE (93). Instead, other adhesion molecules such as VCAM-1 and ICAM-1 have been reported to mediate T cell recruitment in EAE. We performed qPCR in the spinal cord of WT and CD43$^{-/-}$ mice immunized with MOG, and found that ICAM-1 was upregulated in both WT and CD43$^{-/-}$ mice, in contrast to E-Selectin, which was undetectable in both groups (Fig. 3.23A). Interestingly, one previously reported function of CD43 was its ability to bind to soluble ICAM-1 in an *in vitro* system that involved soluble human ICAM-1 and immortalized cancer cell lines overexpressing CD43 (94). We therefore hypothesized that CD43 contributes to Th17 adhesion to ICAM-1 and regulates Th17 cell recruitment in EAE.

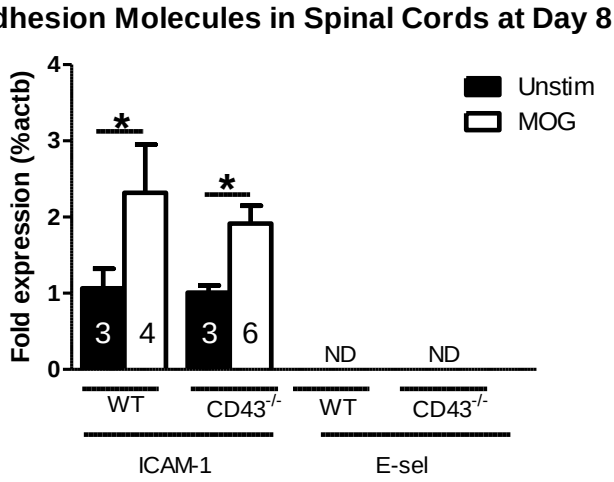

Figure 3.23: WT and CD43$^{-/-}$ upregulate ICAM-1 at similar levels upon immunization with MOG.

A. WT and CD43 $^{-/-}$ mice were immunized with MOG emulsified in CFA 1:1 ratio. Spinal cords were harvested on Day 8 and used for qPCR to assess for ICAM-1 and E-selectin. WT and CD43 $^{-/-}$ mice immunized with PBS were used as a negative control. Data representative of ≥3 independent experiments. ND= not detected. Data show the mean ± SD values. *p<0.05

To test this hypothesis, we differentiated WT and CD43$^{-/-}$ CD4 T cells into Th17 cells, treated them with PMA to induce the active conformation state of integrins such as LFA-1, required to bind to ICAM-1 (Fig 3.24A), and performed adhesion experiments under flow conditions over coverslips coated with ICAM-1. We observed that the number of CD43$^{-/-}$ Th17 cells that adhered to ICAM-1 was significantly decreased as compared to WT Th17 cells (CD43$^{-/-}$ = 47.86 ± 2.972 cells/mm^2 vs WT = 75.48 ± 4.19 cells/mm^2). As expected, unactivated Th17 cells showed very little adhesion to ICAM-1 with 9.091 ± 2.064 cells/mm^2 binding at background level (Fig. 3.24B).

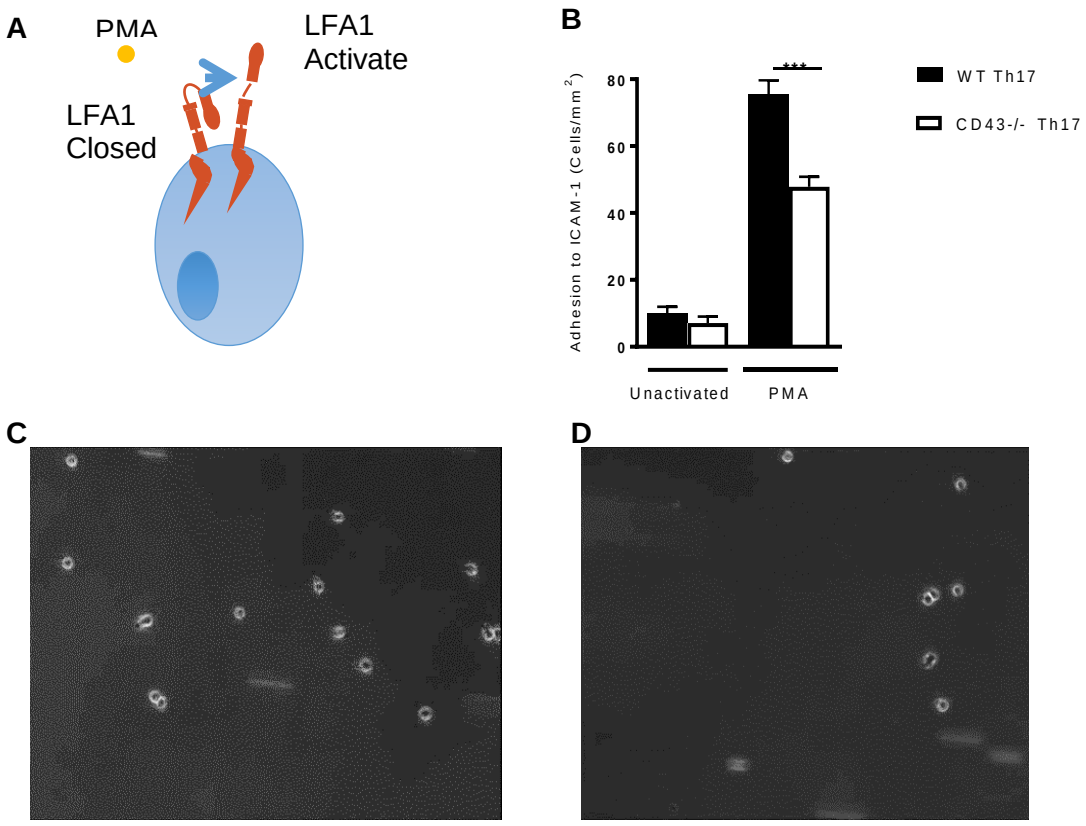

Figure 3.24: CD43$^{-/-}$ Th17 cells have impaired adhesion to ICAM-1 as compared to WT.

A, Representative image of Th17 cells treated with PMA to induce integrin conformational changes. **B.** WT and CD43 $^{-/-}$ Th17 cells were perfused over ICAM-1 coated coverslips at 1 dyne/cm ^{2}. Cells were left untreated or were treated with 50ng of PMA (5 minutes) prior to perfusion over ICAM-1. **B-C.** Representative images of WT Th17 cells adhering to ICAM-1 **(B)** and CD43 $^{-/-}$ Th17 cells **(C)** adhering to ICAM-1. Representative images of N≥ 3 independent experiments, with 6 fields of view per each recording. *p<0.05, **p<0.01, ***p<0.001.

To determine whether this was a subset specific effect we perfused Th1 cells over ICAM-1 coated coverslips. We observed no significant differences between Th1 cells from WT (adhering at 69.23 ± 5.276 cells/mm^2) and CD43$^{-/-}$ mice (adhering at 62.53 ± 4.171 cells/mm^2) in adhesion to ICAM-1 (Fig. 3.25). Our results demonstrate that the lack of CD43 in Th17 cells significantly impairs the adhesion of these cells to ICAM-1 under shear

stress conditions in a subset specific manner. We therefore next focused on understanding the role of CD43 in Th17 cells adhesion to ICAM-1.

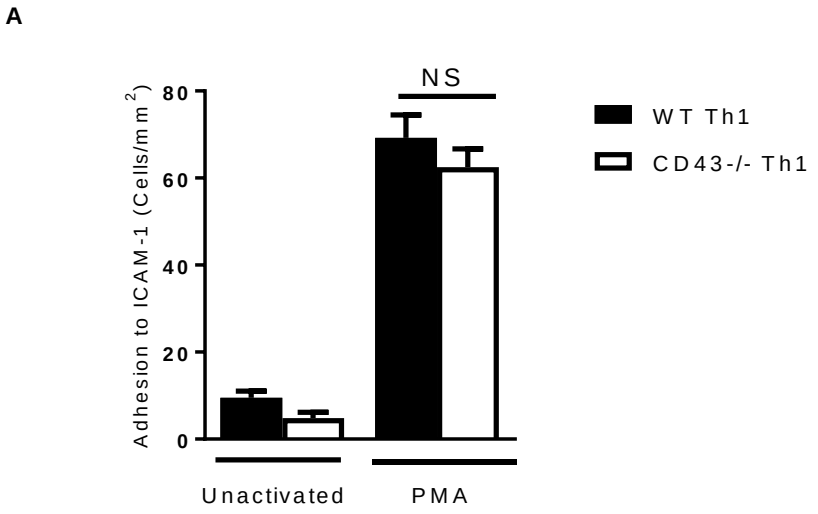

Figure 3.25: CD43$^{-/-}$ and WT Th1 cells adhere to ICAM-1 in similar numbers.

A. WT and CD43 $^{-/-}$ Th1 cells were perfused over ICAM-1 coated coverslips at a shear stress of 1 dyne/cm ^{2}. Cells were activated with 50ng of PMA for 5 mins, or left unactivated prior to being perfused. 6 fields of view were recorded per each condition. WT and CD43 $^{-/-}$ Th1 cells adhered similarly to ICAM-1. Data representative of 3-5 experiments.

3.2.3. Function blocking of LFA-1 does not completely abolish adhesion of WT Th17 cells to ICAM-1 but it does so in CD43$^{-/-}$ Th17 cells.

While absence of CD43 seems to impair Th17 cell adhesion to ICAM-1, most of the observed adhesion is likely mediated by the main ligand of ICAM-1, LFA-1. To determine whether CD43 is directly contributing in Th17 cell adhesion to ICAM-1, we next used an LFA-1 function blocking antibody (α-LFA-1) or an isotype control antibody (IgG) and quantified the adhesion of WT and CD43$^{-/-}$ Th17 cells to ICAM-1. Th17 cells from WT and CD43$^{-/-}$ mice were incubated with α-LFA-1 antibody for 20 minutes before being perfused over ICAM-1. Treatment with α-LFA-1 on WT Th17 cells resulted in decreased adhesion to ICAM-1 compared to IgG treated cells (difference of 49.43 ± 5.786 cells/mm^2 between

α-LFA-1 and IgG treated WT Th17 cells). However, WT Th17 cell adhesion to ICAM-1 was not completely abolished as compared to unactivated cells (difference of 70.96 ± 9.104 cells/mm^2 between α-LFA-1 Th17 cells and unactivated Th17 cells), in contrast to adhesion of CD43$^{-/-}$ Th17 cells to ICAM-1, which was abolished when treated with α -LFA-1 and was comparable to the adhesion observed in unactivated Th17 cells (Fig 3.26A). To ensure that blocking LFA-1 on Th17 cells was not affecting functional aspects of CD43, we perfused IgG and function blocking α-LFA1 treated cells over E-selectin. We observed that there was no difference in adhesion between IgG and α -LFA-1 treated cells in either WT or CD43$^{-/-}$ Th17 cells adhesion to E-selectin. As previously demonstrated in Chapter 3.1, CD43$^{-/-}$ Th17 cells adhered in significantly less numbers to E-selectin as compared to WT Th17 cells (difference of 89.32 ± 17.01 cells/mm^2 between WT and CD43$^{-/-}$ Th17 cells) (Fig. 3.26).

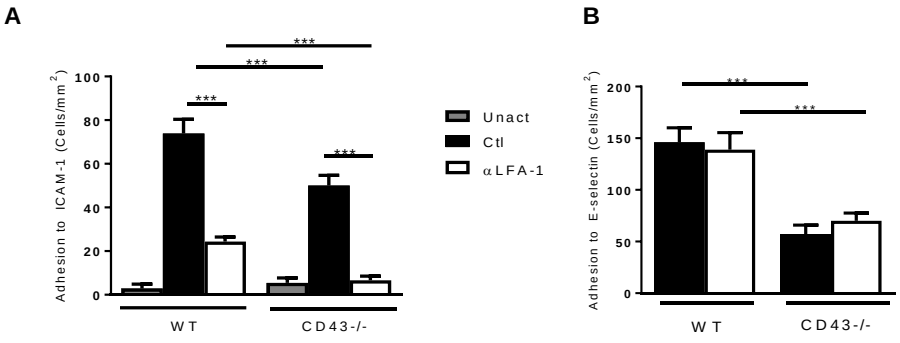

Figure 3.26: CD43 contributes to Th17 cell adhesion to ICAM-1 in an LFA-1 independent manner.

WT and CD43$^{-/-}$ Th17 cells that were treated with function blocking α-LFA-1 or IgG after being activated with PMA and perfused over ICAM-1 **(A)** or E-selectin **(B**) at 1 dyne/cm^2. Data representative of 5 experiments. *p<0.05, **p<0.01, ***p<0.001.

To determine whether CD43 mediated adhesion to ICAM-1 was subset specific, we next performed similar studies using Th1 cells. We found that treatment of PMA activated Th1 cells treated with α- LFA-1 abolished adhesion of Th1 cells to ICAM-1 similarly in WT and

CD43$^{-/-}$ Th1 cells (Fig. 3.27A). Additionally, such treatment did not impact Th1 cell adhesion of WT and CD43$^{-/-}$ cells to E-selectin (Fig 3.28B).

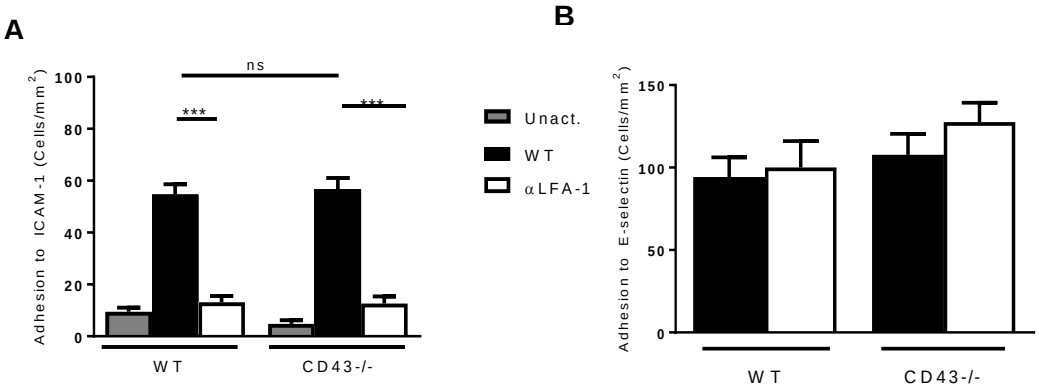

Figure 3.27: Th1 cell adhesion to ICAM-1 is abolished with α-LFA-1 function blocking antibody.

WT and CD43 $^{-/-}$ Th1 cells that were treated with function blocking α-LFA-1 or IgG after being activated with PMA and perfused over ICAM-1 **(A)** or E-selectin **(B)** at 1 dyne/cm^2. Data representative of 5 experiments. *p<0.05, **p<0.01, ***p<0.001.

We next determined whether CD43 and LFA-1 shared a common binding epitope for ICAM-1. To do so, we perfused PMA activated WT and CD43$^{-/-}$ Th17 cells at 1 dyne/cm^2 over ICAM-1 coverslips that were treated with either IgG or function blocking antibody for ICAM-1 (YN1.1) which blocks the domains 1 and 2 of ICAM-1, where LFA-1 binds (Fig 3.28)(95). We observed that both WT Th17 cells and CD43$^{-/-}$ Th17 cells had similar decreased adhesion to ICAM-1 in the YN1.1 condition as compared to IgG treated cells. The remaining adhesion in the YN1.1 conditions is similar in WT and CD43-/- and may reflect suboptimal ICAM-1 blocking, however it does not differ between WT and CD43$^{-/-}$ Th17 cells. Taken together, these data suggest that both LFA-1 and CD43 interact with ICAM-1, with LFA-1 mediating most of the adhesion but CD43 also contributing and sharing a common epitope with ICAM-1.

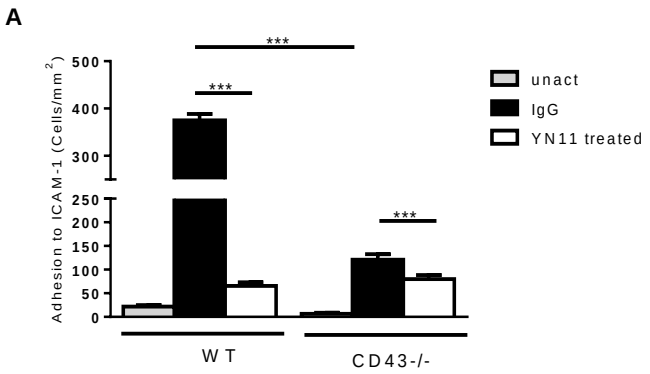

Figure 3.28: CD43 shares a common epitope with LFA-1 for adhesion of Th17 cells to ICAM-1.

WT and CD43 $^{-/-}$ Th17 cells were perfused over ICAM-1 coated coverslips treated with control IgG Isotype or function blocking antibody to ICAM-1. T cells were left unactivated or treated with PMA 5 mins prior to being perfused over coverslips at physiological shear stress conditions. **A.** WT and CD43 $^{-/-}$ Th17 cells that were treated with function blocking α-ICAM-1 coverslips had significantly decreased adhesion as compared to IgG treated coverslips. *p<0.05, **p<0.01, ***p<0.001.

3.2.4. Lack of CD43 does not impair LFA-1 expression in Th17 cells.

Our data demonstrates that in the absence of LFA-1, WT but not CD43$^{-/-}$ cells adhere to ICAM-1 However, most of the adhesion in WT is mediated by LFA-1, not by CD43, suggesting the possibility that CD43 additionally serves as a pro-adhesive molecule that aids LFA-1 adhesion to ICAM-1. T test this hypothesis, we first sought to determine whether the absence of CD43 impaired LFA-1 expression as a possible explanation of the observed decreased CD43$^{-/-}$ Th17 cell adhesion to ICAM-1. We differentiated Th17 cells from WT and CD43$^{-/-}$ mice and stained for LFA-1 using flow cytometry. WT Th17 cells and CD43$^{-/-}$ Th17 cells had similar surface expression of LFA-1 after T cell differentiation (Fig. 3.29A-B).

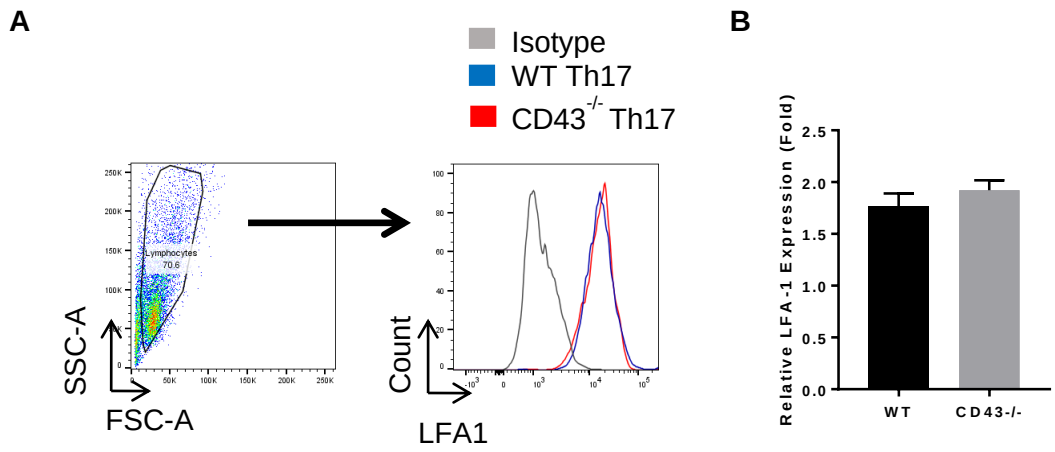

Figure 3.29: WT and CD43 $^{-/-}$ Th17 cells express LFA-1 at similar levels.

A. Representative FACS plot of T cell expression of LFA-1 on WT and CD43 $^{-/-}$ Th17 cells. **B.** Quantification of Th17 cell expression of LFA-1.

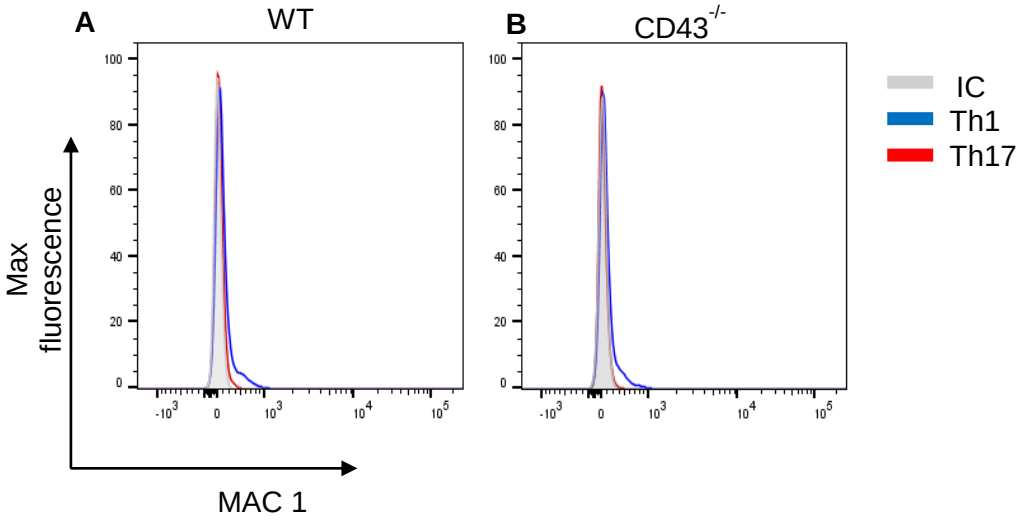

Figure 3.30: WT and CD43 $^{-/-}$ Th17 cells do not express MAC1.

A. Representative pictures of WT **(A)** and CD43 $^{-/-}$ **(B)** Th17 cells in red and Th1 cells in blue stained for MAC1. Data representative of ≥3 independent experiments.

We also evaluated the expression of MAC1, another ICAM-1 ligand, but did not observe any expression of MAC1 in Th17 cells or Th1 cells of WT and CD43$^{-/-}$ mice (Fig. 3.30). These data demonstrate that CD43 does not regulate the expression of LFA-1 in Th17

cells and thus the observed effect in adhesion to ICAM-1 cannot be attributed to an effect of LFA expression.

3.2.5. CD43 does not regulate LFA-1 mediated adhesion strength or polarization on ICAM-1 but contributes to Th17 cells locomotion and transmigration.

While the expression of LFA-1 does not differ between WT and CD43$^{-/-}$ Th17 cells, we next questioned whether the observed defect in adhesion in CD43$^{-/-}$ Th17 cells could be due to a defective function of LFA-1. To determine whether the LFA-1 expressed on CD43$^{-/-}$ Th17 cells was fully functional, we took different approaches involving PMA activated Th17 cell adhesion to ICAM-1 under flow conditions. Our first approach was to evaluate cell spreading, the formation of pseudopods and polarization of Th17 cells upon LFA-1 mediated adhesion to ICAM-1 under flow conditions (96). We found that WT Th17 cells polarized and formed pseudopods upon adhesion to ICAM-1 (Fig. 3.31A). Absence of CD43 did not impair such polarization (Fig. 3.31B).

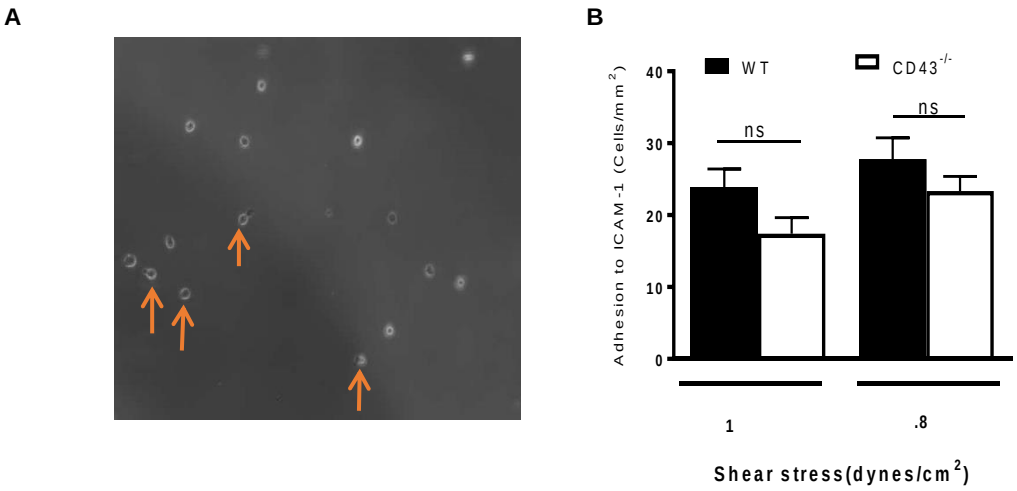

Figure 3.31: WT and CD43 $^{-/-}$ Th17 polarization on ICAM-1 is similar.

A. Representative image of Pseudopod formation of WT Th17 cells after adhesion to ICAM-1. **B.** WT and CD43 $^{-/-}$ Th17 cells were perfused over ICAM-1 coated coverslips at a shear stress of 1 and 0.8 dyne/cm ^{2} and pseudopods were quantified by video microscopy in 6 different fields of view.

A second approach was to determine the role of CD43 in adhesion strength of Th17 cells on ICAM-1 by performing a detachment assay. We perfused PMA activated Th17 cells from WT or CD43$^{-/-}$ mice over ICAM-1 covered coverslips to ensure sufficient adhesion of Th17 cells in the field of view, followed by sequential increases of shear stress from 1 dyne/cm^2 to 10 dyne/cm^2. We monitored the number of WT and Th17 cells that detached or remained adhered at each increasing shear stress and observed that WT Th17 cells consistently adhered in greater numbers to ICAM-1 at shear 1 dyne/cm^2. The CD43$^{-/-}$ Th17 cells that adhered to ICAM-1 remained firmly arrested on ICAM-1 as we increased shear stress, in contrast to WT Th17 cells which slightly detached when the shear was increased from 1 to 2 dynes/cm^2 and then remained arrested as the shear stress increased to 10 dynes/cm^2 (Fig. 3.32). Thus, absence of CD43 does not impact the adhesion strength of Th17 cells ICAM-1. Our data demonstrating initial detachment of WT cells is consistent with the experiments in section 3.2.2 (Fig 3.24) demonstrating that CD43 contributes to ICAM-1 adhesion, and indicated that this possible interaction is weaker than the interaction between LFA-1 and ICAM-1 present in both WT and CD43$^{-/-}$ cells.

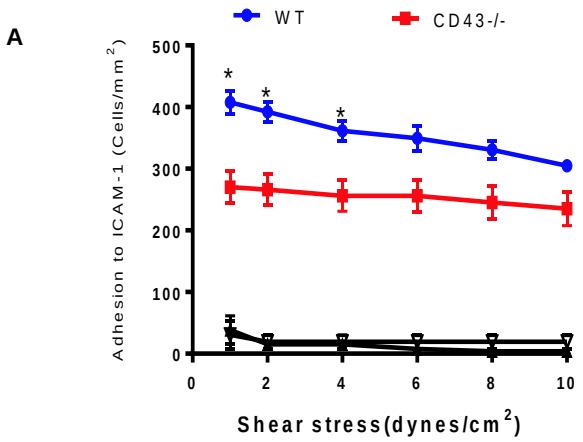

Figure 3.32: WT and CD43 $^{-/-}$ Th17 cells adhesion strength to ICAM-1 is comparable.

A. WT and CD43 $^{-/-}$ Th17 cells were left untreated or activated with PMA for 5 mins, prior to experiment. Cells were perfused at 2 x 10 ^{6} cells/mL over ICAM-1 coated coverslips at a shear stress of 1 dyne/cm ^{2}. Shear stress was increased every 30 seconds until a maximum of shear stress of 10 dyne/cm ^{2} while recording one field of view. *p<0.05, **p<0.01, ***p<0.001.

Our third approach was to evaluate Th17 cell locomotion on ICAM-1, a mechanism required for T cells to apically migrate on the surface of the endothelium to reach the sites of transmigration (96, 97). To determine whether CD43 regulated locomotion of Th17 cells on ICAM-1, we perfused PMA activated WT and CD43$^{-/-}$ Th17 cells over ICAM-1 and tracked T cell movement on ICAM-1 for 30 minutes. We observed that WT Th17 cell locomotion on ICAM-1 was heterogeneous, with 31.4% of cells locomoting and 68.6% firmly arrested without locomoting (Fig 3.33A). Surprisingly CD43$^{-/-}$ Th17 cells had a decreased percent of cells that locomoted on ICAM-1 as compared to WT Th17 cells (Fig. 3.33B). Within the Th17 cells that locomoted on ICAM-1 we observed that CD43$^{-/-}$ Th17 cells migrated less distance on the ICAM-1 coated coverslip as compared to WT Th17 cells that locomoted (Fig. 3.34A), and locomoted at a significantly decreased velocity as compared to WT Th17 cells (Fig. 3.34B). Taken together, our data suggest that CD43 plays a role in contributing to the amount of Th17 cells that can locomote on ICAM-1, and

within those that locomote, CD43 plays a role in the distance and velocity during locomotion.

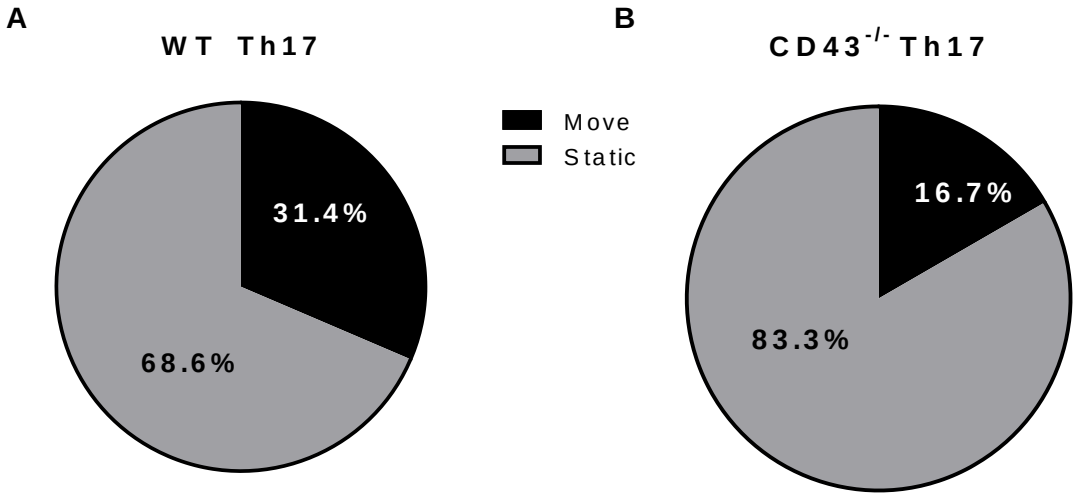

Figure 3.33: CD43 $^{-/-}$ Th17 can bind to ICAM-1 with functional LFA-1 as compared to WT.

A-B. Percentages of locomotion or static cells was calculated from the total average of cells that adhered during 20 mins from 3-5 experiments.

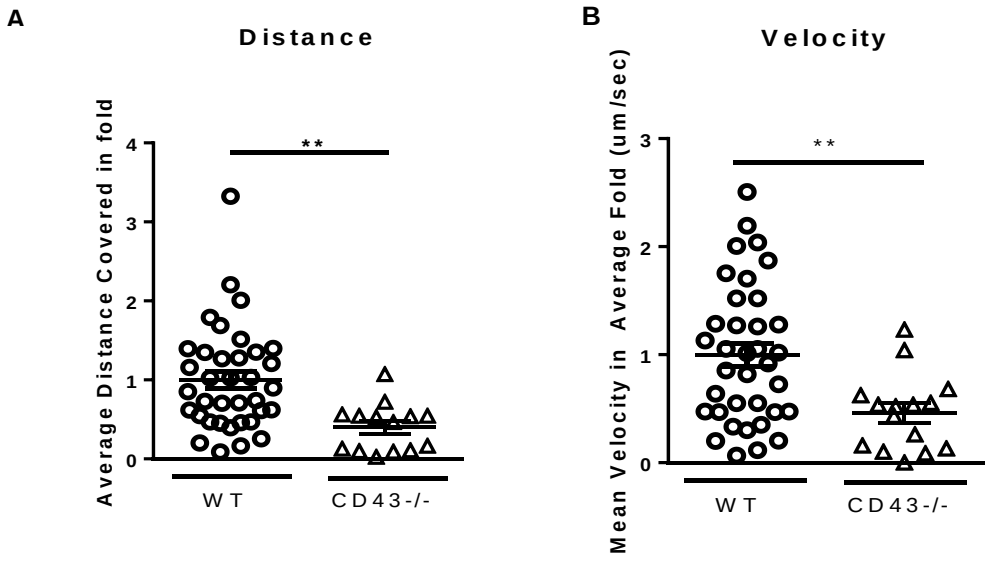

Figure 3.34: CD43 $^{-/-}$ Th17 cells have impaired integrin mediated locomotion on ICAM-1.

A. Total distance covered in µm was traced for each individual Th17 cell that locomoted. Average fold was calculated and cells were normalized to WT Th17 cell distance for each individual experiment. **B.** Velocity of Th17 cells locomoting across ICAM-1 was calculated by the total distance covered in the 20 mins that were recorded. Fold was calculated and normalized to WT Th17 cells for each individual experiment. *p<0.05, **p<0.01, ***p<0.001.

3.2.6. CD43 does not regulate the actin cytoskeletal polymerization in Th17 cells upon adhesion to ICAM-1.

T cell adhesion and locomotion result in cell morphology changes that involve the rearrangement of the actin cytoskeleton. Upon firm adhesion to ICAM-1, T cells undergo this rearrangement and apically migrate or locomote on the vascular endothelium previous to transmigrating across the endothelium. CD43 has been shown to interact with the cytoskeleton through the ezrin/radixinn/moesin (ERM) complex during T cell activation (98). We next sought to determine if CD43 regulates cytoskeleton rearrangement upon ICAM-1 adhesion by evaluating f-actin polymerization. We incubated WT and CD43$^{-/-}$ Th17 cells on coverslips coated with ICAM-1 after being activated with PMA. Cells were then stained for phalloidin to visualize f-actin polymerization. We found that rearrangement of the actin cytoskeleton upon ICAM-1 arrest occurred similarly in both WT and CD43$^{-/-}$ Th17 cells (Fig 3.35 A-B) with no significant changes in the total corrected cell fluorescence (Fig 3.35C). Our data suggest that CD43 does not actively participate in f-actin polymerization of Th17 cells upon adhesion to ICAM-1.

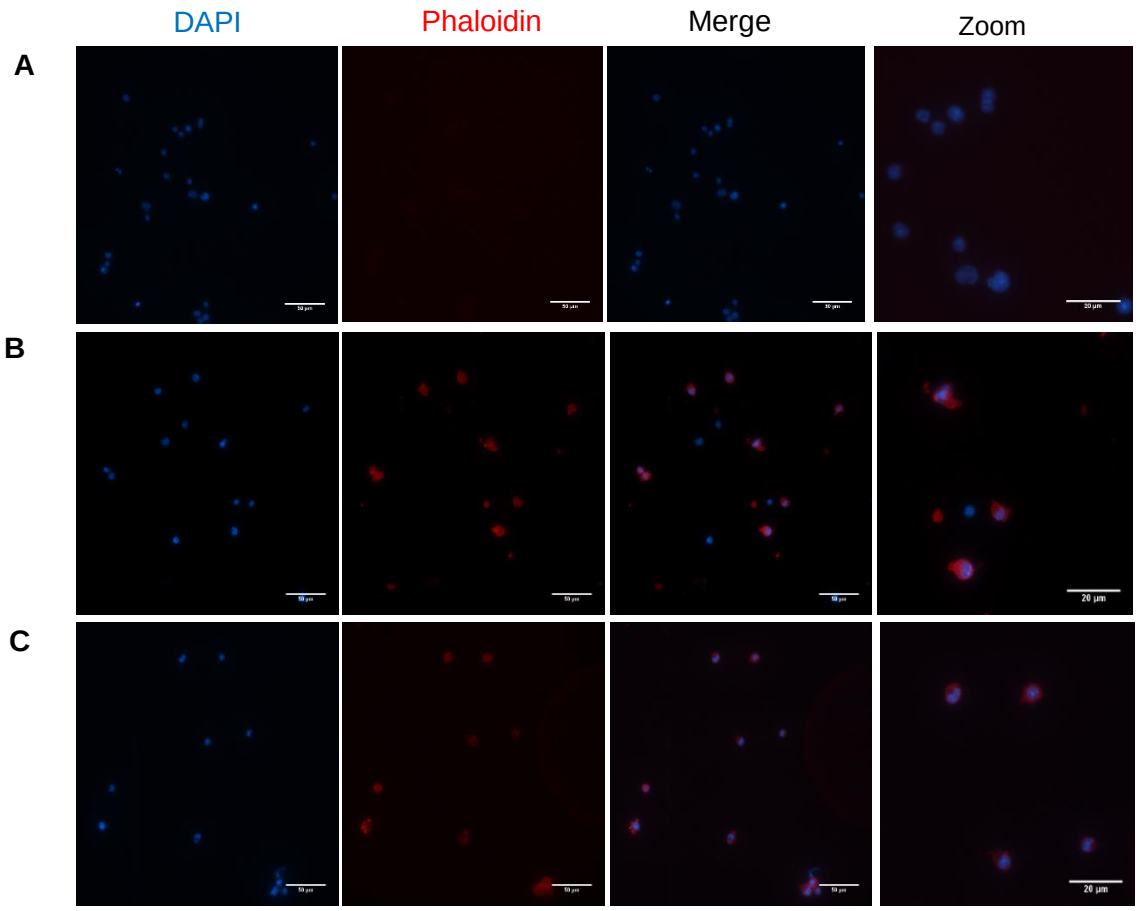
DAPI
Phaloidin
Merge
Zoom
A
B
C
20 µm
20 µm

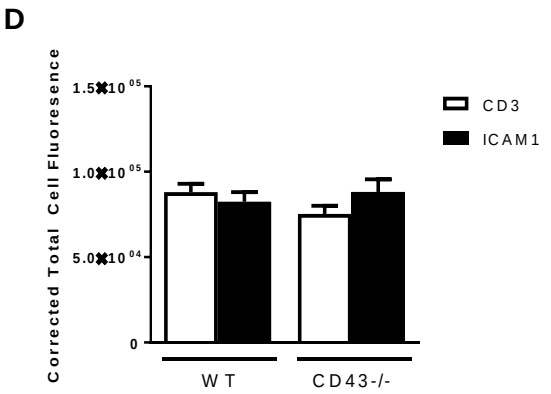
D
Corrected Total Cell Fluoresence
1.5X10 05
1.0X10 05
5.0X10 04
0
CD3
ICAM1
WT
CD43-/-

Figure 3.35: CD43 $^{-/-}$ Th17 cells undergo f-actin polymerization upon adhesion to ICAM-1.

WT and CD43 $^{-/-}$ Th17 cells were differentiated from naïve CD4 T cells and incubated on ICAM-1 coated coverslips before being fixed. Cells were stained for F-actin polymerization using Phalloidin and for DAPI and assessed via immunofluorescence and imaged at 40X. Fourth column is a zoomed image of the merge. **A-C.** IgG **(A)** WT **(B)** and CD43 $^{-/-}$ **(C)** Th17 cells underwent F-actin polymerization upon firm arrest on ICAM-1 as visualized by Phalloidin (red). **D.** WT and CD43 $^{-/-}$ Th17 cells had similar corrected total cell fluorescence as quantified per each individual cell per image.

3.2.7. CD43 regulates Th17 cell ICAM-1 dependent transmigration in response to chemokine CCL20.

Given that CD43 contributes to adhesion of Th17 cells to ICAM-1, and that ICAM-1 mediates both adhesion and transendothelial migration, we next determined whether CD43 played a role on the final step of the leukocyte recruitment cascade, transmigration. We used transwell assays with a size pore defined across ICAM-1 coated surfaces and a specific chemokine such as CCL20 which mediates Th17 cell adhesion to ICAM-1(47) and to endothelial cells(99). Th17 cells were fluorescently labeled and fluorescence was quantified in the bottom well as a read out for transmigration. We observed that ICAM-1 dependent transmigration in response to CCL20 was significantly impaired in CD43$^{-/-}$ vs WT Th17 cells. Interestingly, CCL20 chemotaxis in the absence of ICAM-1 lead to significantly less transwell migration of Th17 cells, and was not significantly different between WT and CD43$^{-/-}$ Th17 cells. This defect in ICAM-1 dependent transmigration can be as a result of the defective locomotion observed in CD43$^{-/-}$ Th17 cells (see Fig 3.36). These data demonstrates that CD43 is essential for effective ICAM-1 dependent transmigration, but not for chemotaxis towards CCL20.

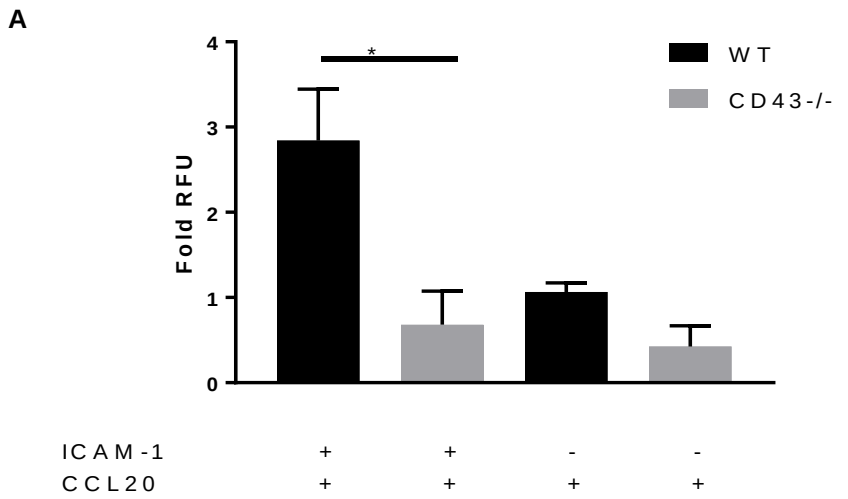

Figure 3.36: Absence of CD43 impacts Th17 cell Transmigration on ICAM-1.

Fluorescently labeled WT and CD43 $^{-/-}$ Th17 cells on transwells were incubated in the presence of CCL20 and/or ICAM-1 and quantified using relative fluorescent units. Samples were averaged to basal transmigration **(A)**. Data representative of N ≥ 3 independent experiments. *p<0.05

3.2.8. Conclusion

In this chapter we investigated the role of CD43 in Th17 cell recruitment to the spinal cord during EAE *in vivo*, and evaluated potential mechanisms regulating such recruitment using *in vitro* approaches. We found that E-selectin is not upregulated in the spinal cord in EAE, in contrast to ICAM-1, highlighting that the protection observed in CD43$^{-/-}$ mice is independent of CD43's ability to function as an E-selectin ligand. While others have reported that CD43 and ICAM-1 can interact in solution *in vitro*, whether this occurs in murine Th17 cells in the context of T cell adhesion and transmigration during physiological shear flow conditions, had not been addressed. We demonstrated that absence of CD43 significantly impairs Th17 cell adhesion to ICAM-1, but this does not occur in Th1 cells. This was interesting given that CD43 is not the main ligand of ICAM-1 on T cells. We used functional shear flow assays to test whether CD43 was contributing to adhesion of Th17

cells to ICAM-1 independently or by altering the functionality of LFA-1, the main T cell ligand for ICAM-1. We observed that blocking LFA-1 does not effectively abolish WT Th17 cell adhesion to ICAM-1, while it does for CD43$^{-/-}$ Th17 cells. Furthermore, blocking ICAM-1 using an antibody known to block the ICAM-1 epitope region where LFA-1 binds, abolished equally adhesion of WT and CD43$^{-/-}$ Th17 cells, suggesting that CD43 adheres to ICAM-1 through a shared epitope with LFA-1. Interestingly, the expression and function of LFA-1, the polarization and the strength of adhesion to ICAM-1 are not affected by the lack of CD43. In contrast, we observed that absence of CD43 affected other functions of LFA-1, such as LFA-1 integrin mediated motility and locomotion, and ICAM-1 dependent transmigration in response to CCL20. These data lead us to conclude two roles for CD43 that contribute to Th17 cell adhesion to ICAM-1 and could explain limited Th17 cell recruitment *in vivo* in tissues expressing ICAM-1, such the spinal cord in EAE. The first is that CD43 mediates Th17 cells weak interactions with ICAM-1 through a common ICAM-1 shared epitope with LFA-1. The second is that CD43 is involved in further steps of the leukocyte recruitment cascade by impacting locomotion/apical migration and transmigration. We speculate that absence of CD43 and its negative charges impacts how the cell can polarize, independently of proper F-actin cytoskeleton polarization, and this is further discussed in the discussion section of the present thesis. Taken together, this chapter demonstrates that CD43 plays an essential role in the recruitment of Th17 cells in EAE, and unveils new adhesion pathways in which CD43 contributes specifically in Th17 cells.

In this chapter we investigated the role of CD43 in Th17 cell recruitment to the spinal cord during EAE *in vivo*, and evaluated potential mechanisms regulating such recruitment using *in vitro* approaches. We found that E-selectin is not upregulated in the spinal cord in EAE, in contrast to ICAM-1, highlighting that the protection observed in $CD43^{-/-}$ mice is independent of CD43's ability to function as an E-selectin ligand. While others have reported that CD43 and ICAM-1 can interact in solution *in vitro*, whether this occurs in murine Th17 cells in the context of T cell adhesion and transmigration during physiological shear flow conditions, had not been addressed. We demonstrated that absence of CD43 significantly impairs Th17 cell adhesion to ICAM-1, but this does not occur in Th1 cells. This was interesting given that CD43 is not the main ligand of ICAM-1 on T cells. We used functional shear flow assays to test whether CD43 was contributing to adhesion of Th17 cells to ICAM-1 independently or by altering the functionality of LFA-1, the main T cell ligand for ICAM-1. We observed that blocking LFA-1 does not effectively abolish WT Th17 cell adhesion to ICAM-1, while it does for $CD43^{-/-}$ Th17 cells. Furthermore, blocking ICAM-1 using an antibody known to block the ICAM-1 epitope region where LFA-1 binds, abolished equally adhesion of WT and $CD43^{-/-}$ Th17 cells, suggesting that CD43 adheres to ICAM-1 through a shared epitope with LFA-1. Interestingly, the expression and function of LFA-1, the polarization and the strength of adhesion to ICAM-1 are not affected by the lack of CD43. In contrast, we observed that absence of CD43 affected other functions of LFA-1, such as LFA-1 integrin mediated motility and locomotion, and ICAM-1 dependent transmigration in response to CCL20. These data lead us to conclude two roles for CD43 that contribute to Th17 cell adhesion to ICAM-1 and could explain limited Th17 cell recruitment *in vivo* in tissues expressing ICAM-1, such the spinal cord in EAE. The first is that CD43 mediates Th17 cells weak interactions with ICAM-1 through a common ICAM-1 shared epitope with LFA-1. The second is that CD43 is involved in further steps of the leukocyte recruitment cascade by impacting locomotion/apical migration and

transmigration. We speculate that absence of CD43 and its negative charges impacts how the cell can polarize, independently of proper F-actin cytoskeleton polarization, and this is further discussed in the discussion section of the present thesis. Taken together, this chapter demonstrates that CD43 plays an essential role in the recruitment of Th17 cells in EAE, and unveils new adhesion pathways in which CD43 contributes specifically in Th17 cells.

Chapter 3.3

3.3. Determine the role of CD43 in cardiovascular disease (CVD) using the *in vivo* mouse model of Thoracic Aortic Constriction (TAC).

Rationale: Heart**:** Failure (HF) is primarily a clinical diagnosis that develops secondary to left ventricular (LV) dysfunction in response to ischemic, infections or non-ischemic/non-infectious triggers, including myocardial infarct, viral, bacterial or protozoan infections, or hypertension, respectively. HF involves the interplay of several factors, including inflammation (62, 63). In humans, studies demonstrate a positive correlation between inflammatory cytokines potentially produced by T cells and LV dysfunction in patients with HF (68, 100, 101). While much of what has been studied of the immune system in HF has focused on the innate immune response and the adaptive immune responses in infection, ischemic injury and autoimmunity (69), our lab and others have demonstrated a clear role for the adaptive immune system in non-ischemic/ non-infectious induced HF (74). We found that T cells are infiltrated in the LV of patients with non-ischemic/ non-infectious HF (74). Using the model of Thoracic Aortic Constriction (TAC) as a model of non-ischemic/ non-infectious HF we have demonstrated that absence of T cells is protective from the development of fibrosis and other pathological hallmarks of HF (74, 102). Additionally we have also demonstrated that intracellular adhesion molecule 1 (ICAM-1) regulates left ventricular leukocyte recruitment after TAC (75), and that both E-selectin and ICAM-1 are upregulated in the LV in response to TAC (74). However, it remains unclear whether the ligands of adhesion molecules present in T cells, play a role in leukocyte recruitment during HF. This chapter will focus on the role of CD43 in T cell recruitment during TAC induced HF.

3.3.1. CD43 is upregulated in T cells in WT mice in response to TAC.

Our studies demonstrating the importance of CD43 in E-selectin and ICAM-1 mediated Th17 cell recruitment, together with the observed upregulation of these molecules in the LV in HF, the role that T cells play in TAC induced HF (74, 102), and a few reports demonstrating a role for CD43 in two models of cardiovascular disease, prompted us to study whether CD43 played a role in TAC induced HF. We initially evaluated the expression of CD43 in T cells in response to 4 weeks TAC, the time when mice develop cardiac dysfunction. We observed that in response to TAC, WT mice had higher levels of the highly glycosylated from of CD43 in T cells isolated from cardiac draining lymph nodes as compared to WT Sham mice (Fig 3.37A-B).

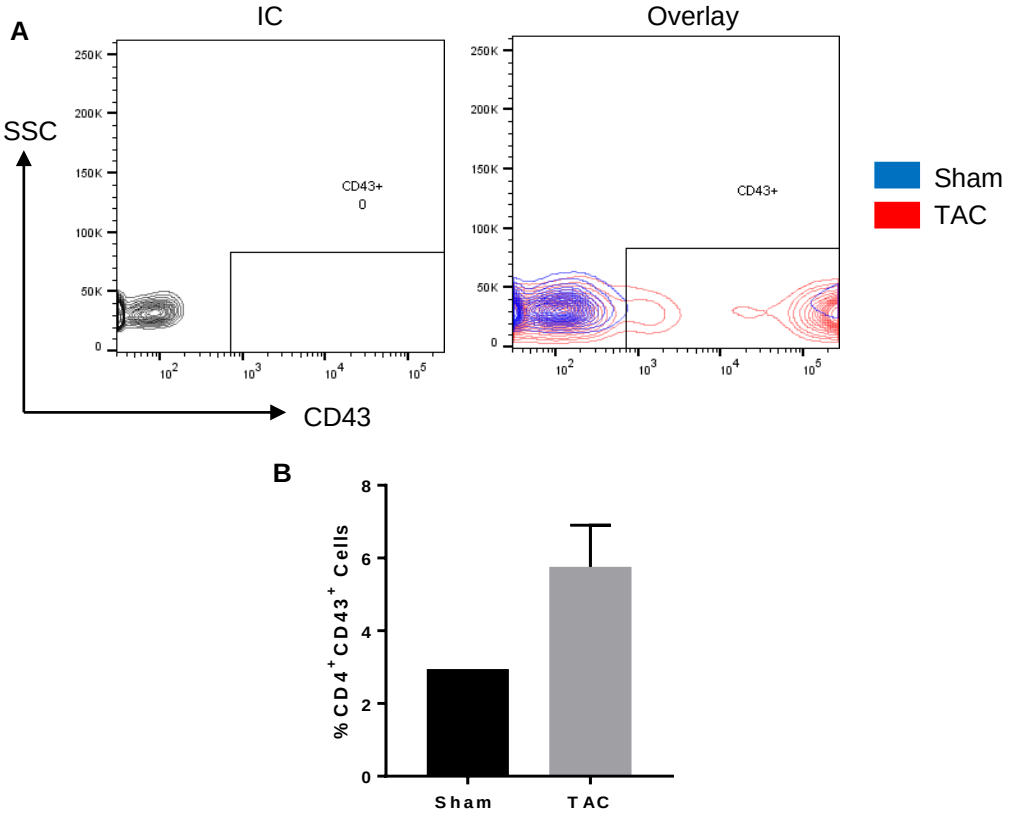

Figure 3.37: CD43 is highly expressed in WT TAC mice in response to TAC.

(A-B) Representative FACS plot demonstrates WT Sham and TAC mice with IgG and CD43 (clone 1B11) **(A)** were stained for at 4 wks after TAC from the CLN. **B.** Quantification of relative percentages from FACS Gating.

These data, together with the intra-myocardial upregulation of E-selectin and ICAM-1 reported in mice in response to TAC, led us to further investigate the role of CD43 in TAC induced HF.

3.3.2. CD43$^{-/-}$ mice have improved survival to TAC induced HF and develop similar cardiac hypertrophy as compared to WT mice.

Recent studies have demonstrated a role for CD43 in cardiovascular disease in different mouse models (22, 23). To determine whether CD43 played a role in TAC induced HF. WT and CD43$^{-/-}$ mice underwent TAC or a control Sham operation and were harvested 4 weeks post TAC. 80% of the mice survived to TAC, as compared to 50% survival in WT mice (Fig. 3.38). The majority of the mice, WT and CD43$^{-/-}$, succumbed to TAC within the first week post-surgery.

A

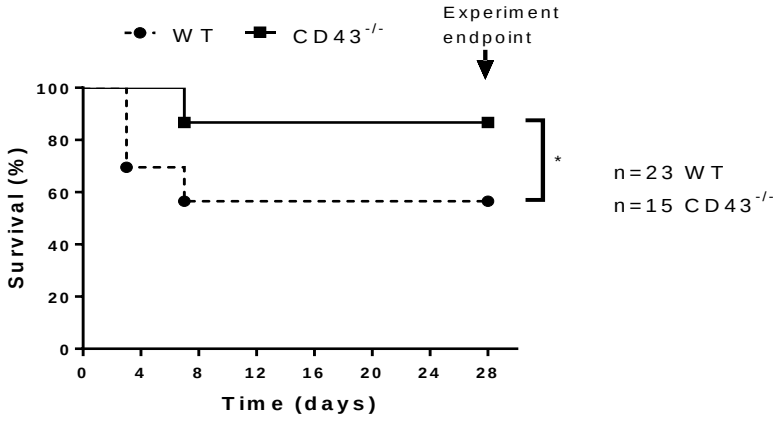

Figure 3.38: CD43$^{-/-}$ mice have improved survival to TAC induced HF as compared to WT mice.

A. WT and CD43$^{-/-}$ mice were followed for 4 wks after TAC. . *p, 0.05,

Left Ventricular (LV) weight is an indicator of LV remodeling in response to pressure overload. We observed that both WT and CD43$^{-/-}$ mice had increased LV weight normalized to tibia length (Fig 3.39A). Such increase was independent of body weight, which remained similar in both mice groups (Fig 3.39B). Increased lung weight is an indicator of pulmonary edema resulting from the inability of the heart to pump blood efficiently, and is a marker of congestive HF. While lung weight was significantly increased in WT mice, this was not significantly increased in CD43$^{-/-}$ mice. (Fig 3.39C).

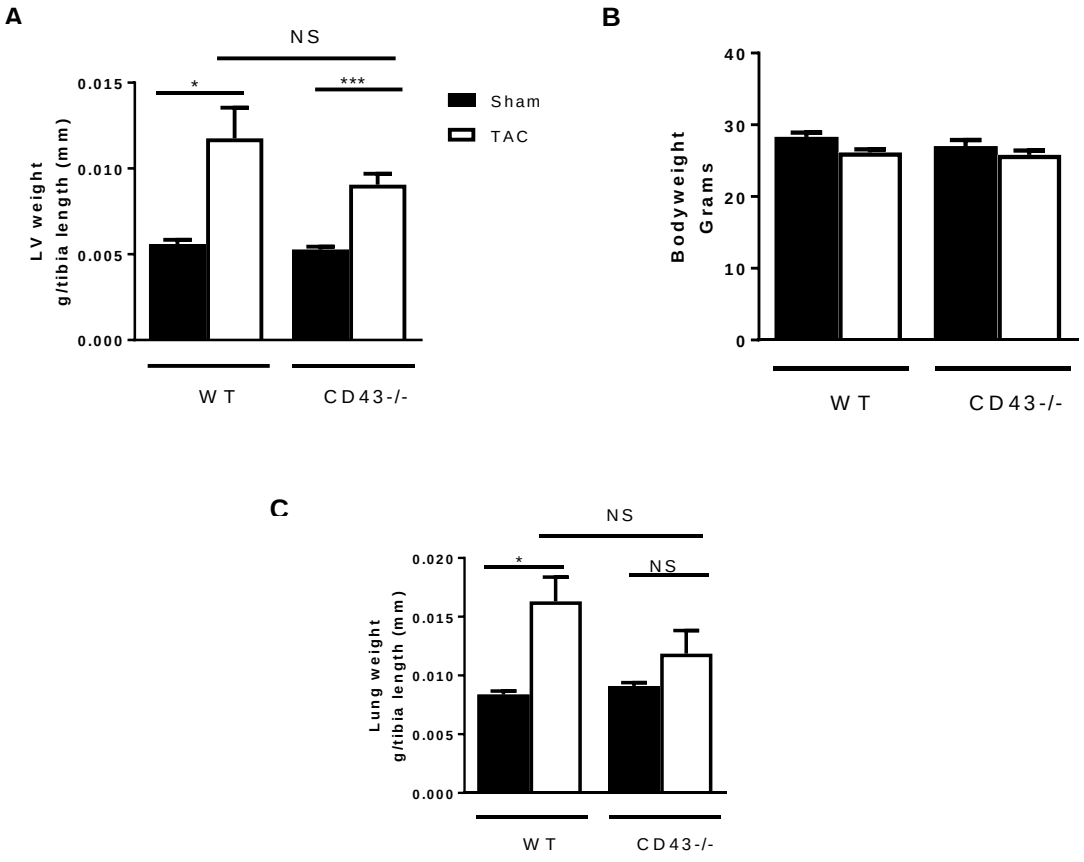

Figure 3.39: CD43$^{-/-}$ develop LV hypertrophy in response to TAC similarly to WT TAC mice.

WT and CD43$^{-/-}$ mice were sacrificed at 4 weeks. Left ventricle **(A)** was separated from right ventricle and weighed and normalized to tibia length of each mouse. **B.** Total bodyweight of WT and CD43$^{-/-}$ mice at end of 4 wks post-TAC. **C**. Lungs of WT and CD43$^{-/-}$ mice were harvested and immediately weighed and normalized to tibia length of each mouse. N=14 mice for CD43$^{-/-}$ (7 Shame, 7 TAC) and N=13 from WT (5 Sham, 8 TAC). *p, 0.05, ***p, 0.001

Increased LV weight is normally as a result of cardiomyocyte hypertrophy and/or cardiac fibrosis in response to TAC. Thus, we next sought to determine these two parameters in WT and CD43$^{-/-}$ mice to study whether CD43 played a role in such mechanisms. To evaluate cardiomyocyte hypertrophy, we determined cardiomyocyte area in WT and CD43$^{-/-}$ LV cross-sections stained with H&E by tracing cardiomyocytes and measuring their area. We observed that both WT TAC mice (Fig 3.40A) and CD43$^{-/-}$ TAC mice (Fig 3.40B) had increased cardiomyocyte area, in comparison to their respective Sham controls. More importantly the area measured between WT TAC and CD43$^{-/-}$ TAC mice was similar (Fig 3.40C). Taken together, our data demonstrate that WT and CD43$^{-/-}$ mice both develop cardiomyocyte and LV hypertrophy in response to TAC, but that CD43$^{-/-}$ mice have an increased survival rate.

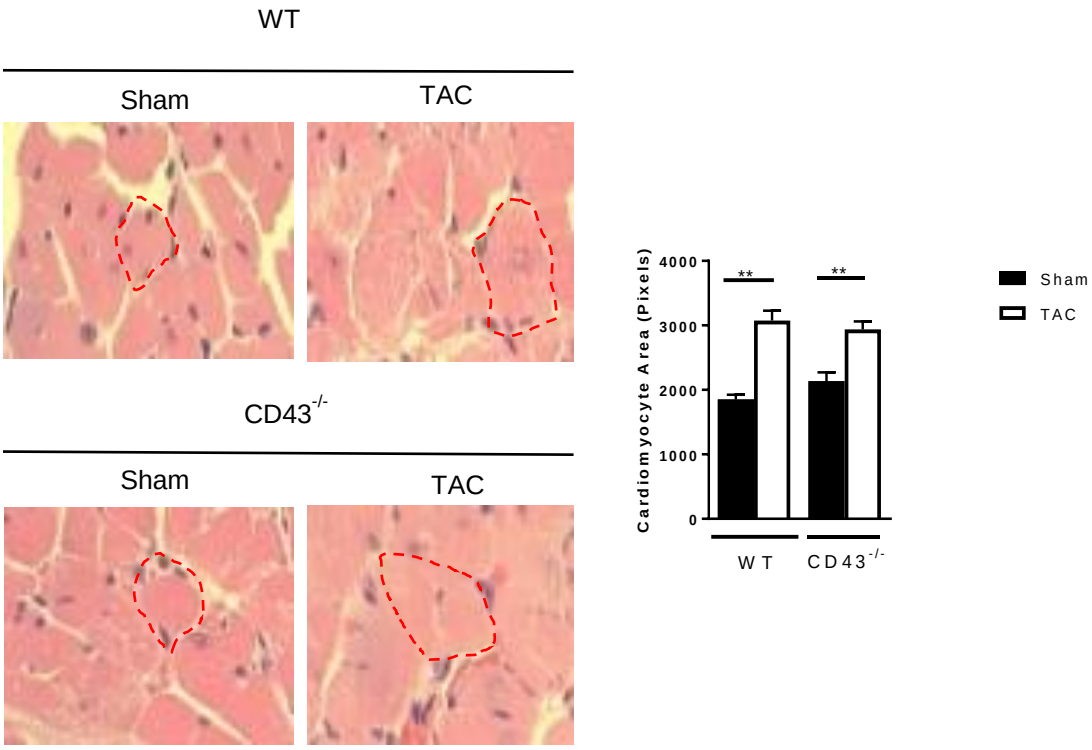

Figure 3.40: WT and CD43$^{-/-}$ mice have increased cardiomyocyte area in response to TAC induced HF.

A-B. Representative images of H&E sections of the LV at 40X of Sham and TAC WT and CD43$^{-/-}$ mice. In response to TAC WT (A) and CD43$^{-/-}$ (B) mice develop similar LV hypertrophy as observed with increased cardiomyocyte area. C. Quantification of cardiomyocyte area from 20X in pixels. 10 cardiomyocyte were measured per each field of view with 3 fields of view of the LV obtained for each individual mouse. . **p, 0.01,

This data confirms that in response to TAC, CD43-/- and WT mice develop similar LV hypertrophy. However, CD43-/- mice have an increased survival rate to TAC as compared to WT mice, therefore supporting a protective role for CD43 in HF.

3.3.3. LV fibrosis is reduced in CD43$^{-/-}$ mice as compared to WT mice.

Another hallmark of pathological cardiac remodeling leading to HF is cardiac fibrosis. Given that CD43$^{-/-}$ mice had increased survival, we hypothesized that such protection was

in part mediated by decreased fibrosis in response to TAC. To determine fibrosis, we stained LV cross-sections with Picrosirius Red and quantified collagen deposition and LV fibrosis based in the positive staining. We observed that CD43$^{-/-}$ TAC mice developed significantly less perivascular fibrosis as compared to WT TAC mice, which had increased perivascular fibrosis as compared to its Sham control (Fig 3.41A-B). Indeed, the CD43$^{-/-}$ mice have the same levels of perivascular fibrosis as does the CD43$^{-/-}$ Sham mice (Fig 3.41C).

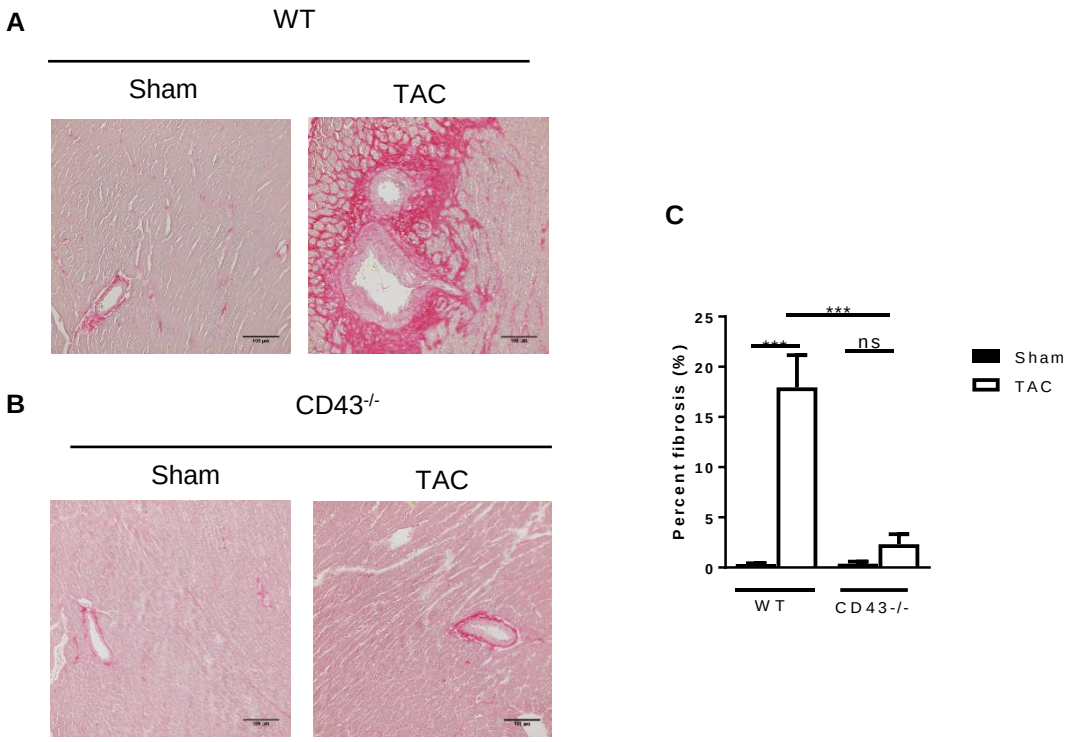

Figure 3.41: CD43 is necessary for the development of perivascular fibrosis.

A-B. Representative images of WT and CD43$^{-/-}$ mice at 40X of picrosirius red strained sections of Sham and TAC mice. **C.** Quantification of perivascular fibrosis of WT and CD43$^{-/-}$ Sham and TAC mice. 3 fields of view were acquired per each mouse for quantification using ImageJ. N=14 mice for CD43$^{-/-}$ (7 Sham, 7 TAC) and N=13 from WT (5 Sham, 8 TAC). ***p, 0.001

Interstitial fibrosis, although increased in CD43$^{-/-}$ TAC mice vs Sham, it was also significantly decreased in CD43$^{-/-}$ TAC mice compared to WT TAC mice (Fig 3.42A-C).

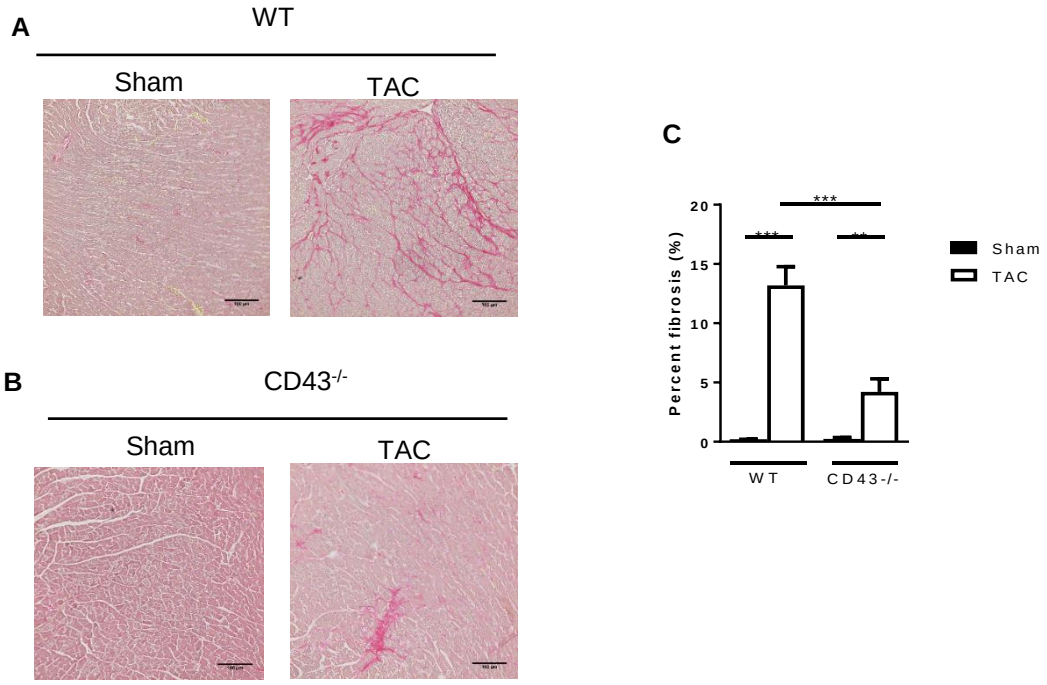

Figure 3.42: CD43$^{-/-}$ develop less interstitial fibrosis the LV in response to TAC as compared to WT mice.

A-B. Representative images of WT and CD43$^{-/-}$ mice at 40X of picrosirius red strained sections of Sham and TAC mice. **C.** Quantification of interstitial fibrosis of WT and CD43$^{-/-}$ Sham and TAC mice. 3 fields of view were acquired per each mouse for quantification using ImageJ. N=14 mice for CD43$^{-/-}$ (7 Sham, 7 TAC) and N=13 from WT (5 Sham, 8 TAC). **p, 0.01, ***p, 0.001

Our data demonstrates that CD43$^{-/-}$ mice do not develop perivascular fibrosis, and develop significantly less interstitial fibrosis in response to TAC as compared to WT mice. These findings could suggest a mechanism contributing to the increased survival to TAC induced HF observed in CD43$^{-/-}$ mice.

3.3.4. CD43$^{-/-}$ mice have decreased leukocyte infiltration into the Left Ventricle in response to TAC.

Our lab and others have previously demonstrated that T cell dependent LV inflammation contributes to pathological cardiac remodeling and HF since T cell deficient mice are protected from perivascular and interstitial fibrosis (74, 75, 102). LV inflammation is indeed directly associated with LV fibrosis. We hypothesized that CD43 contributes to immune cell infiltration and inflammation in the LV in response to TAC. To test this, we determined LV inflammation by analyzing infiltrated leukocytes in LV cross-sections stained with H&E in Sham and TAC mice. We observed that CD43$^{-/-}$ TAC mice had significantly reduced, almost inexistent LV inflammation as compared to WT TAC mice and this was comparable to the level of leukocyte infiltration found in Sham control mice (Fig. 3.43A-C).

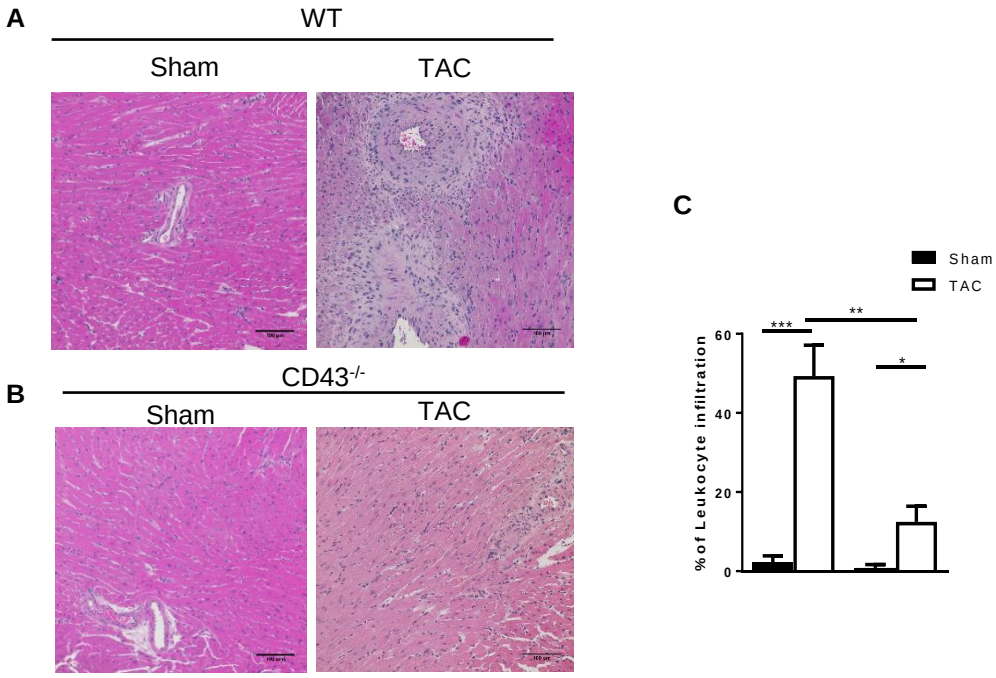

Figure 3.43: CD43$^{-/-}$ mice have decreased leukocyte infiltration into the Left Ventricle after 4 wks of TAC.

A-B. Representative images of WT and CD43$^{-/-}$ left ventricle H&E sections of Sham and TAC mice. **C**. Quantification of leukocyte infiltration into the LV of WT and CD43$^{-/-}$ mice was calculated from 3 representative fields of view per each individual sample. N=10 mice for CD43$^{-/-}$ (5 Shame, 5 TAC) and N=10 from WT (5 Sham, 5 TAC). *p, 0.05, **p, 0.01

Interestingly, LV leukocyte infiltration correlated with LV fibrosis in perivascular areas of WT TAC mice in the same LV cross sections. (Fig 3.44 A-B). The CD43$^{-/-}$ TAC mice had little leukocyte infiltration, and barely any positive stain for perivascular fibrosis as compared to CD43$^{-/-}$ Sham mice and WT TAC mice (Fig 3.44 C-D).

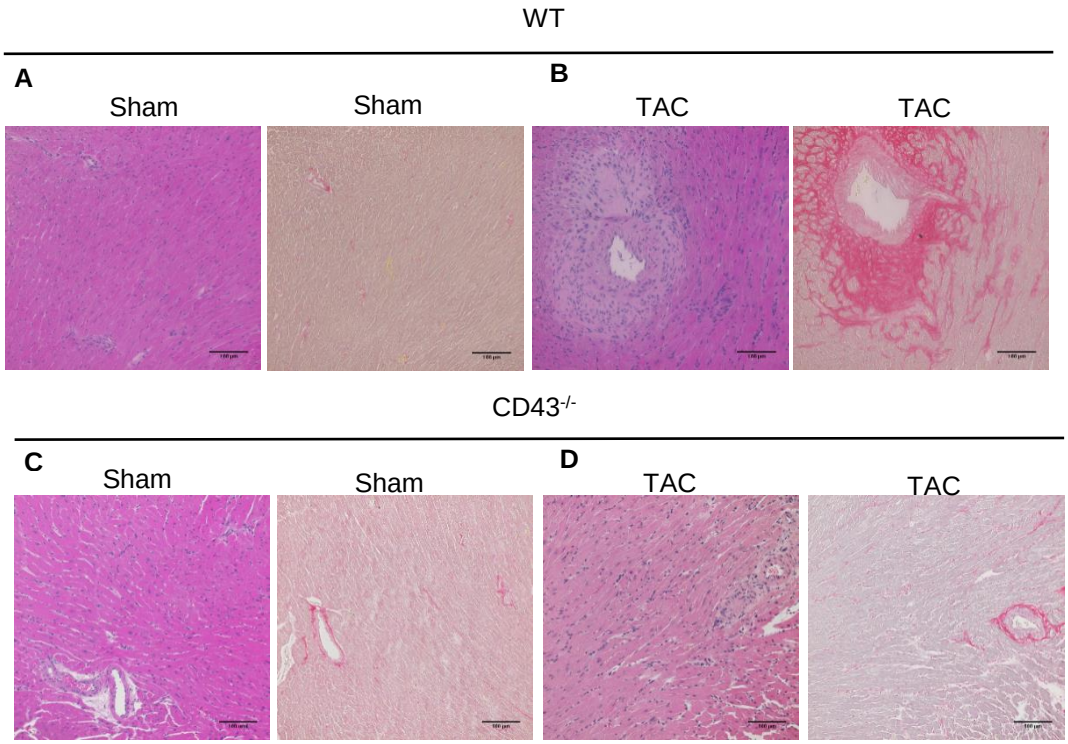

Figure 3.44: CD43$^{-/-}$ mice have decreased leukocyte infiltration into the Left Ventricle after 4 wks of TAC.

A-D. Representative images of Sham and TAC WT and CD43$^{-/-}$ mice of H&E and Picosirius red staining pointing at leukocyte infiltration and fibrosis around the vessel. Scale bar measures 10um. Images shown at 20X magnification.

Our data demonstrates that CD43$^{-/-}$ mice have decreased LV fibrosis and leukocyte infiltration into the LV. Moreover, leukocyte infiltration co-localizes with fibrosis in the same cross-sections. These data are in line with previous work demonstrating that T cells regulate cardiac fibrosis in the model of TAC, and highlights a new role for CD43 in leukocyte infiltration to the heart and in cardiac fibrosis.

3.3.5. Cardiac function is preserved in CD43$^{-/-}$ mice in response to TAC.

We have shown that CD43$^{-/-}$ mice develop LV hypertrophy and cardiac myocyte hypertrophy in response to TAC. Additionally our findings establish a role for leukocyte infiltration associated with perivascular fibrosis in WT mice but not in CD43$^{-/-}$ mice in response to TAC. These findings brought to question whether in CD43-/- mice hypertrophy was sufficient to induce cardiac dysfunction. Thus, we next determined the cardiac function using non-invasive hemodynamics such as Echocardiography. We observed that while WT mice had decreased ejection fraction, a parameter also decreased in patients with HF, CD43$^{-/-}$ TAC mice had a preserved Ejection Fraction (Fig 3.45A). Additionally we observed that CD43$^{-/-}$ TAC mice also had preserved Fractional Shortening (Fig 3.45B), which is an estimate of myocardial contractility, as compared to WT TAC mice, which had a significantly decreased Fractional Shortening. Echocardiography also determined other parameters such as anterior and posterior wall thicknesses, which were both similarly increased in WT and CD43$^{-/-}$ mice in response to TAC. This is in line with CD43$^{-/-}$ developing similar hypertrophy as WT mice. The heart rate was significantly increased in

WT TAC mice as compared to Sham mice, in contrast to TAC CD43$^{-/-}$, which had lower heart rates, another indicator of better heart function in response to TAC (Table 3.1).

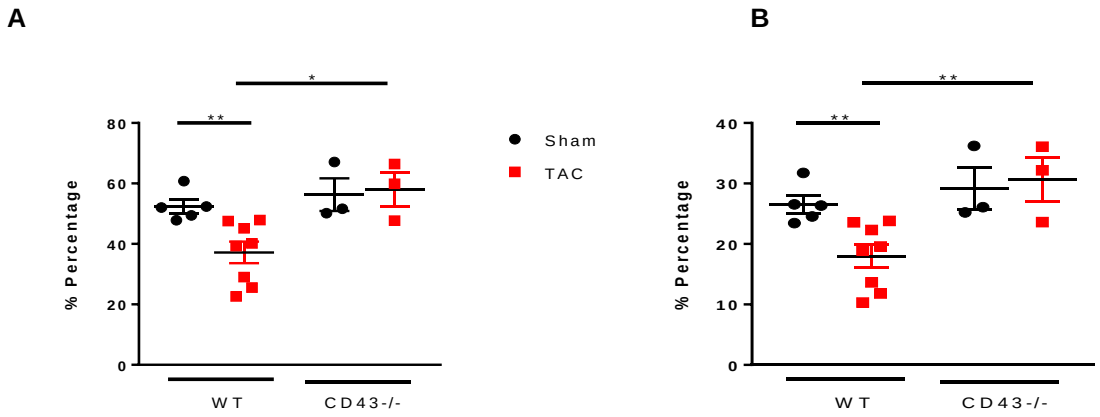

Figure 3.45: Cardiac function is preserved in CD43$^{-/-}$ mice in response to TAC.

A. Ejection Fraction of WT and CD43$^{-/-}$ mice in response to TAC as compared to Sham Controls was determined by echocardiography. **B.** Fractional shortening of WT and CD43$^{-/-}$ mice in response to TAC as determined by echocardiography. N= 6 mice for CD43$^{-/-}$ (3 Shame, 3 TAC) and N=13 from WT (5 Sham, 8 TAC). . *p, 0.05, **p, 0.01,

Parameter	WT Sham	WT TAC	CD43$^{-/-}$ Sham	CD43$^{-/-}$ TAC
Posterior Wall Thickness	0.8821 ± 0.0394	1.327 ± 0.1088 *	0.9717 ± 0.1273	1.278 ± 0.0814 *
Anterior Wall Thickness	0.8841 ± 0.0324	1.219 ± 0.06778 *	1.168 ± 0.1717	1.367 ± 0.0375 *
Heart Rate	417.5 ± 23.58	515.9 ± 18.13 *	431.5 ± 2.5	419.3 ± 18.94 #

Table 3.1: Cardiac function parameters in WT and CD43$^{-/-}$ mice.

TAC indicates thoracic aortic constriction; WT, wild-type; and LV, Left ventricle. Values are means ± SD, *P<0.05, 4 weeks of TAC versus Sham for each genotype. # P<0.05, 4 weeks of TAC between genotypes. N= 6 mice for CD43$^{-/-}$ (3 Sham, 3 TAC) and N=13 from WT (5 Sham, 8 TAC). . *p, 0.05, **p, 0.01,

These data indicate that CD43$^{-/-}$ mice have preserved cardiac function as compared to WT mice in response to TAC.

3.3.6. CD43$^{-/-}$ mice have decreased LV CD4+ and CD11b+ infiltration as compared to WT mice in response to TAC.

Our data indicates that CD43$^{-/-}$ mice have an increased survival rate in response to TAC likely as a result of preserved cardiac function and decreased fibrosis of the LV. Additionally we have demonstrated that there is impaired leukocyte recruitment into the LV in response to TAC. More specifically, we have previously shown that absence of T cells during TAC is beneficial and prevents deposition of collagen and preserves cardiac function (74). We next determined T cell and monocyte recruitment in the LV in response to TAC in CD43$^{-/-}$ mice in LV frozen cross-sections stained with CD4^{+} T cells and CD11b^{+} monocytes using immunohistochemistry. We observed that CD43$^{-/-}$ TAC mice had significantly decreased CD4^{+} T cell infiltrates (pointed with black arrow) in the LV as compared to WT mice in response to TAC (Fig. 3.46A-B). While CD4^{+} T cells can still be recruited into the LV in response to TAC, absence of CD43 significantly decreases the number of cells found at 4 wks after TAC (Fig 3.46C).

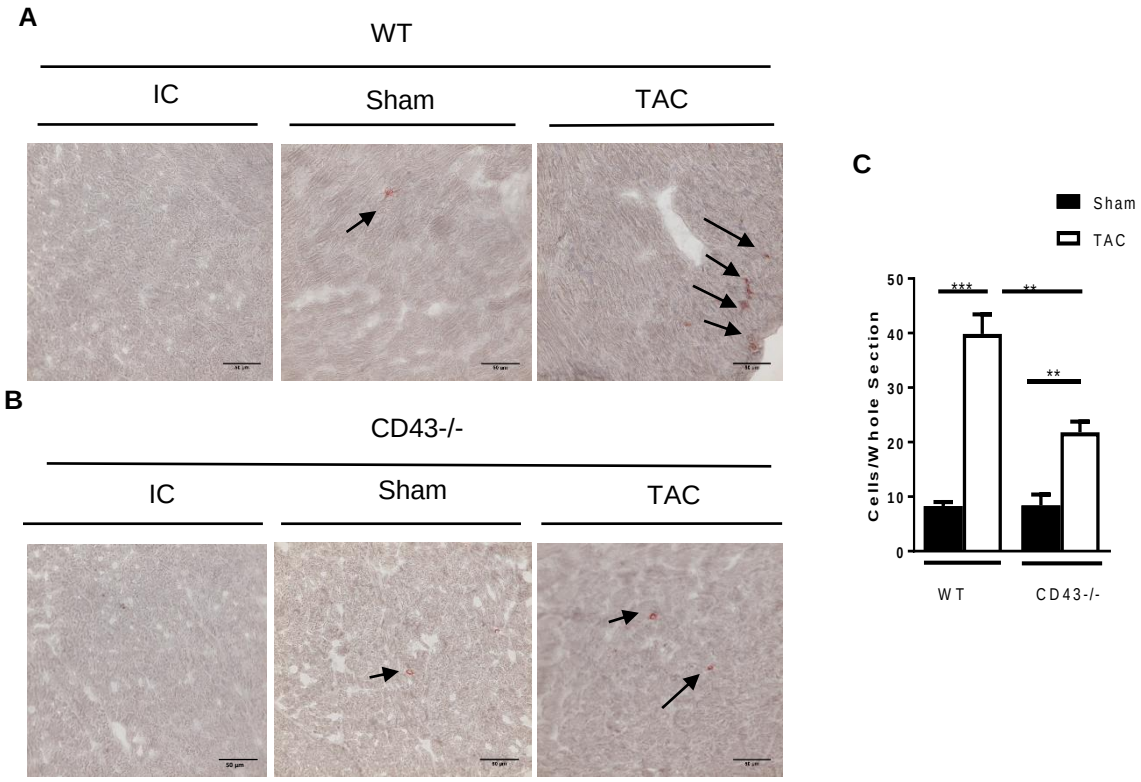

Figure 3.46: CD43$^{-/-}$ regulates recruitment of CD4^{+} T cells into the Left Ventricle in response to TAC.

A-B. Representative images of immunohistochemistry on WT and CD43-/- mice. Arrows indicate positive staining for CD4^{+} **C.** Quantification of CD4 infiltrates in WT and CD43$^{-/-}$ Sham and TAC across the whole LV section. **D.** Quantification of CD4 positive staining's per field of WT and CD43$^{-/-}$ Sham and TAC LV. CD4 infiltrates were calculated by counting CD4 positive stains for each whole section. N=10 mice for CD43$^{-/-}$ (5 Sham, 5 TAC) and N=10 from WT (4 Sham, 7 TAC). **p, 0.01, ***p, 0.001

Interestingly we observed that there were significantly less CD11b^{+} cells in the LV of CD43$^{-/-}$ TAC mice as compared to TAC (Fig. 3.47-AB). However, this decrease in monocytes being recruited into the LV was not as pronounced as the amount of CD4^{+} T cells (Fig 3.47C).

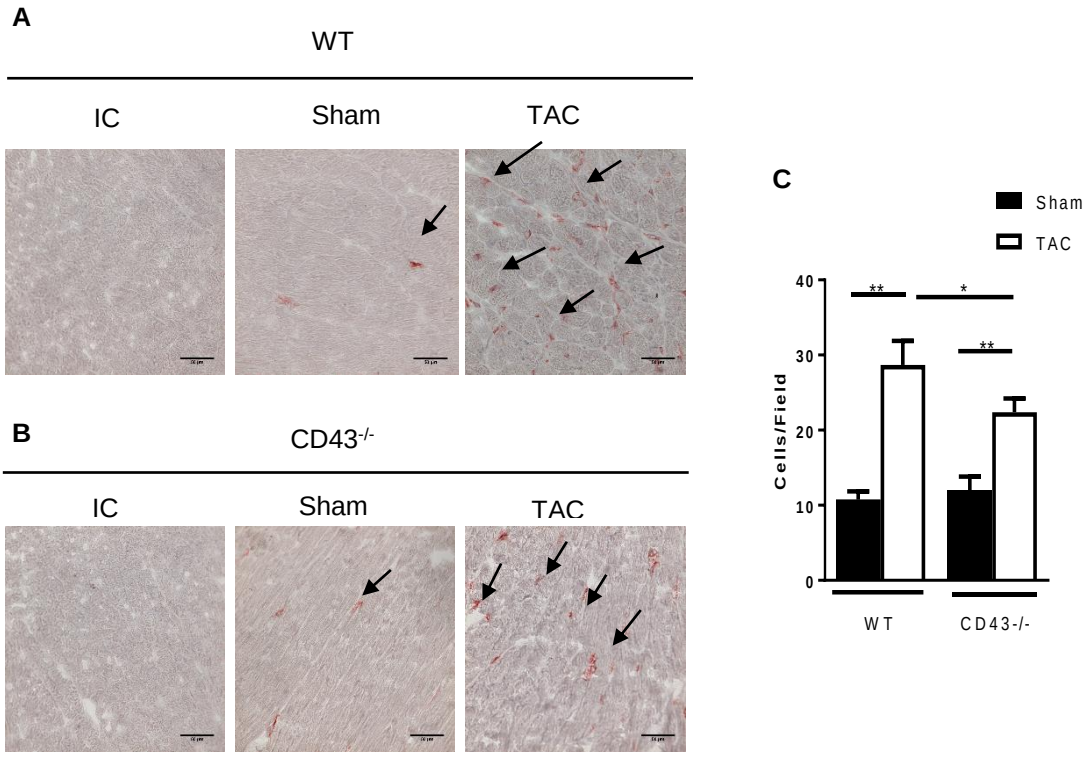

Figure 3.47: CD43$^{-/-}$ mice have decreased CD11b^{+} infiltrates into the Left Ventricle as compared to WT in response to TAC.

A-B. Representative images of immunohistochemistry on WT and CD43$^{-/-}$ mice. Arrows indicate positive staining for CD11b^{+} **C.** Quantification of CD11b^{+} infiltrates in WT and CD43$^{-/-}$ Sham and TAC across the whole LV section. **D.** Quantification of CD11b positive staining's per field of WT and CD43$^{-/-}$ Sham and TAC LV. CD11b^{+} infiltrates were calculated by using the average of CD11b positive stains for 3 fields of vision per each section. N=10 mice for CD43$^{-/-}$ (5 Sham, 5 TAC) and N=10 from WT (4 Sham, 7 TAC). . *p, 0.05, **p, 0.01,

Specific adhesion molecules such as ICAM-1 have been shown to be essential for the recruitment of T cells and monocytes into the LV in response to TAC (75). To determine whether the significant decrease in CD4^{+} T cell recruitment and CD11b^{+} monocyte cells was due to absence of CD43 or to a defect in ICAM-1, we stained sections of the LV for this adhesion molecule. We observed that WT TAC mice (Fig 3.48A) and CD43$^{-/-}$ TAC mice (Fig 3.48B), both had upregulation of ICAM-1 on sections of the LV, suggesting that

the decrease in leukocyte infiltration into the LV in response to TAC is due to absence of CD43 in the leukocytes but not to a defect in upregulation of LV ICAM-1.

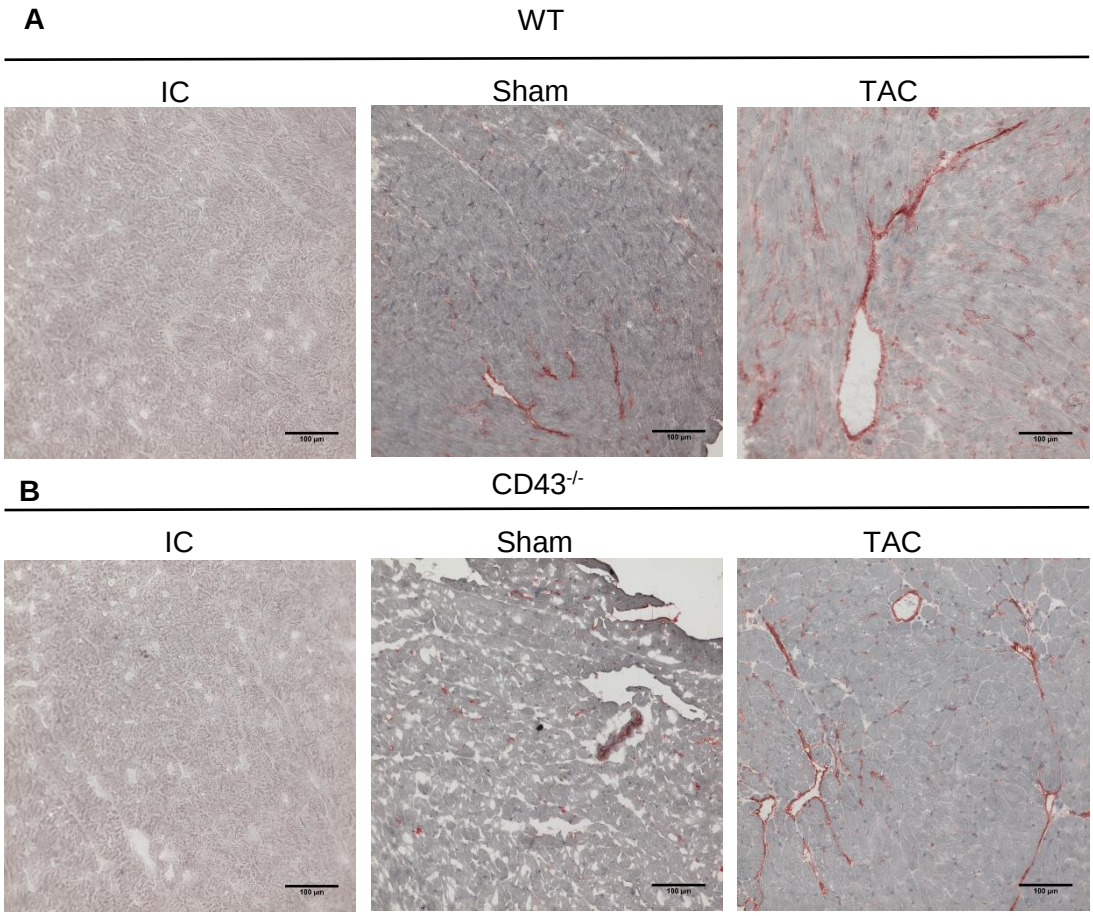

Figure 3.48: Expression of ICAM-1 in the LV in response to TAC is not affected by absence of CD43.

A-B. Representative images of immunohistochemistry on WT and CD43$^{-/-}$ mice. In brown is the staining for ICAM-1. Imaging was captured at 20X magnification with 3 fields of vision per each sample.

Our data demonstrates that absence of CD43 impacts CD4^{+} T cell and CD11b^{+} monocyte recruitment to the LV in response to TAC.

3.3.7. CD43$^{-/-}$ mice have similar T cell activation in the cardiac draining lymph nodes as WT mice in response to TAC.

We have demonstrated that CD43 contributes to leukocyte recruitment, cardiac fibrosis cardiac dysfunction and survival in TAC induced HF. However, as previously mentioned in the present thesis, CD43 is involved in a number of different functions aside of leukocyte recruitment, and these include T cell signaling and differentiation in specific mouse strains and specific models of autoimmunity in such strains (18, 21, 24, 90). It has previously been reported that CD4^{+} T cells but not CD8^{+} T cells are the main players in TAC as CD4$^{-/-}$ mice, but not CD8$^{-/-}$ mice are protected from TAC induced HF (102). Moreover, we have previously reported that T cells become activated in the cardiac draining lymph node of TAC mice. we next sought to determine whether T cell activation in response to TAC was occurring in CD43$^{-/-}$ mice. To this end, we isolated the cardiac draining lymph nodes of WT and CD43$^{-/-}$ Sham and TAC mice and counted total cell numbers. Isolated cells were then stained for CD4, CD44 and CD62L and assessed via flow cytometry to determine effector T cell activation (CD4^{+}CD44highCD62Llow). We observed that CD43$^{-/-}$ TAC mice and WT TAC mice both had an increase in CD4 T cells in the cardiac draining lymph node as compared to their Sham counterparts (Fig 3.49A-B), as well as an increase in activated cells (CD4^{+}CD44^{high}CD62L^{low}) (Fig 3.49C-D).

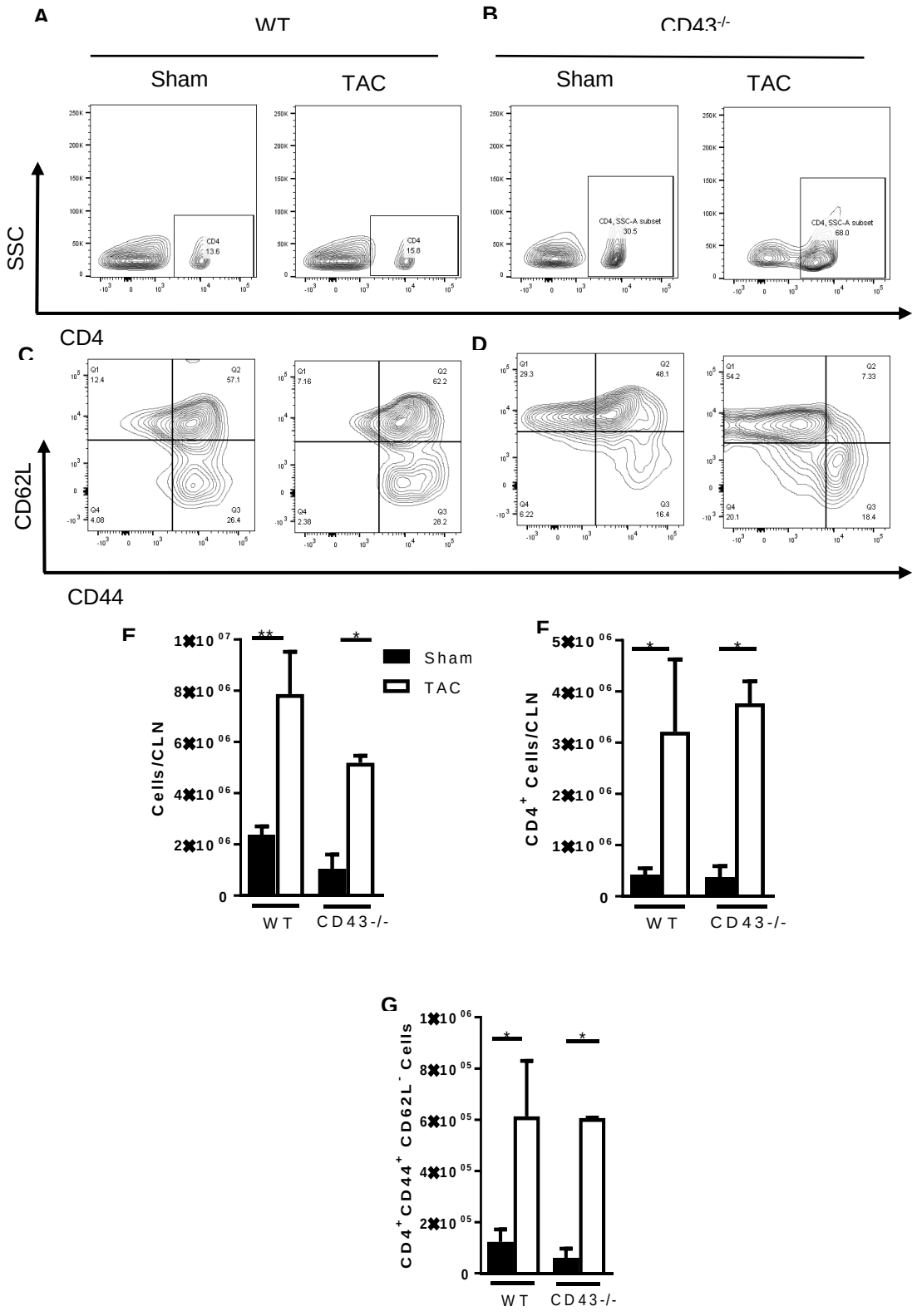
A
WT
Sham
TAC
B
CD43-/-
Sham
TAC
SSC
CD4
CD4
13.6
CD4
15.8
CD4, SSC-A subset
30.5
CD4, SSC-A subset
68.0
C
D
CD62L
CD44
Q1
12.4
Q2
57.1
Q4
4.08
Q3
26.4
Q1
7.16
Q2
62.2
Q4
2.38
Q3
28.2
Q1
29.3
Q2
48.1
Q4
6.22
Q3
16.4
Q1
54.2
Q2
7.33
Q4
20.1
Q3
18.4
E
Cells/CLN
Sham
TAC
WT
CD43-/-
F
CD4+ Cells/CLN
WT
CD43-/-
G
CD4+CD44+CD62L- Cells
WT
CD43-/-

Figure 3.49: CD43 does not impact T cell activation in the cardiac lymph node at 4 wks in response to TAC.

A-D. Representative FACS staining for CD4 cells **(A-B)** of Sham and TAC mice from WT **(A)** and CD43$^{-/-}$**(B)** mice and Activated T cells **(C-D)**. **E.** Quantification of total cells per cardiac lymph node was calculated after cell counting and CD4 T cell numbers **(F)** were calculated form the percentage obtained in the FACS of each sample and back calculating to total cells. Activated T cell **(G)** numbers were back calculated from CD4 cell numbers. N=4 mice for CD43$^{-/-}$ (2 Sham, 2 TAC) and N=8 from WT (3 Sham, 5 TAC). . *p, 0.05, **p , 0.01,

We demonstrate that CD43 does not contribute to T cell activation in the cardiac draining lymph nodes in response to TAC. Hence, the protection observed in CD43$^{-/-}$ mice is not due to a lack of T cell activation in response to TAC, but to leukocyte recruitment.

3.3.8. Conclusion

In this chapter we have demonstrated that CD43 plays a crucial role in leukocyte recruitment to the LV in response to TAC in the model of TAC induced HF. We found that WT mice T cells express higher levels of CD43 in response to TAC as compared to Sham mice. Absence of CD43 resulted in higher survival to TAC when compared to WT mice which succumbed to TAC within the first week post-surgery. Our results demonstrate for the first time a role for CD43 in TAC induced HF that is associated with the development of cardiac fibrosis, T cell and monocyte LV infiltration, and systolic dysfunction, but not with LV or myocyte hypertrophy. While we have shown that absence of CD43 can impact CD4^{+} T cell recruitment, the decrease in the amount of CD11b^{+} monocytes we observed was not expected, as CD43 has not been previously reported to mediate monocyte adhesion to the vascular endothelium. It is therefore very likely that the absence of CD4^{+} T cells being able to successfully infiltrate the LV after TAC regulates subsequent recruitment of other CD11b^{+} leukocytes. We also demonstrate that CD43$^{-/-}$ mice had similar T cell activation as did WT mice in the cardiac draining lymph nodes in response

to TAC, thus the impaired LV infiltration of $CD4^+$ T cells is likely due to failure in recruitment but not in T cell activation in response to TAC.

Chapter 4: Discussion

4.1. Overview

In this section we discuss the role of CD43 in Th17 cell recruitment in inflammation, autoimmunity and cardiovascular disease. CD43 is uniquely expressed in Th17 cells as compared to Th1 cells, and functions as an E-selectin ligand and a pro-adhesive molecule that aids in adhesion to ICAM-1, apical migration and transmigration. Additionally, CD43 is critical for the development of cardiac fibrosis and loss of cardiac function in a model of pressure overload induced heart failure. Each of these findings correspond to the three chapters in the results section in this thesis that describe different aspects and functions of CD43 and are discussed in further detail in this section. Chapter 3.1 of this section discusses the role of CD43 as an E-selectin ligand in Th17 cells *in vitro* and *in vivo* in models of recruitment and E-selectin dependent rolling. Chapter 3.2 in this section discusses the role of CD43 in trafficking of antigen specific Th17 cells to the CNS in a model of EAE and the mechanisms of CD43 regulation of Th17 interactions with ICAM-1 at different steps of the leukocyte recruitment cascade. Finally Chapter 3.3 in this section discusses a novel role for CD43 regulating the development of the pathology and immune cell recruitment that leads to heart failure. Taken together, our data contributes to our understanding of novel mechanisms behind the interaction between the cardiovascular system and the immune system and how Th17 cells are recruited in the context of autoimmune and cardiovascular disease.

4.2. Discussion Chapter 3.1: Determine the role and functionality of CD43 mediating Th17 cell interactions with E-selectin and the activated vascular endothelium.

In this chapter, we have investigated the contribution of E-selectin ligands expressed by T cells to adhesion of murine Th17 cells to E-selectin *in vitro* and identified the glycoprotein CD43 as a major functional Th17 cell E-selectin ligand *in vitro* that also regulates Th17 cell recruitment and rolling interactions with the vascular endothelium *in vivo*. We report for the first time a detailed description of the expression and functionality of T cell expressed E-selectin ligands in murine Th17 cells, and suggest that there are no additional glycoproteins that function as E-selectin ligands expressed on Th17 cells. Moreover, we present CD43 as a major E-selectin ligand with the unique feature of mediating Th17 cell adhesion to E-selectin and the activated vascular endothelium without requiring the cooperation of PSGL-1. We suggest that this specificity of E-selectin ligand expression contributes to the differences in T cell subset recruitment during inflammation.

Multiple studies over the years have identified glycoconjugates that function as E-selectin ligands. Most molecules were characterized in neutrophils (15, 77, 84) or activated T cells, including murine Th1 cells (50, 51) and human Cutaneous Lymphocyte Antigen (CLA^+) T cells (43), before the pro-inflammatory Th17 T cell subset emerged in 2008. Except for the best characterized and initially described E-selectin ligand, PSGL-1, which is also a ligand for P-selectin and functional in neutrophils and T cells (15), the other two T cell described E-selectin ligands known as CD43 and CD44, were shown to be functional only in cooperation with PSGL-1 (50, 51, 77). CD44 acts as an E-selectin ligand in neutrophils (14) and T cells (77), and CD43 does so in T cells only (50, 51). Our data confirms the expression of all three described T cell E-selectin ligands on Th17 cells, and reveals that among the three, the highly glycosylated form of CD43 has a unique expression pattern

by FACS different than the classic bimodal expression described for Th1 cells (103). This may reflect a difference in the glycoconjugates decorating CD43 in Th17 and Th1 cells, possibly sialyl Lewis X (sLx), the minimal E-selectin ligand (20). The known antibodies to detect sLx are for humans, and not mice, preventing us from testing this hypothesis. In addition, our findings indicate, that CD43 is on its own a uniquely important E-selectin ligand and does not require cooperation with PSGL-1 to mediate adhesion to E-selectin, and this is T cell subset specific, as it is not observed on Th1 cells. Our data demonstrates that sorted Th1 cells expressing high CD43 or medium CD43 both adhere to E-selectin in lower numbers than Th17 cells, suggesting that CD43 functions differently in both T cell subsets. A glycomics analysis of Th1 and Th17 cell subsets would define whether CD43 glycosylation in Th17 and Th1 cells can definitively explain this subset specificity. Our conclusion is supported by our studies evaluating E-selectin ligand functionality under shear flow conditions using two different approaches. First by showing that each ligand directly purified from Th17 cells supports rolling interactions with E-selectin, and second by generating Th17 cells from different E-selectin ligand deficient mice and evaluating their interactions with E-selectin immobilized on glass coverslips.

Our blot rolling studies indicate quantitative differences in the number of E-selectin dependent rolling events mediated by Th17 cell expressed PSGL-1, CD43 and CD44: PSGL-1 and CD43 support significantly more E-selectin dependent rolling than CD44 that was abrogated in the presence of EDTA and not observed with CHO-MOCK cells that do not express E-selectin. Our second approach further supports our findings indicating that PSGL-1$^{-/-}$ Th17 cells have decreased adhesion to E-selectin, and PSGL-1$^{-/-}$CD43$^{-/-}$ an even greater decrease in adhesion with CD43$^{-/-}$ Th17 cells binding in similar numbers to PSGL-1$^{-/-}$CD43$^{-/-}$ Th17 cells. In contrast, Th17 cells that lack CD44 in addition to PSGL-1 (PSGL-1$^{-/-}$CD44$^{-/-}$) do not show further decreased adhesion to E-selectin as compared

with PSGL-1$^{-/-}$, indicating that CD44 is not a functional E-selectin ligand for Th17 cells *in vitro.* This differs somewhat from what we observed in the blot rolling assays where CD44 played a minor, but functional role on E-selectin dependent adhesion. We believe this discrepancy between the two approaches is likely due to our striking finding that CD43 plays a major role in Th17 cell adhesion to E-selectin. The PSGL-1$^{-/-}$ CD44$^{-/-}$ Th17 cells express CD43, which may be obscuring the minor role for CD44 observed in the blot rolling assays performed on immunopurified CD44 from Th17 cells and therefore in the absence of CD43. Our data using PSGL-1$^{-/-}$CD44$^{-/-}$ Th1 cells to control for Th17 cell specificity slightly differs from a recent publication demonstrating that PSGL-1$^{-/-}$CD44$^{-/-}$ Th1 cells have impaired adhesion to E-selectin *in vitro* as compared with PSGL-1$^{-/-}$ Th1 cells (77) which could be due to the different *in vitro* adhesion assays used by Nacher et al (static) vs ours (flow conditions on immobilized E-selectin). Our combined results using both approaches as well as highly expressing sorted CD43 Th17 and Th1 cells support the idea that CD43 is a major prominent ligand that mediates Th17 cell, but not Th1 cell, adhesion to E-selectin, and that its different role in T cell subsets is not exclusively due to different expression levels, but also potentially to different functionality of CD43 itself in Th17 cells.

Our rationale to study potential novel E-selectin ligands expressed on Th17 cells comes from our results indicating that TKO Th17 cells showed residual adhesion to immobilized E-selectin implying that uncharacterized and potentially novel E-selectin ligands may exist. However, the two approaches we used suggested that this is not the case. First, treatment of TKO Th17 cells with the cysteine-protease bromelain, which should remove all surface proteins (85), did not completely eliminate TKO Th17 cell E-selectin activity. Second, using blot rolling assays we could not detect any area that supported E-selectin dependent rolling on whole Th17 cells lysates generated from TKO mice. These studies cannot rule out the possibility of glycolipids acting as E-selectin ligands, as previously postulated in T

cells (86, 104, 105). Since glycolipids migrate with the dye front when loaded on SDS-PAGE gel they are hence lost. If other glycoprotein ligands exist besides PSGL-1 and CD43 that mediate Th17 cell adhesion to E-selectin, they are below detectable levels using our two approaches.

We used the dermal air pouch model to study Th17 cell recruitment in response to defined stimuli *in vivo*. We used CCL20, being a specific chemoattractant towards $CCR6^{+}$ cells such as Th17 cells, and TNF-α, which recruits several leukocytes and T cell subsets besides Th17 cells (47, 54, 106-108) . Our studies support the role for CD43 in Th17 cell recruitment, and also exemplify the complexity of addressing the relevance of functional E-selectin ligands to E-selectin interactions *in vivo.* This is due primarily to an existing redundancy between E-selectin and P-selectin in mediating leukocyte recruitment, as demonstrated in several studies, including the air pouch model, employing E-$selectin^{-/-}$ mice (47, 109-111) and PSGL-$1^{-/-}$ mice (51). Secondly, the redundant repertoire of functional E-selectin ligands expressed on leukocytes (15) together with the involvement of several leukocyte types recruited expressing this repertoire. Our data using CCL20 as a chemoattractant supports a non-redundant role of CD43 as an E-selectin ligand in Th17 cells. Using TNF-α as a pro-inflammatory stimulus, we find this role is T cell subset specific *in vivo,* since both Th1 and Th17 cells are recruited in WT mice whereas impaired Th17 cell recruitment is observed in $CD43^{-/-}$ mice. Our results are in line with previous studies demonstrating that $CD43^{-/-}$ and WT mice have similar inflammation and leukocyte recruitment in response to delayed type hypersensitivity, implying that CD43 alone does not regulate recruitment (50, 51) in this model mediated mainly by Th1 cells and neutrophils (89, 112) where CD43 does not itself function as an E-selectin ligand.

It is worth mentioning that our observations using this model cannot be attributed to Th17 cell- E-selectin mediated interactions, given that T cell recruitment into the air pouch does

not exclusively depend on the adhesion molecule E-selectin (47). A likely possibility is that CD43 can adhere to other adhesion putative ligands. Among these other adhesion molecules, we discard CD43 regulating Th17 cell interactions with P-selectin based on our *in vitro* data demonstrating that CD43$^{-/-}$ and WT Th17 cells adhere similarly to P-selectin. We can however speculate that CD43 may regulate adhesion to ICAM-1 as an alternative mechanism that explains the decreased recruitment to the air pouch, as CD43 expressed by human T cells were shown to bind soluble ICAM-1 (94). Further studies were deemed necessary to determine whether this mechanism takes place, and if it is specific for Th17 cells, and those were included in Chapter 3.2 and are now discussed in the next section of the discussion.

It has previously been demonstrated that CD43$^{-/-}$ mice have impaired neutrophil emigration in a mouse model of recruitment to the peritoneum (113). Because neutrophils are recruited into the air pouch, our studies cannot conclude whether the observed lack of recruitment is exclusively mediated by Th17 cell CD43-E-selectin interactions with the activated endothelium. Our competitive rolling assays using a model that is highly dependent on E-selectin (13, 47) combined with an anti-E-selectin function blocking antibody specific approach, addressed directly whether CD43 regulates Th17 cell rolling on the vascular endothelium *in vivo* in a T cell subset specific and E-selectin specific way. Our data indicate a unique Th17 cell dependency on CD43 in their interactions with the vascular endothelium via E-selectin. It has been demonstrated previously that CD43$^{-/-}$ activated T cells adhered to post-capillary venules similarly than WT in competitive migration assays using intravital microscopy (114). However, this study involved ConA activated lymphoblasts and not specific T cell subsets, including Th17 cells, which had not been described at the time.

In summary our work contributes to understanding the role of E-selectin ligands on Th17 cells, identifies CD43 as a unique E-selectin ligand for Th17 cells *in vitro* that also specifically regulates Th17 cell interactions with the vascular endothelium and recruitment to the air pouch and the microvasculature *in vivo* (Fig 4.1), and contributes to our understanding of the processes regulating Th17 cell recruitment, which takes place in various inflammatory diseases.

Our results suggest the intriguing possibility that different T cell subsets utilize the repertoire of E-selectin ligands differently to migrate into tissues during inflammation, therefore opening the possibility of interfering with T cell specific subset recruitment to treat T cell mediated diseases. While we have shown differences in adhesion of these T cell subsets to E-selectin, we have also demonstrated that T cells which express the same level of CD43H adhere differently in different T cell subsets. This leads us to speculate that there are molecular differences that regulate the addition of sugars to the highly glycosylated form of CD43, which in turn impact adhesion to E-selectin. One such example is whether there are other modifications added on to CD43 that are present only on Th17 cells and not Th1 cells, or whether there is more addition of one type of sugar, like Sialyl Lewis X, on CD43 in Th17 cells than in Th1 cells. Another example is the plasticity that might exist between these modifications as a Th17 cell becomes more Th1 cell like or vice versa. These results set the ground to investigate the molecular mechanisms that will help us understand the mechanisms by which CD43 functions differently in Th17 and Th1 cells.

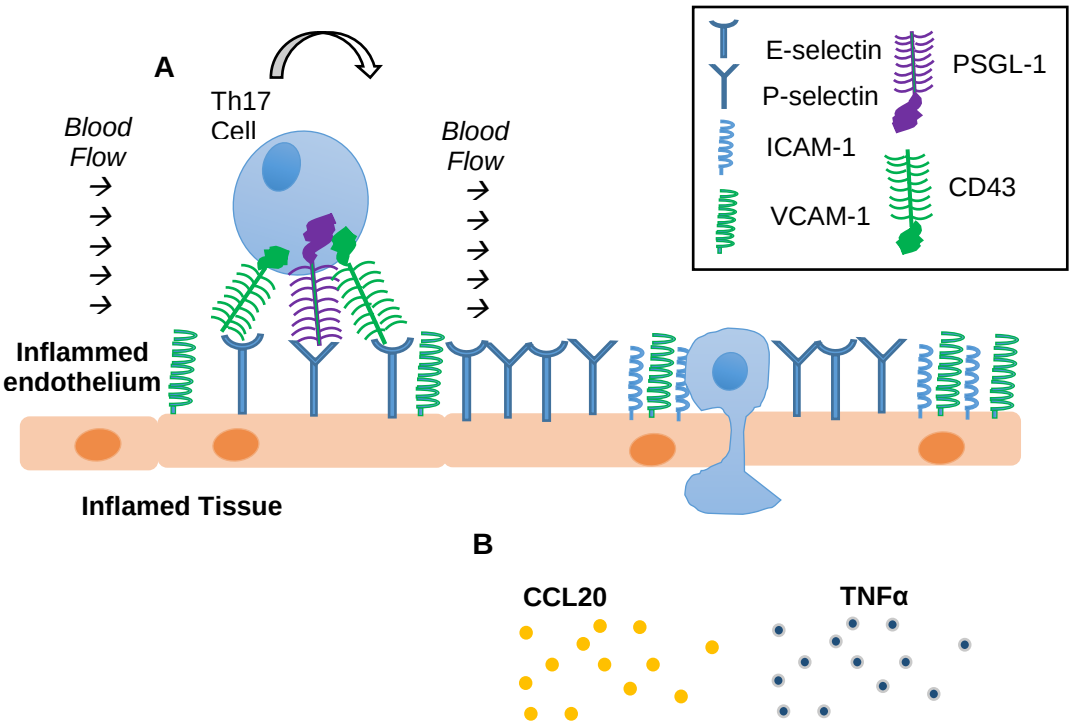

Figure 4.1: CD43 is a critical E-selectin ligand that regulates Th17 cell Trafficking.

Upon inflammatory stimulus, the vascular endothelium upregulates adhesion molecules such as selectins and integrin ligands. Th17 cells use CD43 as a major E-selectin ligand which participates in Th17 cell recruitment to TNFα and CCL20 induced inflammatory responses.

4.3. Discussion Chapter 3.2: Investigate the role of CD43 in the context of autoimmune disease using the mouse model of EAE, and evaluate CD43 mediated Th17 cell interaction with ICAM-1.

In this chapter, we have investigated the role of CD43 in antigen specific Th17 cell recruitment using the model of EAE. Moreover, we have identified potential mechanisms by which CD43 regulates Th17 cell recruitment to sites of inflammation that are independent of its interactions with E-selectin. We report that $CD43^{-/-}$ mice are protected from EAE, have decreased Th17 infiltration in the CNS but unaltered Th17 differentiation in response to MOG immunization. We found upregulation of ICAM-1 but not of E-selectin in the CNS, and we further explored the role of CD43 in regulating Th17 cell interactions with ICAM-1. Our results indicate that CD43 likely adheres to ICAM-1 but also functions as a pro-adhesive molecule that contributes to LFA-1 mediated locomotion and ICAM-1 dependent transmigration. We suggest that CD43 regulates several pathways that facilitate Th17 cell recruitment even to sites of inflammation and autoimmune reactions which do not express E-selectin. It had previously been shown that $CD43^{-/-}$ mice are protected from EAE (24), a disease where Th17 cell recruitment into the central nervous system plays a critical pathogenic role (56, 115). This study, however, was performed before Th17 cells emerged and had only addressed the severity of the disease, as well as CD4 T cell recruitment. Given the importance of Th17 cells in autoimmune diseases, such as EAE, we therefore addressed whether the protection could be attributable to specific Th17 cell recruitment defect.

We have now investigated this directly and for the first time in our knowledge, our data indicates that Th17 cells, do not infiltrate in the spinal cord of mice with EAE at the peak of disease, suggesting that this is one additional reason of the observed disease protection. Our data also indicates that unlike in certain mouse strains such as Balb/c

where CD43 regulates T cell activation, signaling and differentiation in response to immunization with OVA peptide (21, 113), this is not the case in C57/BL6 in response to MOG. In fact, we demonstrate that CD43 does not play a role in antigen specific Th17 cell differentiation, but does alter specific Th17 cell recruitment into the spinal cord.

Our data also indicate that E-selectin is not expressed in the spinal cord during EAE. This is in line with previous reports indicating that the recruitment of immune cells to the spinal cord in EAE is not dependent on E- and P-selectin, and instead relies on vascular cell adhesion molecule 1 (VCAM-1) and intracellular adhesion molecule 1 (ICAM-1). These studies prompted the development of antibodies towards VLA-4, the ligand of VCAM-1, and the development of Natalizumab. However, Natalizumab has been known to have severe side-effects in humans (116). Additionally mouse studies focusing on using antibodies towards VLA-4 have demonstrated the existence of new routes for Th17 cells to infiltrate into the CNS, proving ineffective in controlling T cell recruitment during EAE and highlighting other recruitment molecules such as ICAM-1(117, 118). Indeed, ICAM-1 has been reported to be crucial for the development of EAE in mice. Studies have demonstrated how the expression of one ICAM-1 isoform, is sufficient for the development of EAE (119, 120). Furthermore, the expression levels of ICAM-1 in the spinal cord can influence T cell crawling and effectively the type of diapedeses that will follow. Therefore, a better understanding of how leukocytes traffic during autoimmune disease using adhesion molecules such as ICAM-1 and VCAM-1, is necessary to understand how to prevent undesired immune cell infiltration without compromising the immune system. Our data suggest that blocking LFA-1 in the $CD43^{-/-}$ Th17 cells is much more effective in preventing adhesion to ICAM-1, implying that blocking CD43 may be required to prevent the pro-inflammatory actions mediated by ICAM-1. We suggest that the interaction

between CD43 and ICAM-1 is a possible mechanism for the defect of Th17 cell recruitment into the spinal cord in EAE (90).

We observed that CD43$^{-/-}$ Th17 cells have impaired adhesion to ICAM-1 and believe this phenotype to be T cell subset specific, since no significant differences were observed in CD43$^{-/-}$ Th1 cell adhesion to ICAM-1. We found that CD43 only slightly contributed to Th17 adhesion to ICAM-1 as compared to LFA-1, as most of the adhesion was prevented in the presence of a blocking antibody to LFA1, reducing adhesion to background levels of unactivated cells. We also found that Th17 detachment from ICAM-1 occurs only in WT but not CD43$^{-/-}$ Th17 cells, suggesting that CD43 can function as a weak ligand for ICAM-1. Moreover, this adhesion occurs through the same ICAM-1 epitope used by LFA-1, as indicated in our experiments with the function blocking antibody to ICAM-1.

Our LFA-1 blocking studies are in line with previous results indicating LFA-1 is the main ligand for ICAM-1 in T cells (121). We report that this is the case in Th17 cells as well, but that in Th17 cells, unlike in Th1 cells, CD43 contributes to such adhesion as well although this contribution is weaker than the interaction between LFA-1 and ICAM-1. While our studies demonstrate that blocking LFA-1 does not impact the ability of CD43 to function as an E-selectin ligand, ours studies also raise the possibility that CD43 function may regulate the function of the main ligand of ICAM-1 on T cells, LFA-1.

We found that CD43 does not contribute to LFA-1 expression or adhesion strength, but does contribute to other functions of LFA-1 such as LFA-1 mediated locomotion as well as transmigration. It is important to note that while CD43 has been previously implied to interact with ICAM-1, this was observed in an *in vitro* model, where CD43 was overexpressed and ICAM-1 was in its soluble form. Additionally these studies were done in a static system (94), while we have incorporated a dynamic measure of adhesion and function. This is the first instance, to our knowledge, where CD43 has been shown to aid

in adhesion of one specific T cell effector subset to ICAM-1 under physiological flow conditions.

Our data suggest that CD43$^{-/-}$ Th17 cells have an intact interaction between LFA-1 and ICAM-1, while WT Th17 cells have additional pro-adhesiveness to ICAM-1 mediated by CD43.

LFA-1 mediated locomotion is required for effective transmigration of T cells. This process requires actin remodeling leading to cytosketelon reorganization to support cell movement (122, 123). We observed that WT Th17 cells had a significant number of cells that locomoted across ICAM-1, while CD43$^{-/-}$ Th17 cells had less. Indeed, we observed that WT Th17 cells significantly locomoted much more rapidly and covering more distance than CD43$^{-/-}$ Th17 cells. However, F-actin polymerization was very similar between WT and CD43$^{-/-}$ Th17 cells. Several studies support that CD43 interacts with the ezrin, radixin, moesin (ERM) complex, to regulate the actin cytoskeleton in the context of antigen presentation (98). Our data indicates that this is not the case in the context of ICAM-1 mediated locomotion, and highlight a novel mechanism regulated by CD43 in LFA-1-ICAM-1 mediated Th17 cell locomotion in a way that does not directly impact F-actin polymerization. One limitation in our studies is that the actin polymerization studies were performed under static conditions, therefore there is the possibility that under shear stress with cells crawling on ICAM-1, CD43 may also regulate cytoskeleton polymerization. Since LFA-1 integrin mediated locomotion is a precursor to transendothelial migration, we tested for chemotaxis of WT and CD43$^{-/-}$ Th17 cells over ICAM-1 coated transwells. We observed that CD43$^{-/-}$ Th17 cells had impaired transmigration in the presence of CCL20 and ICAM-1 as compared to WT Th17 cells. This defect in transmigration explains the lack of integrin mediated motility we observed during the locomotion assays. We speculate that CD43 localization to the opposite side of where the T cell is interacting with a ligand might provide

the spatial organization and polarization of the cell that is needed for locomotion as well as transmigration. The absence of CD43 in our Th17 cells thus results in the inability of the cell to locomote using LFA-1 across ICAM-1.

Our study shows a novel role for the sialoglycoprotein, CD43, on Th17 cells as a pro-adhesive molecule that aids in adhesion to ICAM-1 as illustrated in Figure 4.2. The role of CD43 in Th17 cell recruitment regulates how this T cell subset traffics during inflammation and autoimmune diseases, adding to the list of functions of CD43. While CD43 has been known as a pro-adhesive and anti-adhesive molecule, how it interacts with ICAM-1 is controversial. Indeed CD43 has also been shown to play a role as a costimulatory molecule in human T cells (124). However, absence of CD43 does not have an impact on T cell differentiation, or in generation of T cell subsets in the model of EAE as previously described (90). Instead our data supports two roles for CD43 in adhesion to ICAM-1. The first is CD43 serving as a pro-adhesive molecule that aids in Th17 cell adhesion to ICAM-1in a subset specific manner (Fig. 4.2 A). The second role is with CD43 aiding in Th17 cell apical migration and transmigration (Fig 4.2B-C). How CD43 functions as a pro-adhesive molecule in Th17 cells but not Th1 cells may be controlled in changes in expression of CD43 as well as difference in glycosylation between different T cell subsets. As a result absence of CD43 in Th17 cells, but not Th1 cells, impairs the amount of cells that can adhere and infiltrate into the spinal cord during EAE, giving a level of protection from the disease. Thus, we propose adhesion of CD43 to ICAM-1 in Th17 cells as an alternative mechanism that aids LFA-1 in adhesion and transmigration during autoimmune and inflammatory conditions such as EAE.

Additionally, it is possible that it is not the polarization of the T cell by moving CD43 to the distal part of the cell where there is contact with ICAM-1 that affects locomotion or transmigration. It is possible that CD43 regulates these LFA-1 mediated functions by

affecting key components of the inside-outside signaling cascade that occurs through LFA-1. Future studies will focus on demonstrating direct binding of CD43 with ICAM-1, as well as what signaling components are participating during locomotion and transmigration.

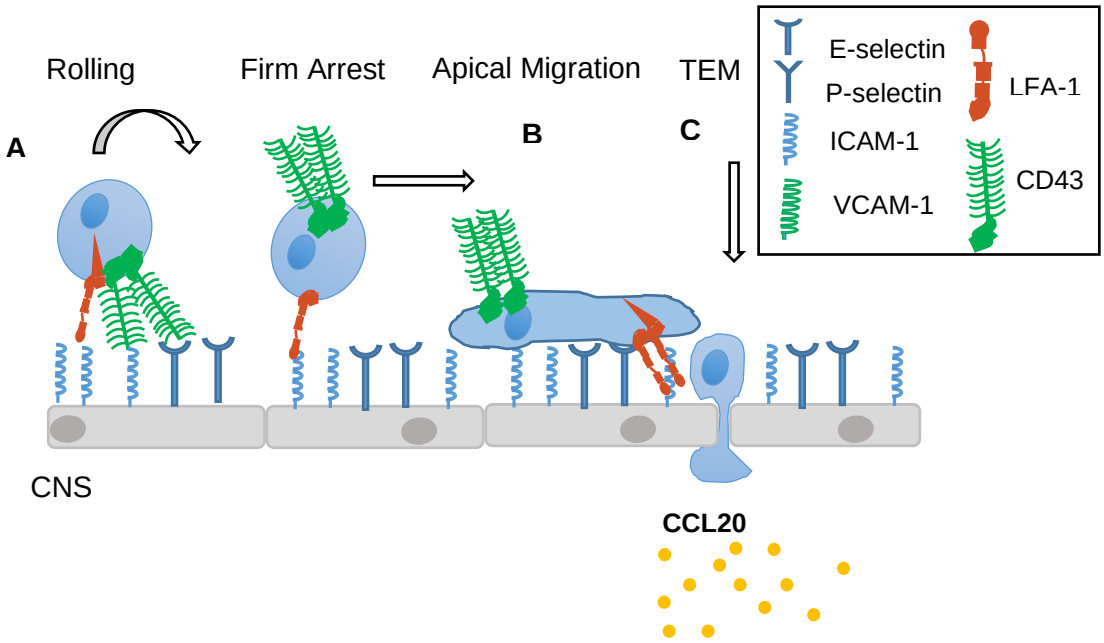

Figure 4.2: CD43 functions as a pro-adhesive molecule to ICAM-1, regulating Th17 cell infiltration into the spinal cord.

CD43 aids Th17 cells in adhesion of ICAM-1 though two working models. CD43 aids LFA-1 adhesion to ICAM-1 by serving as a pro-adhesive molecule that shares a common epitope **(A)**, impacts apical migration **(B)** affecting TEM **(C)** into the CNS.

4.4. Discussion Chapter 3.3: Determine the role of CD43 in cardiovascular disease (CVD) using the *in vivo* mouse model of Thoracic Aortic Constriction (TAC).

In this chapter, we have investigated the role of CD43 in cardiovascular disease using a mouse model of non-ischemic heart failure (HF). HF is a complex syndrome in which T cell recruitment to the heart has been found to be critical in contributing to different aspects of pathological cardiac remodeling including cardiac hypertrophy, cardiac fibrosis and cardiac inflammation (65, 66). We demonstrate for the first time that $CD43^{-/-}$ mice are protected from cardiac dysfunction and HF induced by TAC. CD43 have increased survival that is associated with decreased cardiac T cell and monocyte infiltration and decreased cardiac fibrosis. Interestingly, T cell activation in the cardiac draining lymph nodes is not impaired in $CD43^{-/-}$ TAC mice. Our results indicate that CD43 regulates cardiac leukocyte infiltration and fibrosis in response to TAC. Given our findings of CD43 as a regulator of Th17 cell recruitment, we are very interested in determining which T cell subsets are infiltrating into the LV in response to TAC. Our lab has shown that the transcription factors for Th1 and Th17 cells can be detected at 4 wks after TAC in the LV, suggesting to us that these cells play a critical role in the development of cardiac fibrosis and the loss of cardiac function that lead to HF (74). While we have demonstrated that CD43 can regulate Th17 cell recruitment, the same can't be said about Th1 cells. Further investigation into what T cell subsets could be playing a role in this model are needed to determine the protection mediated by CD43 regulation of leukocyte infiltration.

E-selectin and ICAM-1 are significantly upregulated in the left ventricle in response to TAC (74), and we have further demonstrated that ICAM-1 is crucial for T cell and pro-inflammatory leukocyte recruitment to the LV in response to TAC. However, which adhesion molecule ligands play a role in the leukocytes in order to infiltrate the LV is not

clearly understood. Our results indicate that T cells from mice undergoing TAC express higher levels of CD43 than Sham operated mice, and suggest that leukocyte CD43 could play such recruitment role. CD43 has the ability to mediate both E-selectin ligand and ICAM-1 adhesion in Th17 cells. However, attributing the protective effects observed in $CD43^{-/-}$ mice exclusively to defective Th17 cell interactions with LV E-selectin and/or ICAM-1 is ambitious, since other T cell subsets such as Th1 cells are also recruited in response to TAC (74, 125), and these do not use such pathways for recruitment (Chapter 3.1 and 3.2). Therefore, other mechanisms may be regulated by CD43 that can explain such protection and increased survival to HF. For example, absence of CD43 has been demonstrated to be protective in atherosclerosis as well as in abdominal aortic aneurysms in mechanisms independent of leukocyte recruitment. In atherosclerosis, it is not recruitment that is impaired in macrophages, rather their capacity to process lipids and become foam cells whereas in abdominal aortic aneurysms, the impact of CD43 is through IFNγ production of CD8 T cells (22, 23). Given the characteristics of CD43 being a protruding glycoprotein on the cell surface of all hematopoietic cells, it is a very likely candidate for having an impact on leukocytes in interaction with the vascular endothelium and in subsequently affecting other leukocytes as a result.

We interpret our findings that $CD43^{-/-}$ mice develop LV hypertrophy but not fibrosis or systolic dysfunction as supporting the intriguing possibility that CD43 normally promotes a pathological cardiac hypertrophy program, whereas deletion of CD43 is sufficient to retain a compensatory hypertrophy phenotype during TAC. The lack of LV fibrosis also support this model in which the heart compensates to the induced pressure but without inducing other pathological changes such as fibrosis or inflammation. Altogether, this can explain the improved systolic function observed in $CD43^{-/-}$ mice. Interestingly, this lack of fibrosis can be associated with the decreased T cell infiltration, in line with our recent work

showing a direct association between cardiac fibrosis and T cell infiltration (Fig. 4.3) (74). Additionally, monocytes can contribute to cardiac fibrosis (125), thus CD43's contribution to cardiac fibrosis may be related with the decreased observed monocyte infiltration in CD43$^{-/-}$ mice.

Our data further demonstrates that LV ICAM-1 is similarly upregulated in WT and CD43$^{-/-}$ mice, suggesting that it is defective CD43 in the leukocytes what is mediating this recruitment. Moreover, T cells were similarly activated in the cardiac draining lymph nodes, further supporting the role of CD43 in regulating T cell infiltration in the LV but not T cell activation, as demonstrated in different mouse strains and in different contexts of inflammation (21). However, we do not discard the possibility that in addition to recruitment of key T cell subsets that are in turn impacting the recruitment of other immune cells and monocytes, there may be another function that CD43 is playing in other cells involved in pressure overload induced HF.

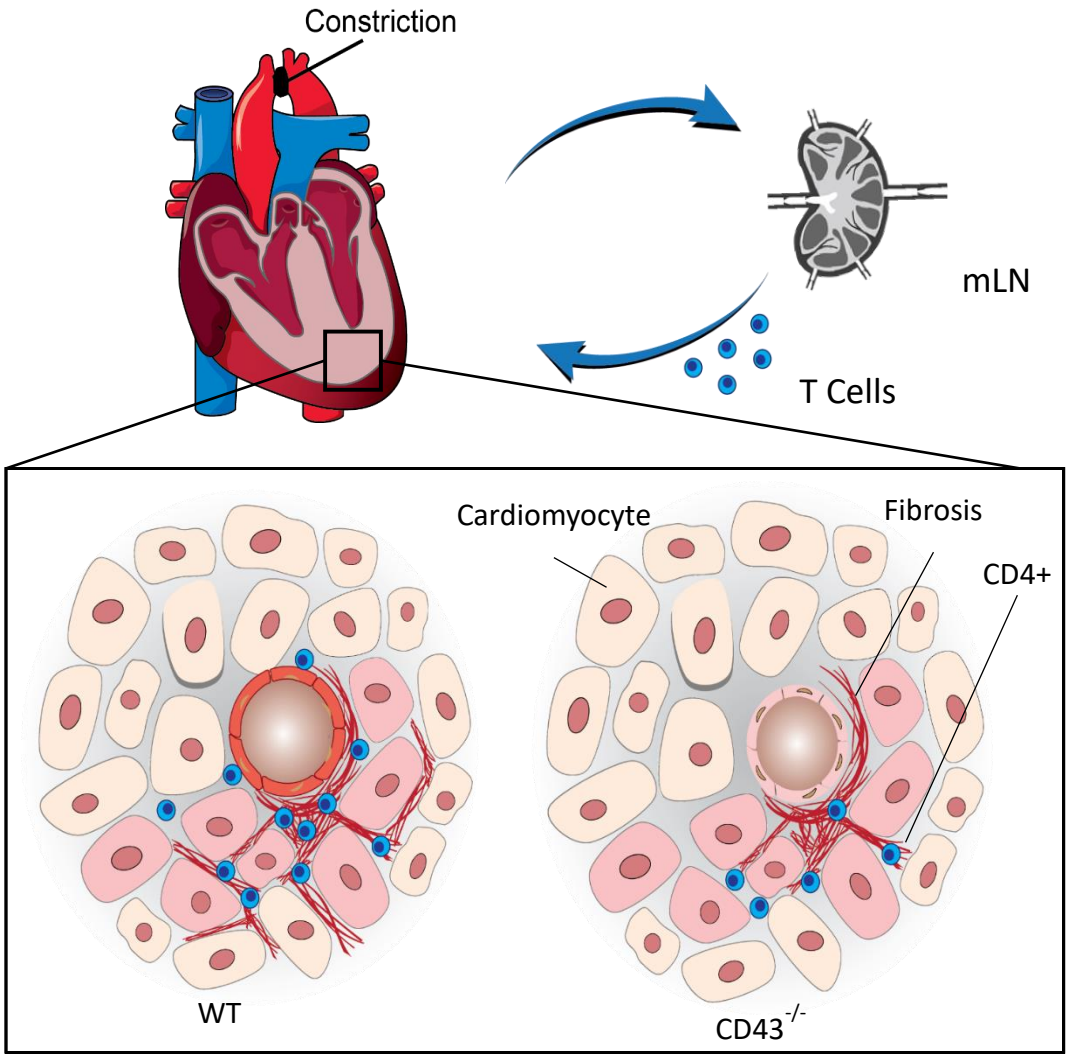

Figure 4.3: CD43 is necessary for PO induced HF in the model of TAC.

In response to TAC **(A)**, T cells become activated in the Cardiac Lymph Nodes and T cells get recruited **(B)** into the LV. The presence of CD43 is necessary for the induction of the classical hallmark signs of HF: cardiomyocyte hypertrophy, cardiac fibrosis, and cardiac dysfunction **(C)**. This is dependent on T cell infiltration into the heart.

4.5. Overall Significance

The major focus of the work on this doctoral thesis dissertation is the role of the syaloglycoprotein CD43 in Th17 cell recruitment, autoimmunity and pathological cardiac remodeling (Fig 4.4). CD43 is a molecule with multiple functions, various ligands it can bind to, and implied in a number of diseases. We report that it regulates Th17 cell trafficking specifically in EAE, and also plays a role in pathological cardiac remodeling that may be not directly associated with Th17 cells. Our data also suggest that the function of CD43 seems to be heavily dependent on the level of expression as well as in the differences found in the manner the molecule is glycosylated between different T cell subsets. The results reported in this thesis dissertation identify new roles for CD43 in Th17 cell recruitment and in more complex chronic inflammation scenarios such as adverse cardiac remodeling in heart failure.

CD43 in Th17 cell recruitment

Our findings using, both *in vitro* and *in vivo* approaches, demonstrate a unique migration phenotype for Th17 cells in three different models of inflammation that is regulated by CD43 that includes E-selectin and ICAM-1. These models include the Air Pouch, the inflamed cremaster muscle, and EAE. We demonstrated that Th17 cells, but not Th1 cell recruitment is impaired in $CD43^{-/-}$ mice, providing protection in EAE, and that such protection is independent of E-selectin, leading us to identify a new role for CD43 in recruitment in Th17 cells. We found that CD43 functions in Th17 cells as a crucial E-selectin ligand that controls Th17 recruitment during inflammation, and as a pro-adhesive molecule that contributes to ICAM-1 apical migration and transmigration (Fig. 4.4A). Perhaps our most interesting finding is that not only expression of CD43, but also alternative glycosylation in Th17 and Th1 cell subsets are responsible for its different functionality. Indeed this difference between subsets does not seem to be exclusive to just

CD43 as an E-selectin ligand but also as it mediates adhesion to ICAM-1. Future studies will be required to evaluate this possibility in detail. Taken together, our studies support the possibility of preventing undesired mediated T cell subset inflammation.

CD43 in Cardiovascular Disease

CD43 has been implied to play a role in a number of diseases, including EAE, atherosclerosis and abdominal aneurysm formation. Whereas the role of CD43 in EAE is directly related to Th17 cell recruitment, its role in aneurysms and atherosclerosis has not been reported to be the same. These results highlight a complex pleiotropic role for CD43. Our work demonstrates that CD43 is required for the development of cardiac fibrosis, cardiac dysfunction and death in TAC induced HF (Fig. 4.4B). Interestingly, we find that CD43 is necessary for leukocyte infiltration, including both CD4 T cells and CD11b monocytes. Hence, the role of CD43 in this setting cannot be specifically attributed to Th17 cell recruitment. Additionally whether CD43 impacts the function of other immune cells in this disease model is not clear, but also a possibility given the role of CD43 in other cardiovascular disease models. Future studies will need to be performed to identify the specific role of CD43 in this context of chronic inflammation. Nevertheless, these findings add to the pool of knowledge of how T cells contribute to the recruitment of other immune cells, such as monocytes, in which CD43 has not been previously reported to contribute to their recruitment and bring to light a novel role for CD43 in TAC induced HF.

All together the present doctoral thesis dissertation has identified new mechanisms for the role and function of CD43 in Th17 cell recruitment and in the pathological contribution it plays in CVD. At the same time it leaves open several questions worth to be addressed in future studies. These include identifying the molecular mechanisms of CD43 glycosylation in Th17 cells whether these contribute to direct interactions between CD43 and ICAM-1, as well as whether any of these mechanisms or alternative ones are responsible for the

protection observed in mice lacking CD43 in HF. This work contributes to the scientific community with novel findings that extend our knowledge in the field of T cell recruitment and cardiovascular immunology. Additionally, it lays the foundation for future studies that can potentially impact the design of useful anti-inflammatory therapies.

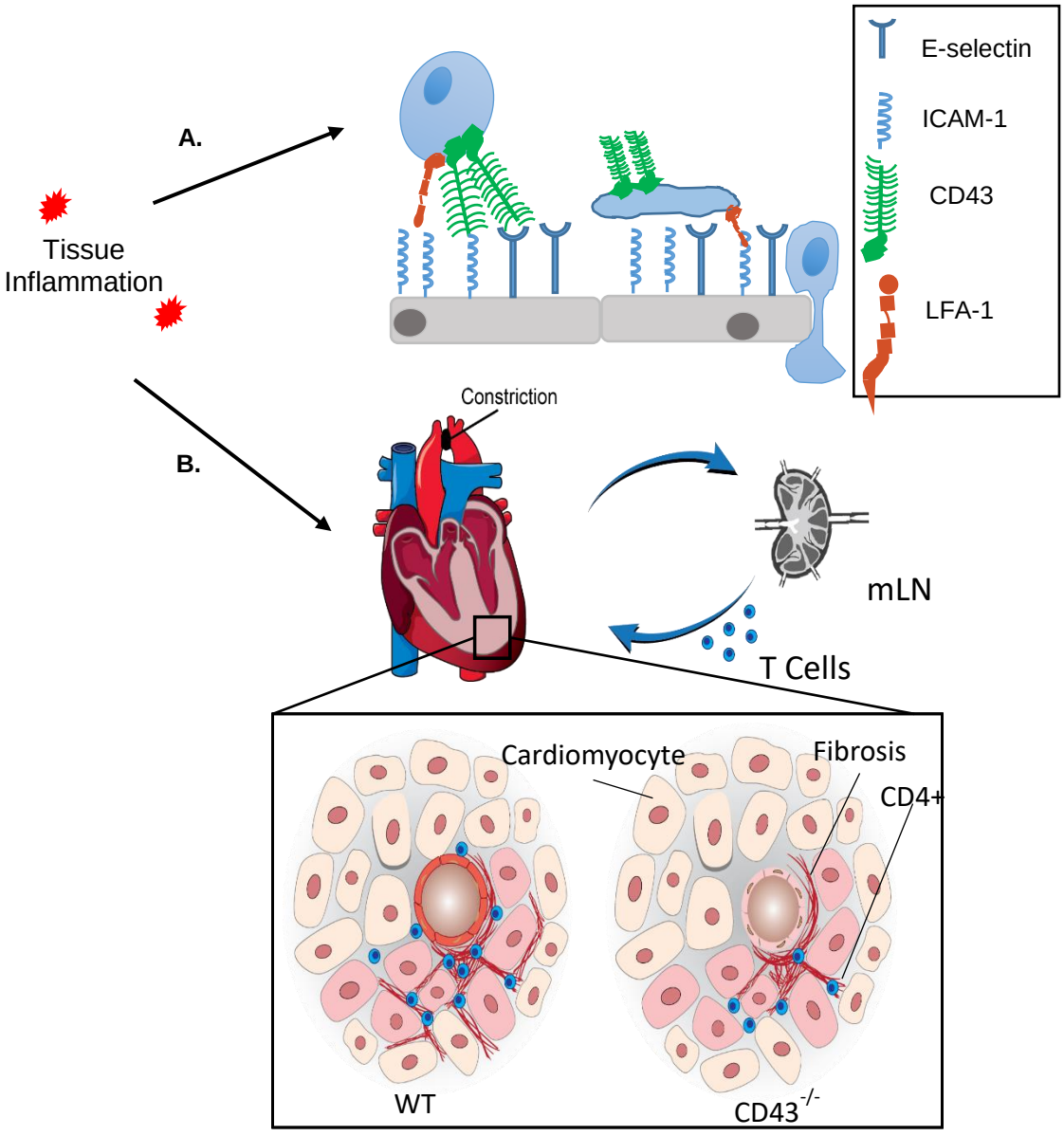

Figure 4.4: CD43 regulates Th17 cell Trafficking and is necessary for the development of cardiovascular disease.

A. Th17 cells use CD43 as a major E-selectin ligand and pro-adhesive molecule to ICAM-1 which participates in Th17 cell recruitment to inflammatory responses and autoimmunity. **B.** CD43 is necessary for activated T cells to infiltrate into the LV and induce cardiac fibrosis, cardiac dysfunction and cardiac hypertrophy.

Chapter 5: Bibliography

1. Alcaide P, Auerbach S, Luscinskas FW. Neutrophil recruitment under shear flow: it's all about endothelial cell rings and gaps. Microcirculation. 2009;16(1):43-57.
2. Schnoor M, Alcaide P, Voisin MB, van Buul JD. Crossing the Vascular Wall: Common and Unique Mechanisms Exploited by Different Leukocyte Subsets during Extravasation. Mediators Inflamm. 2015;2015:946509.
3. Sperandio M. Selectins and glycosyltransferases in leukocyte rolling in vivo. FEBS J. 2006;273(19):4377-89.
4. Williams MR, Azcutia V, Newton G, Alcaide P, Luscinskas FW. Emerging mechanisms of neutrophil recruitment across endothelium. Trends Immunol. 2011;32(10):461-9.
5. Lawrence MB, Kansas GS, Kunkel EJ, Ley K. Threshold levels of fluid shear promote leukocyte adhesion through selectins (CD62L,P,E). J Cell Biol. 1997;136(3):717-27.
6. Marshall BT, Long M, Piper JW, Yago T, McEver RP, Zhu C. Direct observation of catch bonds involving cell-adhesion molecules. Nature. 2003;423(6936):190-3.
7. Berman CL, Yeo EL, Wencel-Drake JD, Furie BC, Ginsberg MH, Furie B. A platelet alpha granule membrane protein that is associated with the plasma membrane after activation. Characterization and subcellular localization of platelet activation-dependent granule-external membrane protein. J Clin Invest. 1986;78(1):130-7.
8. Angiari S, Donnarumma T, Rossi B, Dusi S, Pietronigro E, Zenaro E, et al. TIM-1 glycoprotein binds the adhesion receptor P-selectin and mediates T cell trafficking during inflammation and autoimmunity. Immunity. 2014;40(4):542-53.
9. Munro JM, Lo SK, Corless C, Robertson MJ, Lee NC, Barnhill RL, et al. Expression of sialyl-Lewis X, an E-selectin ligand, in inflammation, immune processes, and lymphoid tissues. Am J Pathol. 1992;141(6):1397-408.
10. McEver RP, Moore KL, Cummings RD. Leukocyte trafficking mediated by selectin-carbohydrate interactions. J Biol Chem. 1995;270(19):11025-8.
11. Ley K, Kansas GS. Selectins in T-cell recruitment to non-lymphoid tissues and sites of inflammation. Nat Rev Immunol. 2004;4(5):325-35.
12. Barthel SR, Gavino JD, Descheny L, Dimitroff CJ. Targeting selectins and selectin ligands in inflammation and cancer. Expert Opin Ther Targets. 2007;11(11):1473-91.
13. Yang J, Hirata T, Croce K, Merrill-Skoloff G, Tchernychev B, Williams E, et al. Targeted gene disruption demonstrates that P-selectin glycoprotein ligand 1 (PSGL-1) is required for P-selectin-mediated but not E-selectin-mediated neutrophil rolling and migration. J Exp Med. 1999;190(12):1769-82.
14. Katayama Y, Hidalgo A, Chang J, Peired A, Frenette PS. CD44 is a physiological E-selectin ligand on neutrophils. J Exp Med. 2005;201(8):1183-9.
15. Zarbock A, Ley K, McEver RP, Hidalgo A. Leukocyte ligands for endothelial selectins: specialized glycoconjugates that mediate rolling and signaling under flow. Blood. 2011;118(26):6743-51.
16. Rosenstein Y, Santana A, Pedraza-Alva G. CD43, a molecule with multiple functions. Immunol Res. 1999;20(2):89-99.
17. Manjunath N, Correa M, Ardman M, Ardman B. Negative regulation of T-cell adhesion and activation by CD43. Nature. 1995;377(6549):535-8.
18. Pedraza-Alva G, Rosenstein Y. CD43 – One molecule, many tales to recount. Signal Transduction2011. p. 372-85.
19. Remold-O'Donnell E, Rosen FS. Sialophorin (CD43) and the Wiskott-Aldrich syndrome. Immunodefic Rev. 1990;2(2):151-74.
20. Tuccillo FM, de LA, Palmieri C, Fiume G, Bonelli P, Borrelli A, et al. Aberrant glycosylation as biomarker for cancer: focus on CD43. Biomed Res Int. 2014;2014:742831.

21. Cannon JL, Collins A, Mody PD, Balachandran D, Henriksen KJ, Smith CE, et al. CD43 regulates Th2 differentiation and inflammation. J Immunol. 2008;180(11):7385-93.
22. Meiler S, Baumer Y, McCurdy S, Lee BH, Kitamoto S, Boisvert WA. Cluster of differentiation 43 deficiency in leukocytes leads to reduced atherosclerosis--brief report. Arterioscler Thromb Vasc Biol. 2015;35(2):309-11.
23. Zhou HF, Yan H, Cannon JL, Springer LE, Green JM, Pham CT. CD43-mediated IFN-gamma production by CD8+ T cells promotes abdominal aortic aneurysm in mice. J Immunol. 2013;190(10):5078-85.
24. Ford ML, Onami TM, Sperling AI, Ahmed R, Evavold BD. CD43 modulates severity and onset of experimental autoimmune encephalomyelitis. J Immunol. 2003;171(12):6527-33.
25. Laudanna C, Kim JY, Constantin G, Butcher E. Rapid leukocyte integrin activation by chemokines. Immunol Rev. 2002;186:37-46.
26. Shamri R, Grabovsky V, Gauguet JM, Feigelson S, Manevich E, Kolanus W, et al. Lymphocyte arrest requires instantaneous induction of an extended LFA-1 conformation mediated by endothelium-bound chemokines. Nat Immunol. 2005;6(5):497-506.
27. Askari JA, Tynan CJ, Webb SE, Martin-Fernandez ML, Ballestrem C, Humphries MJ. Focal adhesions are sites of integrin extension. J Cell Biol. 2010;188(6):891-903.
28. Muller WA. Mechanisms of leukocyte transendothelial migration. Annu Rev Pathol. 2011;6:323-44.
29. Graw F, Regoes RR. Influence of the fibroblastic reticular network on cell-cell interactions in lymphoid organs. PLoS Comput Biol. 2012;8(3):e1002436.
30. Bromley SK, Mempel TR, Luster AD. Orchestrating the orchestrators: chemokines in control of T cell traffic. Nat Immunol. 2008;9(9):970-80.
31. Montresor A, Toffali L, Constantin G, Laudanna C. Chemokines and the signaling modules regulating integrin affinity. Front Immunol. 2012;3:127.
32. Schenkel AR, Mamdouh Z, Muller WA. Locomotion of monocytes on endothelium is a critical step during extravasation. Nat Immunol. 2004;5(4):393-400.
33. Auffray C, Fogg D, Garfa M, Elain G, Join-Lambert O, Kayal S, et al. Monitoring of blood vessels and tissues by a population of monocytes with patrolling behavior. Science. 2007;317(5838):666-70.
34. Ley K, Rivera-Nieves J, Sandborn WJ, Shattil S. Integrin-based therapeutics: biological basis, clinical use and new drugs. Nat Rev Drug Discov. 2016;15(3):173-83.
35. Carman CV, Sage PT, Sciuto TE, de la Fuente MA, Geha RS, Ochs HD, et al. Transcellular diapedesis is initiated by invasive podosomes. Immunity. 2007;26(6):784-97.
36. Vestweber D. Adhesion and signaling molecules controlling the transmigration of leukocytes through endothelium. Immunol Rev. 2007;218:178-96.
37. Muller WA. Leukocyte-endothelial-cell interactions in leukocyte transmigration and the inflammatory response. Trends Immunol. 2003;24(6):327-34.
38. Vestweber D. Regulation of endothelial cell contacts during leukocyte extravasation. Curr Opin Cell Biol. 2002;14(5):587-93.
39. Allport JR, Muller WA, Luscinskas FW. Monocytes induce reversible focal changes in vascular endothelial cadherin complex during transendothelial migration under flow. J Cell Biol. 2000;148(1):203-16.
40. Barreiro O, Yanez-Mo M, Serrador JM, Montoya MC, Vicente-Manzanares M, Tejedor R, et al. Dynamic interaction of VCAM-1 and ICAM-1 with moesin and ezrin in a novel endothelial docking structure for adherent leukocytes. J Cell Biol. 2002;157(7):1233-45.
41. Ley K, Laudanna C, Cybulsky MI, Nourshargh S. Getting to the site of inflammation: the leukocyte adhesion cascade updated. Nat Rev Immunol. 2007;7(9):678-89.

42. Luckheeram RV, Zhou R, Verma AD, Xia B. CD4(+)T cells: differentiation and functions. Clin Dev Immunol. 2012;2012:925135.
43. Fuhlbrigge RC, King SL, Sackstein R, Kupper TS. CD43 is a ligand for E-selectin on CLA+ human T cells. Blood. 2006;107(4):1421-6.
44. Ellies LG, Jones AT, Williams MJ, Ziltener HJ. Differential regulation of CD43 glycoforms on CD4+ and CD8+ T lymphocytes in graft-versus-host disease. Glycobiology. 1994;4(6):885-93.
45. Lee GR, Kim ST, Spilianakis CG, Fields PE, Flavell RA. T helper cell differentiation: regulation by cis elements and epigenetics. Immunity. 2006;24(4):369-79.
46. Yang XO, Nurieva R, Martinez GJ, Kang HS, Chung Y, Pappu BP, et al. Molecular antagonism and plasticity of regulatory and inflammatory T cell programs. Immunity. 2008;29(1):44-56.
47. Alcaide P, Maganto-Garcia E, Newton G, Travers R, Croce KJ, Bu DX, et al. Difference in Th1 and Th17 lymphocyte adhesion to endothelium. J Immunol. 2012;188(3):1421-30.
48. Lim YC, Henault L, Wagers AJ, Kansas GS, Luscinskas FW, Lichtman AH. Expression of functional selectin ligands on Th cells is differentially regulated by IL-12 and IL-4. J Immunol. 1999;162(6):3193-201.
49. Hirata T, Merrill-Skoloff G, Aab M, Yang J, Furie BC, Furie B. P-Selectin glycoprotein ligand 1 (PSGL-1) is a physiological ligand for E-selectin in mediating T helper 1 lymphocyte migration. J Exp Med. 2000;192(11):1669-76.
50. Matsumoto M, Shigeta A, Furukawa Y, Tanaka T, Miyasaka M, Hirata T. CD43 collaborates with P-selectin glycoprotein ligand-1 to mediate E-selectin-dependent T cell migration into inflamed skin. J Immunol. 2007;178(4):2499-506.
51. Alcaide P, King SL, Dimitroff CJ, Lim YC, Fuhlbrigge RC, Luscinskas FW. The 130-kDa glycoform of CD43 functions as an E-selectin ligand for activated Th1 cells in vitro and in delayed-type hypersensitivity reactions in vivo. J Invest Dermatol. 2007;127(8):1964-72.
52. Yen D, Cheung J, Scheerens H, Poulet F, McClanahan T, McKenzie B, et al. IL-23 is essential for T cell-mediated colitis and promotes inflammation via IL-17 and IL-6. J Clin Invest. 2006;116(5):1310-6.
53. Jiang R, Tan Z, Deng L, Chen Y, Xia Y, Gao Y, et al. Interleukin-22 promotes human hepatocellular carcinoma by activation of STAT3. Hepatology. 2011;54(3):900-9.
54. Yamazaki T, Yang XO, Chung Y, Fukunaga A, Nurieva R, Pappu B, et al. CCR6 regulates the migration of inflammatory and regulatory T cells. J Immunol. 2008;181(12):8391-401.
55. Jirmanova L, Giardino Torchia ML, Sarma ND, Mittelstadt PR, Ashwell JD. Lack of the T cell-specific alternative p38 activation pathway reduces autoimmunity and inflammation. Blood. 2011;118(12):3280-9.
56. Komiyama Y, Nakae S, Matsuki T, Nambu A, Ishigame H, Kakuta S, et al. IL-17 plays an important role in the development of experimental autoimmune encephalomyelitis. J Immunol. 2006;177(1):566-73.
57. Li H, Nourbakhsh B, Cullimore M, Zhang GX, Rostami A. IL-9 is important for T-cell activation and differentiation in autoimmune inflammation of the central nervous system. Eur J Immunol. 2011;41(8):2197-206.
58. Stromnes IM, Cerretti LM, Liggitt D, Harris RA, Goverman JM. Differential regulation of central nervous system autoimmunity by T(H)1 and T(H)17 cells. Nat Med. 2008;14(3):337-42.
59. Osnes LT, Nakken B, Bodolay E, Szodoray P. Assessment of intracellular cytokines and regulatory cells in patients with autoimmune diseases and primary immunodeficiencies - novel tool for diagnostics and patient follow-up. Autoimmun Rev. 2013;12(10):967-71.

60. Baldeviano GC, Barin JG, Talor MV, Srinivasan S, Bedja D, Zheng D, et al. Interleukin-17A is dispensable for myocarditis but essential for the progression to dilated cardiomyopathy. Circ Res. 2010;106(10):1646-55.
61. Wu L, Ong S, Talor MV, Barin JG, Baldeviano GC, Kass DA, et al. Cardiac fibroblasts mediate IL-17A-driven inflammatory dilated cardiomyopathy. J Exp Med. 2014;211(7):1449-64.
62. Cowie MR, Mosterd A, Wood DA, Deckers JW, Poole-Wilson PA, Sutton GC, et al. The epidemiology of heart failure. Eur Heart J. 1997;18(2):208-25.
63. Lloyd-Jones D, Adams R, Carnethon M, De Simone G, Ferguson TB, Flegal K, et al. Heart disease and stroke statistics--2009 update: a report from the American Heart Association Statistics Committee and Stroke Statistics Subcommittee. Circulation. 2009;119(3):480-6.
64. Braunwald E. Shattuck lecture--cardiovascular medicine at the turn of the millennium: triumphs, concerns, and opportunities. N Engl J Med. 1997;337(19):1360-9.
65. Ahmad T, Fiuzat M, Felker GM, O'Connor C. Novel biomarkers in chronic heart failure. Nat Rev Cardiol. 2012;9(6):347-59.
66. Jessup M, Brozena S. Heart failure. N Engl J Med. 2003;348(20):2007-18.
67. Mann DL, McMurray JJ, Packer M, Swedberg K, Borer JS, Colucci WS, et al. Targeted anticytokine therapy in patients with chronic heart failure: results of the Randomized Etanercept Worldwide Evaluation (RENEWAL). Circulation. 2004;109(13):1594-602.
68. Chung ES, Packer M, Lo KH, Fasanmade AA, Willerson JT, Anti TNFTACHFI. Randomized, double-blind, placebo-controlled, pilot trial of infliximab, a chimeric monoclonal antibody to tumor necrosis factor-alpha, in patients with moderate-to-severe heart failure: results of the anti-TNF Therapy Against Congestive Heart Failure (ATTACH) trial. Circulation. 2003;107(25):3133-40.
69. Abbate A, Bonanno E, Mauriello A, Bussani R, Biondi-Zoccai GG, Liuzzo G, et al. Widespread myocardial inflammation and infarct-related artery patency. Circulation. 2004;110(1):46-50.
70. Fukunaga T, Soejima H, Irie A, Sugamura K, Oe Y, Tanaka T, et al. Relation between CD4+ T-cell activation and severity of chronic heart failure secondary to ischemic or idiopathic dilated cardiomyopathy. Am J Cardiol. 2007;100(3):483-8.
71. Ismahil MA, Hamid T, Bansal SS, Patel B, Kingery JR, Prabhu SD. Remodeling of the mononuclear phagocyte network underlies chronic inflammation and disease progression in heart failure: critical importance of the cardiosplenic axis. Circ Res. 2014;114(2):266-82.
72. Shim SH, Kim DS, Cho W, Nam JH. Coxsackievirus B3 regulates T-cell infiltration into the heart by lymphocyte function-associated antigen-1 activation via the cAMP/Rap1 axis. J Gen Virol. 2014;95(Pt 9):2010-8.
73. Smith SC, Allen PM. Myosin-induced acute myocarditis is a T cell-mediated disease. J Immunol. 1991;147(7):2141-7.
74. Nevers T, Salvador AM, Grodecki-Pena A, Knapp A, Velazquez F, Aronovitz M, et al. Left Ventricular T-Cell Recruitment Contributes to the Pathogenesis of Heart Failure. Circ Heart Fail. 2015;8(4):776-87.
75. Salvador AM, Nevers T, Velazquez F, Aronovitz M, Wang B, Abadia Molina A, et al. Intercellular Adhesion Molecule 1 Regulates Left Ventricular Leukocyte Infiltration, Cardiac Remodeling, and Function in Pressure Overload-Induced Heart Failure. J Am Heart Assoc. 2016;5(3):e003126.
76. McEver RP. P-selectin and PSGL-1: exploiting connections between inflammation and venous thrombosis. Thromb Haemost. 2002;87(3):364-5.

77. Nacher M, Blazquez AB, Shao B, Matesanz A, Prophete C, Berin MC, et al. Physiological contribution of CD44 as a ligand for E-Selectin during inflammatory T-cell recruitment. Am J Pathol. 2011;178(5):2437-46.
78. Edwards JC, Sedgwick AD, Willoughby DA. The formation of a structure with the features of synovial lining by subcutaneous injection of air: an in vivo tissue culture system. J Pathol. 1981;134(2):147-56.
79. Pino PA, Cardona AE. Isolation of brain and spinal cord mononuclear cells using percoll gradients. J Vis Exp. 2011(48).
80. Rockman HA, Ross RS, Harris AN, Knowlton KU, Steinhelper ME, Field LJ, et al. Segregation of atrial-specific and inducible expression of an atrial natriuretic factor transgene in an in vivo murine model of cardiac hypertrophy. Proc Natl Acad Sci U S A. 1991;88(18):8277-81.
81. Fujinami RS, von Herrath MG, Christen U, Whitton JL. Molecular mimicry, bystander activation, or viral persistence: infections and autoimmune disease. Clin Microbiol Rev. 2006;19(1):80-94.
82. Jacobs AK, Kushner FG, Ettinger SM, Guyton RA, Anderson JL, Ohman EM, et al. ACCF/AHA clinical practice guideline methodology summit report: a report of the American College of Cardiology Foundation/American Heart Association Task Force on Practice Guidelines. J Am Coll Cardiol. 2013;61(2):213-65.
83. Fuhlbrigge RC, King SL, Dimitroff CJ, Kupper TS, Sackstein R. Direct real-time observation of E- and P-selectin-mediated rolling on cutaneous lymphocyte-associated antigen immobilized on Western blots. J Immunol. 2002;168(11):5645-51.
84. Yago T, Shao B, Miner JJ, Yao L, Klopocki AG, Maeda K, et al. E-selectin engages PSGL-1 and CD44 through a common signaling pathway to induce integrin alphaLbeta2-mediated slow leukocyte rolling. Blood. 2010;116(3):485-94.
85. Ritonja A, Rowan AD, Buttle DJ, Rawlings ND, Turk V, Barrett AJ. Stem bromelain: amino acid sequence and implications for weak binding of cystatin. FEBS Lett. 1989;247(2):419-24.
86. Alon R, Feizi T, Yuen CT, Fuhlbrigge RC, Springer TA. Glycolipid ligands for selectins support leukocyte tethering and rolling under physiologic flow conditions. J Immunol. 1995;154(10):5356-66.
87. Ding ZM, Babensee JE, Simon SI, Lu H, Perrard JL, Bullard DC, et al. Relative contribution of LFA-1 and Mac-1 to neutrophil adhesion and migration. J Immunol. 1999;163(9):5029-38.
88. Hafezi-Moghadam A, Ley K. Relevance of L-selectin shedding for leukocyte rolling in vivo. J Exp Med. 1999;189(6):939-48.
89. Austrup F, Vestweber D, Borges E, Lohning M, Brauer R, Herz U, et al. P- and E-selectin mediate recruitment of T-helper-1 but not T-helper-2 cells into inflammed tissues. Nature. 1997;385(6611):81-3.
90. Velazquez F, Grodecki-Pena A, Knapp A, Salvador AM, Nevers T, Croce KJ, et al. CD43 Functions as an E-Selectin Ligand for Th17 Cells In Vitro and Is Required for Rolling on the Vascular Endothelium and Th17 Cell Recruitment during Inflammation In Vivo. J Immunol. 2016;196(3):1305-16.
91. Lee Y, Awasthi A, Yosef N, Quintana FJ, Xiao S, Peters A, et al. Induction and molecular signature of pathogenic TH17 cells. Nat Immunol. 2012;13(10):991-9.
92. Miller SD, Karpus WJ, Davidson TS. Experimental autoimmune encephalomyelitis in the mouse. Curr Protoc Immunol. 2010;Chapter 15:Unit 15 1.
93. Doring A, Wild M, Vestweber D, Deutsch U, Engelhardt B. E- and P-selectin are not required for the development of experimental autoimmune encephalomyelitis in C57BL/6 and SJL mice. J Immunol. 2007;179(12):8470-9.

94. Rosenstein Y, Park JK, Hahn WC, Rosen FS, Bierer BE, Burakoff SJ. CD43, a molecule defective in Wiskott-Aldrich syndrome, binds ICAM-1. Nature. 1991;354(6350):233-5.
95. Staunton DE, Dustin ML, Erickson HP, Springer TA. The arrangement of the immunoglobulin-like domains of ICAM-1 and the binding sites for LFA-1 and rhinovirus. Cell. 1990;61(2):243-54.
96. Horwitz AR, Parsons JT. Cell biology - Cell migration - Movin' on. Science. 1999;286(5442):1102-3.
97. Ramsay AG, Evans R, Kiaii S, Svensson L, Hogg N, Gribben JG. Chronic lymphocytic leukemia cells induce defective LFA-1-directed T-cell motility by altering Rho GTPase signaling that is reversible with lenalidomide. Blood. 2013;121(14):2704-14.
98. Allenspach EJ, Cullinan P, Tong J, Tang Q, Tesciuba AG, Cannon JL, et al. ERM-dependent movement of CD43 defines a novel protein complex distal to the immunological synapse. Immunity. 2001;15(5):739-50.
99. Ghannam S, Dejou C, Pedretti N, Giot JP, Dorgham K, Boukhaddaoui H, et al. CCL20 and beta-defensin-2 induce arrest of human Th17 cells on inflamed endothelium in vitro under flow conditions. J Immunol. 2011;186(3):1411-20.
100. Aukrust P, Ueland T, Lien E, Bendtzen K, Muller F, Andreassen AK, et al. Cytokine network in congestive heart failure secondary to ischemic or idiopathic dilated cardiomyopathy. Am J Cardiol. 1999;83(3):376-82.
101. Levine B, Kalman J, Mayer L, Fillit HM, Packer M. Elevated circulating levels of tumor necrosis factor in severe chronic heart failure. N Engl J Med. 1990;323(4):236-41.
102. Laroumanie F, Douin-Echinard V, Pozzo J, Lairez O, Tortosa F, Vinel C, et al. CD4+ T cells promote the transition from hypertrophy to heart failure during chronic pressure overload. Circulation. 2014;129(21):2111-24.
103. Lord GM, Rao RM, Choe H, Sullivan BM, Lichtman AH, Luscinskas FW, et al. T-bet is required for optimal proinflammatory CD4+ T-cell trafficking. Blood. 2005;106(10):3432-9.
104. Huang MC, Laskowska A, Vestweber D, Wild MK. The alpha (1,3)-fucosyltransferase Fuc-TIV, but not Fuc-TVII, generates sialyl Lewis X-like epitopes preferentially on glycolipids. J Biol Chem. 2002;277(49):47786-95.
105. Nimrichter L, Burdick MM, Aoki K, Laroy W, Fierro MA, Hudson SA, et al. E-selectin receptors on human leukocytes. Blood. 2008;112(9):3744-52.
106. Griffin GK, Newton G, Tarrio ML, Bu DX, Maganto-Garcia E, Azcutia V, et al. IL-17 and TNF-alpha sustain neutrophil recruitment during inflammation through synergistic effects on endothelial activation. J Immunol. 2012;188(12):6287-99.
107. Wang C, Kang SG, Lee J, Sun Z, Kim CH. The roles of CCR6 in migration of Th17 cells and regulation of effector T-cell balance in the gut. Mucosal Immunol. 2009;2(2):173-83.
108. Tessier PA, Naccache PH, Clark-Lewis I, Gladue RP, Neote KS, McColl SR. Chemokine networks in vivo: involvement of C-X-C and C-C chemokines in neutrophil extravasation in vivo in response to TNF-alpha. J Immunol. 1997;159(7):3595-602.
109. Yoshizaki A, Yanaba K, Iwata Y, Komura K, Ogawa A, Akiyama Y, et al. Cell adhesion molecules regulate fibrotic process via Th1/Th2/Th17 cell balance in a bleomycin-induced scleroderma model. J Immunol. 2010;185(4):2502-15.
110. Labow MA, Norton CR, Rumberger JM, Lombard-Gillooly KM, Shuster DJ, Hubbard J, et al. Characterization of E-selectin-deficient mice: demonstration of overlapping function of the endothelial selectins. Immunity. 1994;1(8):709-20.
111. Ley K, Allietta M, Bullard DC, Morgan S. Importance of E-selectin for firm leukocyte adhesion in vivo. Circ Res. 1998;83(3):287-94.

112. Staite ND, Justen JM, Sly LM, Beaudet AL, Bullard DC. Inhibition of delayed-type contact hypersensitivity in mice deficient in both E-selectin and P-selectin. Blood. 1996;88(8):2973-9.
113. Woodman RC, Johnston B, Hickey MJ, Teoh D, Reinhardt P, Poon BY, et al. The functional paradox of CD43 in leukocyte recruitment: a study using CD43-deficient mice. J Exp Med. 1998;188(11):2181-6.
114. Carlow DA, Ziltener HJ. CD43 deficiency has no impact in competitive in vivo assays of neutrophil or activated T cell recruitment efficiency. J Immunol. 2006;177(9):6450-9.
115. Hofstetter H, Gold R, Hartung HP. Th17 Cells in MS and Experimental Autoimmune Encephalomyelitis. Int MS J. 2009;16(1):12-8.
116. Ransohoff RM. Natalizumab and PML. Nat Neurosci. 2005;8(10):1275.
117. Rothhammer V, Heink S, Petermann F, Srivastava R, Claussen MC, Hemmer B, et al. Th17 lymphocytes traffic to the central nervous system independently of alpha4 integrin expression during EAE. J Exp Med. 2011;208(12):2465-76.
118. Theien BE, Vanderlugt CL, Nickerson-Nutter C, Cornebise M, Scott DM, Perper SJ, et al. Differential effects of treatment with a small-molecule VLA-4 antagonist before and after onset of relapsing EAE. Blood. 2003;102(13):4464-71.
119. Hu X, Barnum SR, Wohler JE, Schoeb TR, Bullard DC. Differential ICAM-1 isoform expression regulates the development and progression of experimental autoimmune encephalomyelitis. Mol Immunol. 2010;47(9):1692-700.
120. Bullard DC, Hu X, Schoeb TR, Collins RG, Beaudet AL, Barnum SR. Intercellular adhesion molecule-1 expression is required on multiple cell types for the development of experimental autoimmune encephalomyelitis. J Immunol. 2007;178(2):851-7.
121. Marlin SD, Springer TA. Purified intercellular adhesion molecule-1 (ICAM-1) is a ligand for lymphocyte function-associated antigen 1 (LFA-1). Cell. 1987;51(5):813-9.
122. del Pozo MA, Sanchez-Mateos P, Nieto M, Sanchez-Madrid F. Chemokines regulate cellular polarization and adhesion receptor redistribution during lymphocyte interaction with endothelium and extracellular matrix. Involvement of cAMP signaling pathway. J Cell Biol. 1995;131(2):495-508.
123. Serrador JM, Nieto M, Sanchez-Madrid F. Cytoskeletal rearrangement during migration and activation of T lymphocytes. Trends Cell Biol. 1999;9(6):228-33.
124. Bravo-Adame ME, Vera-Estrella R, Barkla BJ, Martinez-Campos C, Flores-Alcantar A, Ocelotl-Oviedo JP, et al. An alternative mode of CD43 signal transduction activates pro-survival pathways of T lymphocytes. Immunology. 2017;150(1):87-99.
125. Patel B, Ismahil MA, Hamid T, Bansal SS, Prabhu SD. Mononuclear Phagocytes Are Dispensable for Cardiac Remodeling in Established Pressure-Overload Heart Failure. PLoS One. 2017;12(1):e0170781.